ON THE USE OF A GAS-CAVITATION MODEL TO GENERATE PROTOTYPAL AIR AND HELIUM DECOMPRESSION SCHEDULES FOR DIVERS

A DISSERTATION SUBMITTED TO THE GRADUATE DIVISION OF THE
UNIVERSITY OF HAWAII IN PARTIAL FULFILLMENT
OF THE REQUIREMENTS FOR THE DEGREE OF

DOCTOR OF PHILOSOPHY

IN PHYSICS

AUGUST 1985

By

Donald Clinton Hoffman

Thesis Committee:

David E. Yount, Chairman
Charles F. Hayes
Sandip Pakvasa
Chester A. Vause, III
Edward L. Beckman

We certify that we have read this dissertation and that, in our opinion, it is satisfactory in scope and quality as a dissertation for the degree of Doctor of Philosophy in Physics.

DISSERTATION COMMITTEE

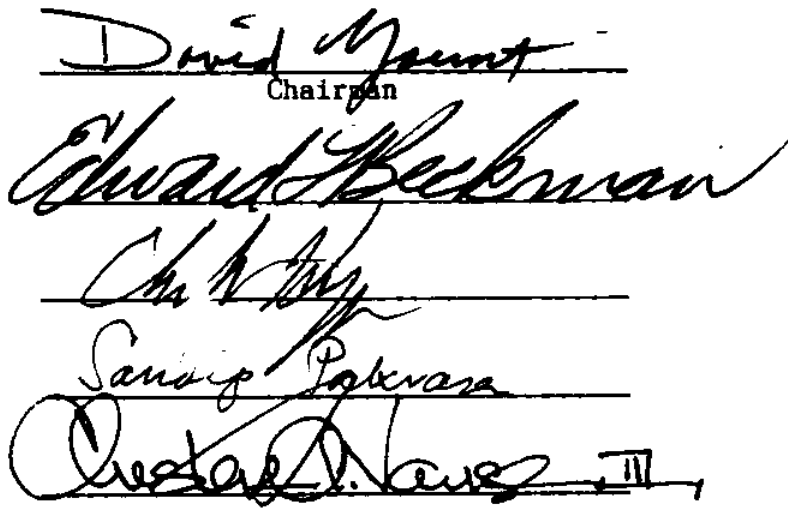

Chairman

ACKNOWLEDGEMENTS

It is a pleasure for me to thank all the colleagues who have participated in the "Tiny Bubble Group" over the years, especially Birch Porter, Tom Kunkle, Jon Pegg, and Claude Harvey. In addition, there were four visitors from the Ecole Centrale des Arts et Manufactures, Chatenay-Malabry, France who have contributed to this ongoing effort: Gilbert Grenié in 1980, Bernard Rémy in 1981, Gildas Herjean in 1982, and Philippe Mazas in 1983.

University of Hawaii Sea Grant
College Program

Project: The Physics of Gas
Bubbles: Medical Applications

Project No.: HP/R-4

ABSTRACT

In the past, the underlying processes of nucleation and growth of gas phases *in vitro* and *in vivo* have been poorly understood. The present decompression schedules for humans have thus evolved from unsupported assumptions, some of which have been shown to be wrong. Although adjusted by trial and error, these diving tables are neither optimal nor entirely safe. To the population at risk, the cost of empirical investigation has been high and is still being paid.

During the last several years, significant progress has been made in elucidating the bubble-nucleation phenomenon in aqueous media. According to the varying-permeability model, cavitation nuclei consist of spherical gas phases that are small enough to remain in solution, yet strong enough to resist collapse, their stability being provided by elastic skins or membranes consisting of surface-active molecules. By tracking the radial size of bubble nuclei during changes in ambient pressure, the model has provided precise quantitative descriptions of bubble-counting experiments in gelatin. It has also been used to trace levels of incidence for decompression sickness in several animal species, including fingerling salmon, rats, and humans. More recently, bubble nuclei have been observed directly in distilled water, gelatin, and blood using a variety of microscopic techniques.

This work details the application of the varying-permeability model to the problem of decompression sickness through the construction of a prototypal set of decompression schedules. These schedules were generated by a short computer program based on the model equations. Once initialized with a group of tissue half-times and four free

parameters selected to optimize decompression safety and speed, the program was used to calculate air diving tables for depths ranging from 30–300 fsw, requiring only the corresponding depth excursions and bottom times as input. Following the reevaluation and readjustment of the program and the model parameters, a similar set of decompression schedules for helium dives was produced.

Chapter I contains a brief introduction to the varying-permeability model and presents several pertinent equations, with ample references to the original work. Chapter II details the supplementary assumptions required to generate decompression schedules. The model constants are defined and the free parameters are adjusted to accommodate air dives in Chapter III, where extensive comparisons are made between the VPM predictions and current air tables. The theoretical extension of the model to include helium dives is considered in Chapter IV, and in Chapter V the VPM helium tables are compared with their USN counterparts and with data from several other sources. Finally, Chapter VI provides an overview of the operation of the computer program and relates the model equations to the sample program listings given in the appendices.

TABLE OF CONTENTS

TABLE OF CONTENTS (CONTINUED)

LIST OF TABLES

LIST OF FIGURES

LIST OF FIGURES (CONTINUED)

LIST OF ACRONYMS AND SYMBOLS

ACRONYMS

Acronym	Definition
DEC	Digital Equipment Corporation
EDU	Experimental Diving Unit
EVA	Extra-vehicular activity
FSW	Feet of sea water
HELIOX	Helium-oxygen
M-Values	Maximum allowed tissue tensions
RNPL	Royal Naval Physiological Laboratory
SCUBA	Self-contained underwater breathing apparatus
USN	United States Navy
VP	Varying permeability
VPM	Varying-permeability model

SYMBOLS

Symbol	Definition
a, A	Algebraic intermediate variables
b, B	" " "
c, C	" " "
D	Depth
D_a	Allowed depth
F	Inert-gas fraction
F_{He}	Helium inert-gas fraction
H	Tissue half-time

LIST OF ACRONYMS AND SYMBOLS (CONTINUED)

Symbol	Definition
H^*	Tissue exponential time-constant
k	Inverse of tissue exponential time-constant
N_{actual}	Actual bubble number
N_{new}	Augmented bubble number
N_o	Bubble number normalization constant
N_{safe}	Safe bubble number
p	Algebraic intermediate variable
P^*	Crushing pressure threshold
P_a	Ambient pressure
P_{crush}	Permeable region crushing pressure
P^*_{crush}	Impermeable region crushing pressure
P_f	Final pressure
P_{in}	Pressure inside bubble nucleus
P_m	Maximum pressure
P_o	Initial ambient pressure
P_R	Pressure outside nucleus, including surface tension
P_S	Pressure inside nucleus, including skin compression
P_{ss}	Allowed supersaturation pressure
P^{new}_{ss}	Augmented allowed supersaturation pressure
P^{safe}_{ss}	Safe, unaugmented allowed supersaturation pressure
P_1	Exposure pressure
P_2	Final pressure
q	Algebraic intermediate variable

LIST OF ACRONYMS AND SYMBOLS (CONTINUED)

Symbol	Definition
r	Nuclear radius
r^*	Nuclear radius at onset of impermeability
r_m	Minimum nuclear radius after crushing
r_o	Minimum nuclear radius required for bubble formation
r_o^{new}	Minimum nuclear radius after augmentation
S	Effective area of surfactant molecule
t	Elapsed time
t_C	Time of maximum released-gas volume
t_D	Total decompression time
v	Depth excursion velocity
$\dot{V}$	Rate of gas-phase inflation
V_C	Critical volume of released gas
α	Varying-permeability model free parameter
β_o	" " " constant
γ	Surface tension
γ_C	Maximum skin compressional strength
δ	Skin thickness
λ	Former VP model free parameter
Π	Surface pressure
τ	Dissolved gas tension
τ_r	Regeneration time constant
χ	Critical-volume proportionality constant

PREFACE

The new decompression methods contained in this work are the result of ongoing research at the University of Hawaii into the phenomena of cavitation in general and gas nuclei in particular. Affectionately nicknamed the "Tiny Bubble Group," the research team has seen many participants over the years, each of whom has made some contribution to the varying-permeability model or the associated table calculations. However, the author is solely responsible for any shortcomings in the material contained herein. It cannot be over-emphasized that the VPM air and helium tables are theoretical in nature, have never been tested using human subjects, and are not intended for general use by the diving community. It is our hope that their dissemination will provide added insight and point out new directions in studying the decompression problem.

CHAPTER I

A. INTRODUCTION

Decompression sickness is caused by a reduction in ambient pressure resulting in supersaturation and the formation of gas bubbles in blood or tissue. This well-known disease syndrome, often called "the bends," is associated with such modern-day activities as deep-sea diving, working in pressurized tunnels and caissons, flying at high altitudes in unpressurized aircraft, and EVA excursions from spacecraft. One striking feature is that almost any body part, organ, or fluid can be stricken, including the skin, muscle, brain and nervous tissue, vitreous humor of the eye, and bone. Medical signs and symptoms range from itching and mild tingling sensations to crippling bone necrosis, permanent paralysis, and death.

The generality of the symptoms of decompression sickness [1] and the fact that humans are comprised mainly of water suggest that the problem of bubble formation in divers may have a simple physical solution. Since bubble formation occurs in nearly all aqueous media, it can be studied in whatever substance is most convenient. The choice for an original series of experiments performed at the University of Hawaii was unflavored Knox gelatin, which is transparent and holds bubbles in place so that they can be counted and measured [2-7]. Distilled water, sea water, agarose gelatin [8], infertile hen's eggs [9], and blood have been used in subsequent experiments.

The main outcome of this line of investigation has been the development of the varying-permeability model (VPM), in which cavitation

nuclei consist of spherical gas phases that are small enough to remain in solution yet strong enough to resist collapse, their stability being provided by elastic skins or membranes consisting of surface-active molecules [10]. The VPM skins are ordinarily permeable to gas, but they become impermeable when subjected to large compressions.

The varying-permeability model has provided accurate quantitative descriptions of several bubble-counting experiments carried out using supersaturated gelatin as the medium [5-7]. The model has also been used to trace levels of incidence for decompression sickness in a variety of animal species, including fingerling salmon, rats, and humans [11,12]. Recently, microscopic evidence has been obtained [13-15] which indicates that spherical gas nuclei--the persistent microbubbles hypothesized by the varying-permeability model--actually do exist and have physical properties consistent with those previously attributed to them [5-7,10]. Nuclear radii, for example, are found to be on the order of one micron or less, and their number density decreases exponentially with increasing radius [5-7,10]. This exponential radial distribution is believed to be a signature of VPM nuclei in thermodynamic equilibrium, and it has been derived from statistical-mechanical considerations [16].

The latest step in the application of the varying-permeability model to decompression sickness has been to calculate comprehensive sets of air and helium diving tables and to compare them with other tables now in use. No claim is made for the validity of the diving schedules listed herein, particularly the VPM schedules, which have never been directly tested using human subjects.

A promising feature of this new approach is that it provides sensible prescriptions for a wide range of diving situations, yet it employs only a few constant parameters and is easily implemented. While many of the VPM schedules described herein were calculated on a DEC VAX-11/780 minicomputer, the program has been expressly designed for microcomputer operation, and the original FORTRAN program has been rewritten using simple BASIC instructions. However, for a BASIC interpreter the execution time required to complete a single decompression schedule may vary from several minutes to several hours, and compilation is recommended. In general, longer schedules require more processor time.

B. THE VARYING-PERMEABILITY MODEL

Experimental evidence suggests that bubble formation in aqueous media is initiated from preexisting gas nuclei. Ordinary samples of sea water, tap water, or even distilled water form visible bubbles when subjected to supersaturation pressures as small as one atmosphere. This is three orders of magnitude below the theoretical breaking strength of pure water and implies that cavitation must be initiated by something other than modest changes in pressure and the random motions of molecules [21,22]. Several experiments have demonstrated that cavitation thresholds can be raised by degassing the sample or by subjecting it to a preliminary application of static pressure [23,24]. These are specific tests for stable gas-filled nuclei. It is surprising that such nuclei exist, since small bubbles (of radius less than one micrometer) should rapidly dissolve under the effect of surface tension,

while larger ones should float. Several mechanisms for the stabilization of gas nuclei have been proposed and subsequently dismissed [25], but the one presented here, the varying-permeability model, remains viable.

According to the VP model, bubble formation nuclei are gas cavities embedded in aqueous media and surrounded and stabilized by skins of surfactant molecules [10]. The model does not track continuous changes in the nuclear permeability, but instead assumes that the skins are either permeable or impermeable to gas transfer. More precisely, skins become impermeable only when subjected to large compressions, typically exceeding eight atmospheres. For smaller compressions and during all decompressions, they are assumed to remain permeable. Since the equations describing the two regimes are somewhat different, a smooth transition must be made between them as the maximum compression passes through the changeover point. The experimentally-determined pressure differential of 8.2 atmospheres [10] has been designated as that point and is one of the model constants. Thus, most of the VPM tables (excursions shallower than 270 fsw) have been calculated using the equations describing the permeable regime. The deepest tables require some use of the impermeable equations but are a modest theoretical extension of their shallower counterparts.

The derivations of the original VPM equations have been previously published [7,10,25], and several of those results will be presented here without proof. It will remain, then, to derive from this basis the final equation for the allowed supersaturation as required by the decompression program. In the following section, we obtain a

preliminary relationship between the model equations and the allowed tissue supersaturation. In Chapter II, several equations which supplement the decompression criterion are developed: the allowed supersaturation is augmented by the dynamic critical-volume hypothesis, a perfusion-limited equation is used to describe the exponential uptake and elimination of gas by the controlling tissue, and the regeneration of crushed nuclei is considered.

C. THE MODEL EQUATIONS

During a rapid compression from an initial ambient pressure P_o to some increased pressure P_m (Fig. 1), each included bubble nucleus is subjected to a "crushing" effect which decreases its radial size. This results in an increased tolerance to supersaturation since smaller nuclei will form macroscopic bubbles less readily than larger ones. The greater the crushing pressure P_{crush}, the greater the supersaturation required to form a given number of harmful bubbles. There is another way to characterize the data: for any pressure schedule, all nuclei which are initially larger than some "critical" radius r_o will grow to form macroscopic bubbles, while the rest will not.

The first of the varying-permeability model equations relates the crushing pressure P_{crush} to the corresponding change in the critical radius from r_o to r_m. At the onset of decompression, r_m characterizes the smallest nucleus which will produce a macroscopic bubble, just as r_o did prior to crushing. For the permeable compression from P_o to P_m, we have [10]

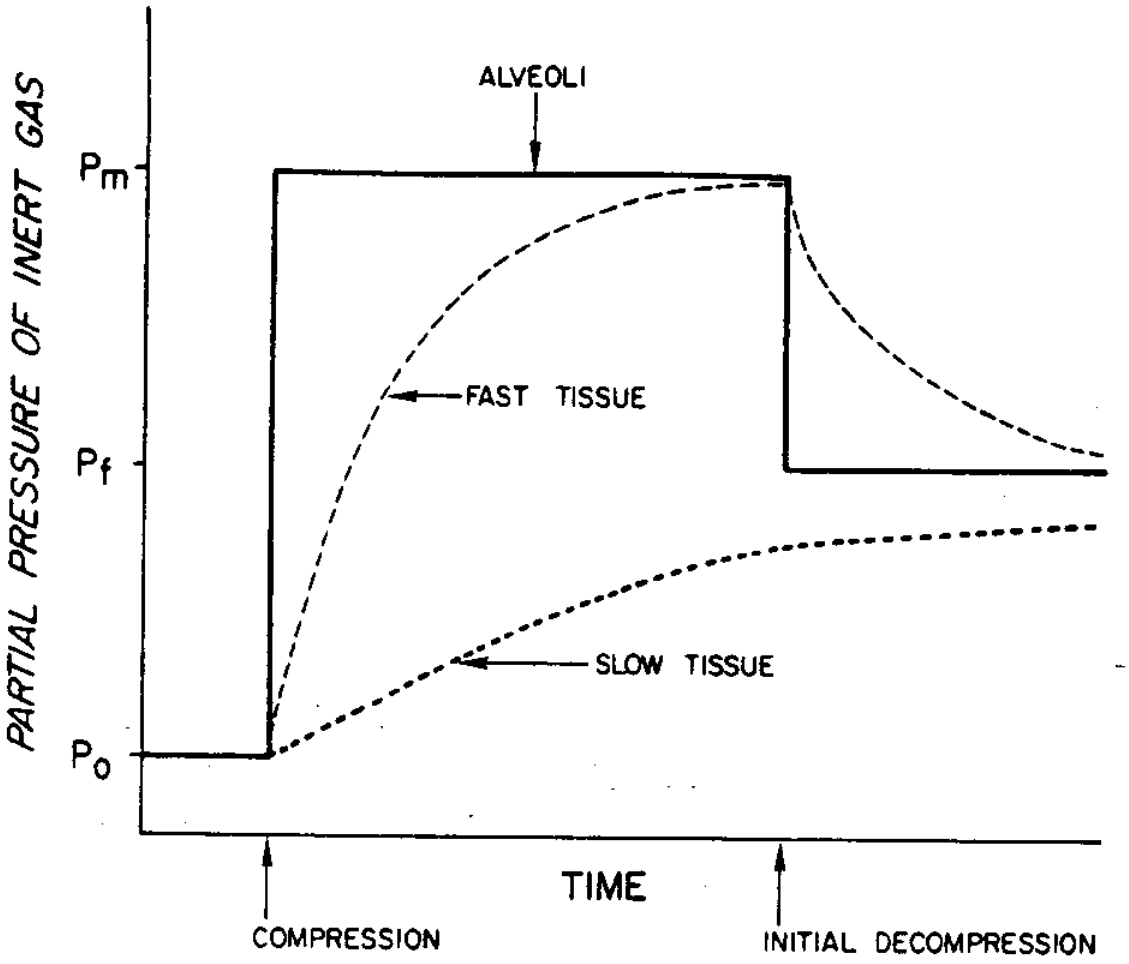

Fig. 1 - Response of fast and slow tissues exposed to a rectangular pressure schedule consisting of a rapid compression from an initial pressure P_o to some maximum pressure P_m and a rapid decompression to an intermediate pressure P_f.

$$P_{crush} = P_m - P_o = 2(\gamma_C - \gamma)(1/r_m - 1/r_o) \quad , \tag{1.1}$$

where γ is the surface tension and γ_c is the "crumbling" or maximum compressional strength of the surfactant skin. When P_m exceeds the changeover point P^* (9.2 atm abs), the equation appropriate to the impermeable region must be used, and for the impermeable compression from P^* to P_m, we have [10]

$$P^*_{crush} = P_m - P^* = 2(\gamma_C - \gamma)(1/r_m - 1/r^*) + P^* + 2P_o + P_o(r^*/r_m)^3, \tag{1.2}$$

where

$$r^* = [(P^*-P_o)/2(\gamma_C-\gamma) + 1/r_o]^{-1} \tag{1.3}$$

is the radius of the critical nucleus at the onset of impermeability, found by replacing P_m and r_m with P^* and r^* in Eq. (1.1).

The allowed supersaturation is given by [7]

$$P_{ss} = P_m - P_f = 2(\gamma/\gamma_C)(\gamma_C - \gamma)/r_m \quad , \tag{1.4}$$

which can be solved by rearranging Eqs. (1.1) and (1.2) to obtain values for r_m. The result is

$$r_m = [P_{crush}/2(\gamma_C-\gamma) + 1/r_o]^{-1} \tag{1.5}$$

for the permeable regime, while for the impermeable regime one must solve the cubic equation,

$$r_m^3 - 2(\gamma_C-\gamma)r_m^2 - (P_o/c)r^{*3} = 0 \tag{1.6}$$

with

$$c = P^*_{crush} - P^* + 2P_o + 2(\gamma_C-\gamma)/r^* \quad . \tag{1.7}$$

The solution is found in standard mathematical tables:

$$p = -2(\gamma_c - \gamma)/c \quad , \tag{1.8}$$

$$q = -P_o r^{*3}/c \quad , \tag{1.9}$$

$$a = -p^2/3 \quad , \tag{1.10}$$

$$b = (2/27)p^3 + q \quad , \tag{1.11}$$

$$A = [-b/2 + (b^2/4 + a^3/27)^{1/2}]^{1/3} \quad , \tag{1.12}$$

$$B = [-b/2 - (b^2/4 + a^3/27)^{1/2}]^{1/3} \quad , \tag{1.13}$$

$$r_m = A + B - p/3 \quad . \tag{1.14}$$

The cubic equation has two additional roots, but it can be shown that they are always negative or imaginary, given realistic values for the model parameters. To attempt a more explicit solution for r_m is impractical, thus the above equations have been inserted directly into the computer program.

It has been shown that the allowed supersaturation can be found for any rectangular pressure schedule by specifying only three parameters: γ, γ_c, and r_o. In addition, it is a feature of the model that the supersaturation is dependent only upon the ratios γ/γ_c and γ/r_o. Thus there is some flexibility afforded in selecting absolute values for γ, γ_c, and r_o. Also, by specifying the given ratios instead, the number of free parameters can be reduced from three to two. As will be shown, the critical-volume hypothesis and nuclear regeneration require one free parameter each, for a total of four.

CHAPTER II

A. THE CRITICAL-VOLUME HYPOTHESIS

In previous applications of the varying-permeability model [11,12], the number of macroscopic bubbles evolved during decompression was used to quantify decompression stress. Schedules which produced the same number of bubbles were assumed to cause the same decompression liability. This method worked remarkably well for rudimentary schedules and outcomes, such as pressure excursion limits and injury versus no-injury situations. The first VPM tables (unpublished) were thus based on the assumption that the body could accommodate a certain number of bubbles. The bubble number was equal to the number of nuclei initially present with radii larger than some critical radius r_o, and the allowed supersaturation was calculated using Eq. (1.4). This method generated schedules th were quite reasonable for lengthy dives but failed in the case of sho r dives, where it required excessive decompression times. In particular, satisfactory no-stop limits could not be produced concurrently with saturation dive schedules using the same nucleation parameters. The no-stops were "too safe" because the bubble number was being limited by the saturation dives.

It is known that tables currently in use often allow many bubbles to form during decompression. These can be detected by Doppler monitoring [26]. Apparently, the body can support some bubbles without outward signs of decompression stress. Of course, the long-term effects of repeated exposure to such bubble formation remain undefined and, perhaps, unsuspected. Among the many possible scenarios are an

increased incidence of osteonecrosis and "punch-drunk" behavior in divers, attributable to the chronic random destruction of cells in brain and bone. The incidence of macroscopic bubble formation in human blood or tissue can no longer be ignored in the creation of decompression tables: merely avoiding the bends may not guarantee diver safety.

The "primary" bubbles formed directly from nuclei may lead to "secondary" bubbles via fission [27] in blood or by the creation of "rosaries" in the interstitial spaces of the firmer tissues [28]. Since tissue deformation and impairment of circulation should depend upon both the size and the number of bubbles, it seems plausible that the total volume of evolved gas would serve as an effective criterion [29]. This would permit the formation of many small bubbles or of very few large ones. The "constant-bubble-number" hypothesis has thus been replaced by the "critical-volume" hypothesis and the number of bubbles has been allowed to fluctuate accordingly. For shorter total decompression times, bubble nuclei have little time during which to inflate. The permissible critical radius is then smaller and the allowed supersaturation larger, resulting in many small bubbles. Conversely, during long decompressions, bubbles may grow very large, so only a few are permitted. Because the number density and size distribution of nuclei *in vivo* are unknown, the table calculations are based upon an iterative procedure which does not explicitly determine the number of bubbles or the volume of released gas.

The original safe-ascent criterion was based on Eq. (1.4) and gave lines of constant bubble number (Fig. 2) [6] which were associated with lines of constant decompression stress. Our latest revision alters that

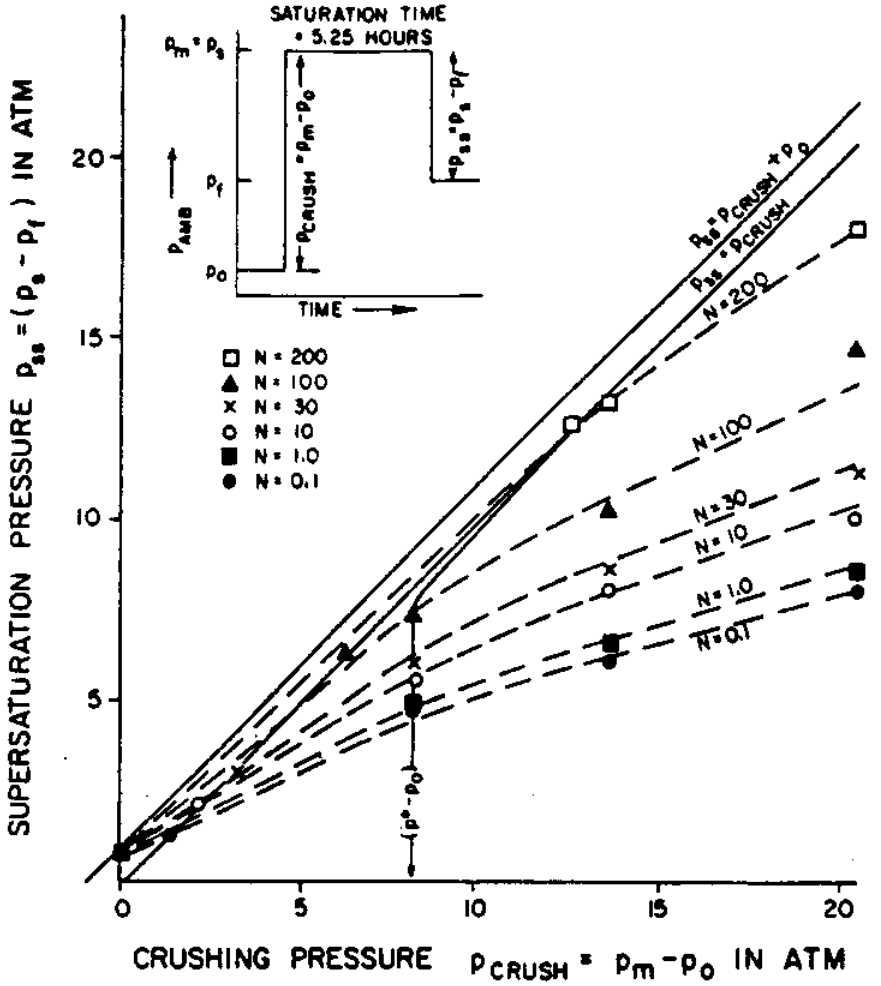

Fig. 2 - Plot of supersaturation versus crushing pressure for various lines of constant bubble number. The sudden decrease in slope at P_{crush} = 8.2 atm indicates the onset of impermeability.

criterion by augmenting the allowed supersaturation. This is accomplished by permitting the gas phase to inflate during decompression, under the constraint that the total volume of free gas never exceeds some critical value V_C. The rate at which the gas phase inflates is assumed to be proportional both to the number of bubbles in excess of the safe-ascent criterion and to the new supersaturation,

$$P_{ss}^{new}(t)(N_{new} - N_{safe}) = \chi \dot{V} \quad , \tag{2.1}$$

where χ is the constant of proportionality. The total volume of released gas must remain below V_C and can be found by integrating Eq. (2.1),

$$\int_o^t P_{ss}^{new}(t)(N_{new} - N_{safe})dt = \chi V_C \ . \tag{2.2}$$

In this case, the integral must reach its maximum value at time t_C so as not to exceed the volume V_C. Since the bubble numbers are constant after the first decompression step, they are independent of time. The new decompression criterion is then

$$(N_{new} - N_{safe}) \int_o^{t_C} P_{ss}^{new}(t)\, dt = \chi V_C \ . \tag{2.3}$$

Adopting a form for P_{ss}^{new} which is positive definite and letting the time t_C go to infinity is one way to guarantee that the integral is maximized. It is therefore assumed that P_{ss}^{new} remains constant during the decompression time t_D and decays exponentially thereafter. In practice, the supersaturation will eventually become slightly negative, since humans equilibrated at atmospheric pressure are inherently unsaturated by some 54 mm Hg [30]. Unfortunately, the time at which the integral would reach its maximum under those conditions is unknown. The

assumed form of P_{ss}^{new} is conservative, since the true value will be a little lower, and the net volume of free gas will be somewhat less than V_C. The integral and its solution are

$$(N_{new} - N_{safe})\{\int_o^{t_D} P_{ss}^{new}\, dt + \int_{t_D}^{\infty} P_{ss}^{new} \exp[(t_D-t)/H^*]dt\} ,$$

$$= (N_{new} - N_{safe})\, P_{ss}^{new}\, (t_D + H^*) = \chi V_C , \qquad (2$$

where P_{ss}^{new} is now a constant, $H^* = H/\ln 2$ is the exponential time constant, and H is the half-time of the controlling tissue.

The new supersaturation criterion is thus

$$P_{ss}^{new} = \chi V_C \,/\, (N_{new} - N_{safe})(t_D + H^*) \quad . \qquad (2.5)$$

The radial distribution of bubble nuclei has been found to follow a decaying exponential function (Fig. 3) [15] in several *in vitro* studies [5-7,10,13-15], and it is reasonable to assume that a similar distribution exists *in vivo*. The number of bubbles formed is [

$$N_{safe} = N_o \exp(-\beta_o S r_o / 2kT) \qquad (2.6)$$

for the original safe-ascent criterion and

$$N_{new} = N_o \exp(-\beta_o S r_o^{new} / 2kT) \qquad (2.7)$$

for the new augmented supersaturation, where N_o is a normalization constant, $\beta_o = 2(\gamma_C - \gamma)/r_o$ is determined from the model parameters, S is the effective surface area of one surfactant skin molecule *in situ*, r_o^{new} is the size of the smallest nucleus that contributes to the new bubble number, k is the Boltzmann constant, and T is the absolute body

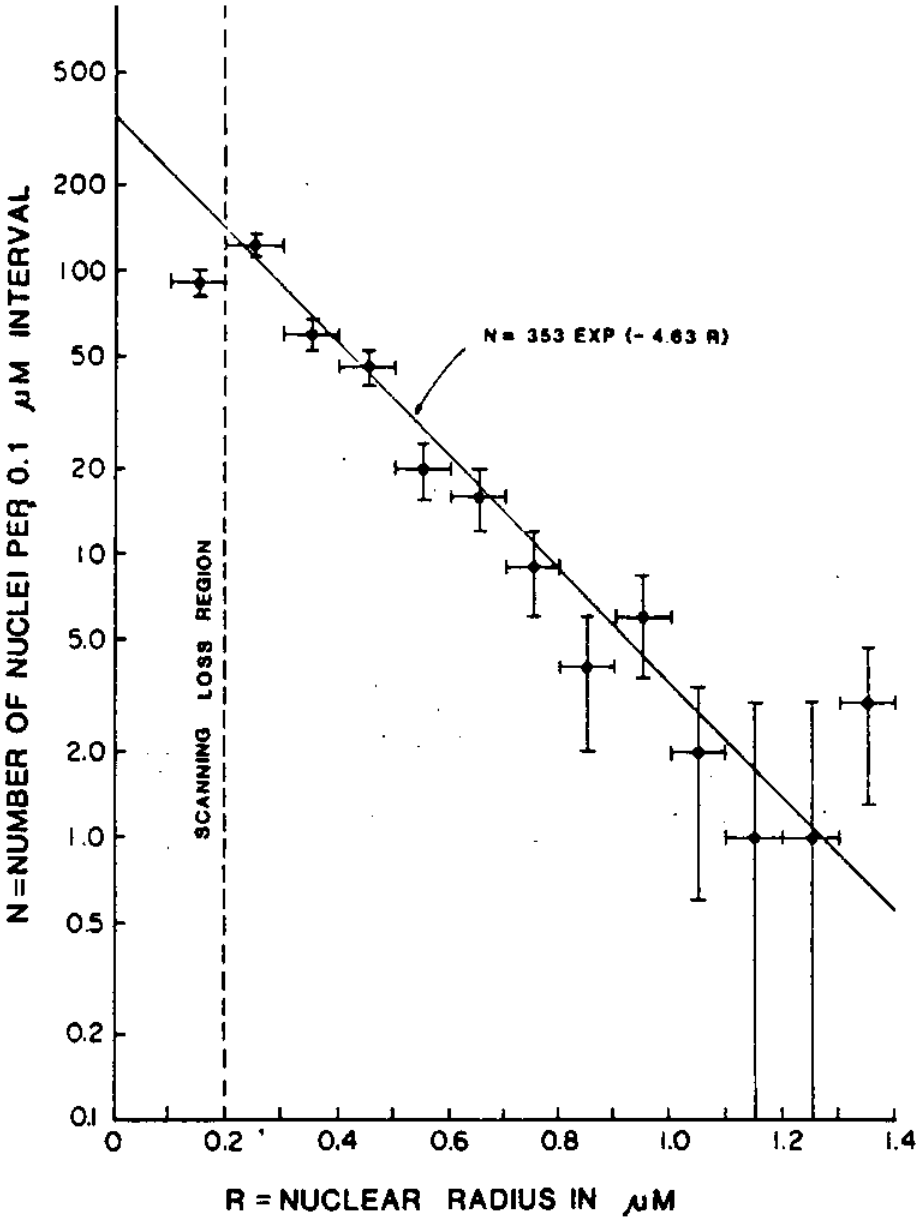

Fig. 3 - Differential radial distribution of gas cavitation nuclei in agarose gelatin. Above 0.2 μm, the points can be described by a decaying exponential. Below 0.2 μm, the microscope scanning efficiency deteriorates rapidly, and data in this region should be disregarded.

temperature. The difference in the bubble numbers can then be written

$$N_{new} - N_{safe} = N_o[\exp(-\beta_o Sr_o^{new}/2kT) - \exp(-\beta_o Sr_o/2kT)]. \quad (2.8)$$

If the exponential arguments are small, this simplifies to

$$N_{new} - N_{safe} \simeq N_o(\beta_o Sr_o^{new}/2kT)(1 - r_o^{new}/r_o) . \quad (2.9)$$

The last approximation is questionable, since the values of the model parameters are neither fixed nor known. If the approximation is not valid, the bubble numbers would simply correspond to a linear nuclear size distribution rather than the linear (small exponent) regime of an exponential distribution.

Eqs. (1.4) and (1.5) can be combined to give

$$P_{ss}^{safe} = 2\gamma(\gamma_C - \gamma)/\gamma_C r_o + (\gamma/\gamma_C)P_{crush} \quad (2.10)$$

and

$$P_{ss}^{new} = 2\gamma(\gamma_C - \gamma)/\gamma_C r_o^{new} + (\gamma/\gamma_C)P_{crush} . \quad (2.11)$$

Although Eq. (1.5) applies strictly only to the permeable regime, it varies little (less than 3%) when compared to the impermeable cubic equation at the maximum P_{crush} (largest deviation) encountered. It is therefore reasonable to use Eqs. (2.10) and (2.11) to simplify Eq. (2.9). The corresponding radii are

$$r_o = 2\gamma(\gamma_C - \gamma)/\{\gamma_C[P_{ss}^{safe} - P_{crush}(\gamma/\gamma_C)]\} \quad (2.12)$$

and

$$r_o^{new} = 2\gamma(\gamma_C - \gamma)/\{\gamma_C[P_{ss}^{new} - P_{crush}(\gamma/\gamma_C)]\} . \quad (2.13)$$

Inserting these results into Eq. (2.9), we obtain

$$N_{new} - N_{safe} \simeq \frac{[\beta_o N_o S r_o / 2kT](P_{ss}^{new} - P_{ss}^{safe})}{P_{ss}^{new} - (\gamma/\gamma_C)P_{crush}} \ . \tag{2.14}$$

The new supersaturation given by Eq. (2.5) is

$$P_{ss}^{new} \simeq \frac{2\chi V_C kT\,[P_{ss}^{new} - (\gamma/\gamma_C)P_{crush}]}{N_o \beta_o S r_o (t_D + H^*)(P_{ss}^{new} - P_{ss}^{safe})} \ , \tag{2.15}$$

which can be expressed in the standard quadratic form

$$(P_{ss}^{new})^2 - b(P_{ss}^{new}) + c = 0 \ , \tag{2.16}$$

where

$$b = P_{ss}^{safe} + \alpha/(t_D + H^*) \ , \tag{2.17}$$

$$c = (\gamma/\gamma_C)P_{crush}[\alpha/(t_D + H^*)] \ , \tag{2.18}$$

and

$$\alpha = 2\chi V_C kT/N_o \beta_o S r_o = \chi V_C kT/N_o(\gamma_C - \gamma)S \ . \tag{2.19}$$

Quantities such as χ, S, V_C, N_o, N_{new}, and N_{safe} are, of course, absorbed into the third free parameter α and are never explicitly determined. The solution for the new allowed supersaturation is

$$P_{ss}^{new} = [b + (b^2 - 4c)^{1/2}]/2 \ , \tag{2.20}$$

which has been inserted directly into the computer program. However, since t_D depends on P_{ss}^{new}, Eq. (2.20) must be iterated to convergence, evident when two successive calculations give virtually the same total decompression time t_D.

B. TISSUE TENSION

The allowed tissue supersaturation provided by Eq. (2.20) must be converted to an allowed depth before a decompression step can be made. So long as the difference between the tissue tension τ and the ambient pressure P_{amb} does not exceed that allowed supersaturation, the critical volume of free gas will not be exceeded. The constraining relationship is therefore

$$\tau(t) - P_{amb}(t) \leq P_{ss}^{new} \quad , \tag{2.21}$$

where the equals sign is adopted to minimize the total decompression time. If the time scale for equilibration of the body with the breathing gas is short compared to the rate of change of depth, the ambient pressure will correspond to the current depth of sea water. The ascent criterion is then

$$D_a(t) = \tau(t) - P_{ss}^{new} \quad , \tag{2.22}$$

in which D_a is the allowed depth. Once the tissue tension is known as a function of time, Eq. (2.22) will provide the exact depth requirements. However, since ascents are normally made in stages rather than continuously, the computer program adjusts D_a in even increments (of 10 fsw) and solves for the elapsed time instead.

The tissue tension calculation is based upon a perfusion-limited rate equation [31],

$$\frac{d\tau(t)}{dt} = k[P_a(t) - \tau(t)] \quad , \tag{2.23}$$

where $k = (\ln 2)/H$ and H is the tissue half-time. The partial pressure

P_a of a single inert gas in the breathing mixture is assumed to be proportional to the ambient pressure P_{amb}, where F is the constant of proportionality. The fraction of nitrogen is fixed at F = 0.79 in all the air-table calculations. Oxygen, carbon dioxide, and water vapor will be taken into account shortly. The rate equation is then

$$\frac{d\tau(t)}{dt} = k[FP_{amb} - \tau(t)]$$

or

$$\frac{d\tau(t)}{dt} + k\,\tau(t) = kFP_{amb} \quad . \tag{2.24}$$

The homogeneous solution to Eq. (2.24) is of the form

$$\tau(t) = Ae^{-kt} \quad . \tag{2.25}$$

The change in the total ambient pressure during any linear (constant velocity) depth excursion from an initial pressure P_o is given by

$$P_{amb} = P_o + vt \quad , \tag{2.26}$$

where v has the units of fsw/min and t is the duration of the excursion in minutes. Inserting Eq. (2.26) into Eq. (2.24), we find that the particular solution to the rate equation is

$$\tau(t) = F(P_o + vt - v/k) \quad . \tag{2.27}$$

The complete solution is the sum of the homogeneous and particular solutions, or

$$\tau(t) = Ae^{-kt} + F(P_o + vt - v/k) \quad . \tag{2.28}$$

To evaluate the constant A, we assume that the excursion begins at time $t = 0$ and at depth $P_{amb} = P_o$. This yields

$$\tau(0) = A + F(P_o - v/k)$$

or

$$A = \tau(0) - F(P_o - v/k) \quad . \tag{2.29}$$

Using the above equations, we may insert any arbitrary starting depth P_o with its corresponding tissue tension $\tau(0)$ and calculate the tissue tension as a function of time, even if there is no excursion (constant depth). To describe the various bodily tissue types, fixed half-times for some fifteen tissue compartments have been included (Fig. 1), ranging (for nitrogen) from one minute to twelve hours [31,32,41,51-55]. They are intended to span the full range of diving experience, from no-stop decompressions to saturation dives. Of these tissue half-times, one will be found to yield the greatest tension via Eq. (2.28) and is thus said to be "controlling" the ascent through Eq. (2.22). The half-times of the controlling tissues tend toward larger values as the elapsed decompression time increases.

Oxygen, carbon dioxide, and water vapor have been treated as a group labeled "active" gases. The details of their treatment have already been published [30], so only a brief statement is presented here. The contribution of the active gases to the inert gas tension can be found by subtracting the "oxygen window" (Fig. 4) from the inspired oxygen pressure. The oxygen window calculation is based upon the

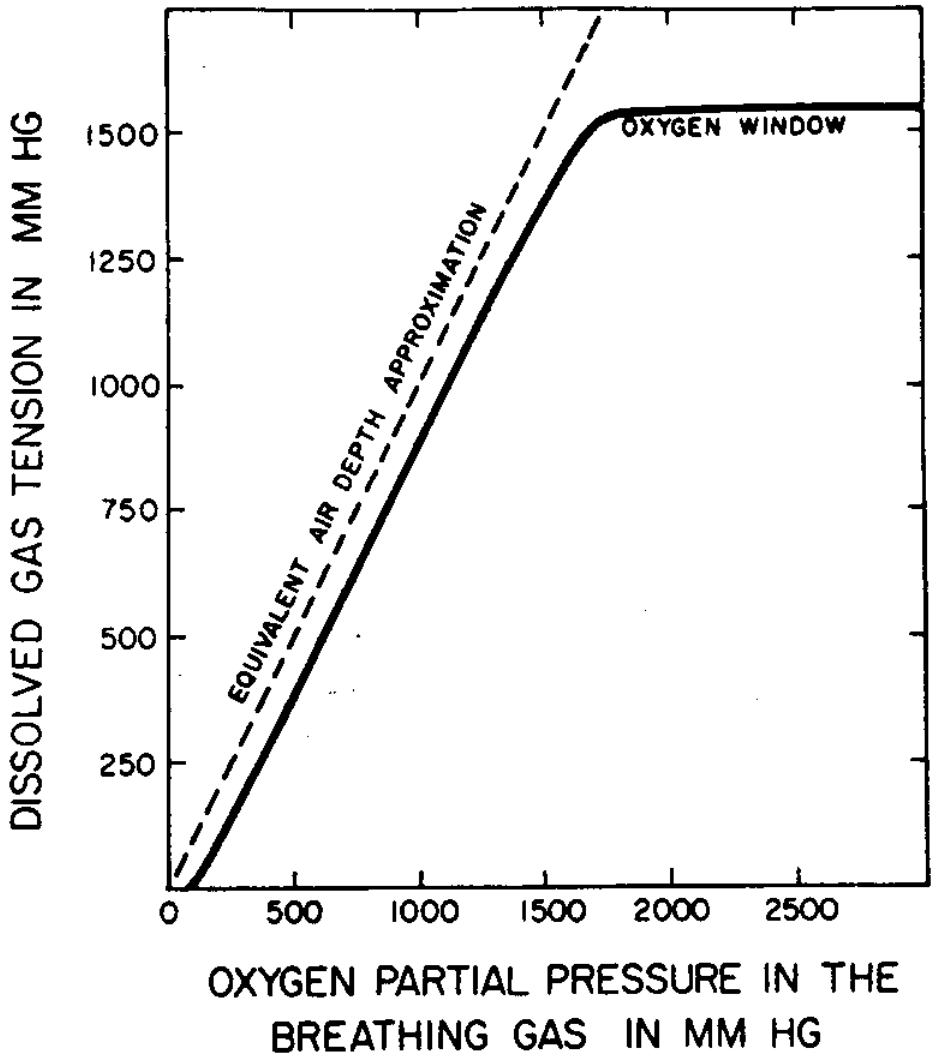

Fig. 4 - Plot of dissolved gas tension versus oxygen partial pressure. The equivalent-air-depth approximation is useful for oxygen partial pressures below 1500 mm Hg.

inhalation of "dry" air containing no carbon dioxide, using the normal values of 47 mm Hg for water vapor pressure and 40 mm Hg for the arterial carbon dioxide pressure. A remarkable fact is that the result of the subtraction is very nearly constant at 102 mm Hg until the oxygen partial pressure reaches about 1500 mm Hg. The active-gas contribution to the inert gas tension has therefore been set at 4.43 fsw (102 mm Hg) for O_2 pressures below 1500 mm Hg, and at 4.43 fsw plus the excess oxygen partial pressure (inspired pressure less 1500 mm Hg) for higher O_2 pressures. For O_2 partial pressures above 360 mm Hg, care must be exercised to guard against oxygen toxicity.

C. NUCLEAR REGENERATION

As illustrated in Fig. 2 [6], samples of knox gelatin display increased resistance to bubble formation following the rapid application of a crushing pressure [5-7]. The same effect occurs <u>in vivo</u>, as can be seen in Figs. 5 [11] and 6 [30]. The larger the exposure pressure, the fewer the bubbles that form with the same allowed supersaturation during decompression. The varying-permeability model dictates that bubble nuclei are "crushed" by the mechanical strength of the initial compression and that the number of nuclei larger than the critical radius decreases. Surfactant molecules are forced out of the nuclear skin into solution, perhaps into a "reservoir" just outside, where they remain available to retake their old positions.

The equilibrium exponential radial distribution of bubble nuclei has been derived from statistical-mechanical considerations, and it has been shown theoretically that a nuclear population, once crushed, is

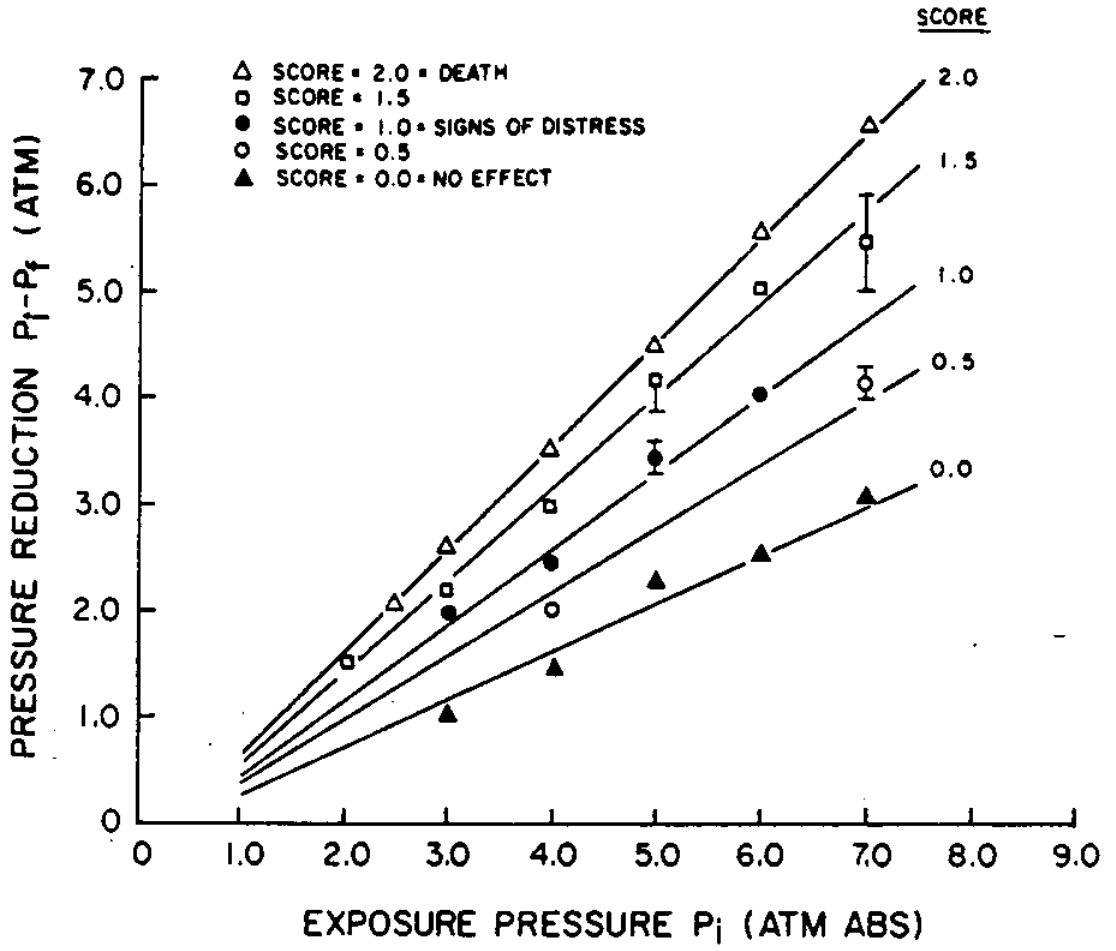

Fig. 5 - Limits of pressure reduction versus exposure pressure for fingerling salmon. The respective VPM predictions are straight lines.

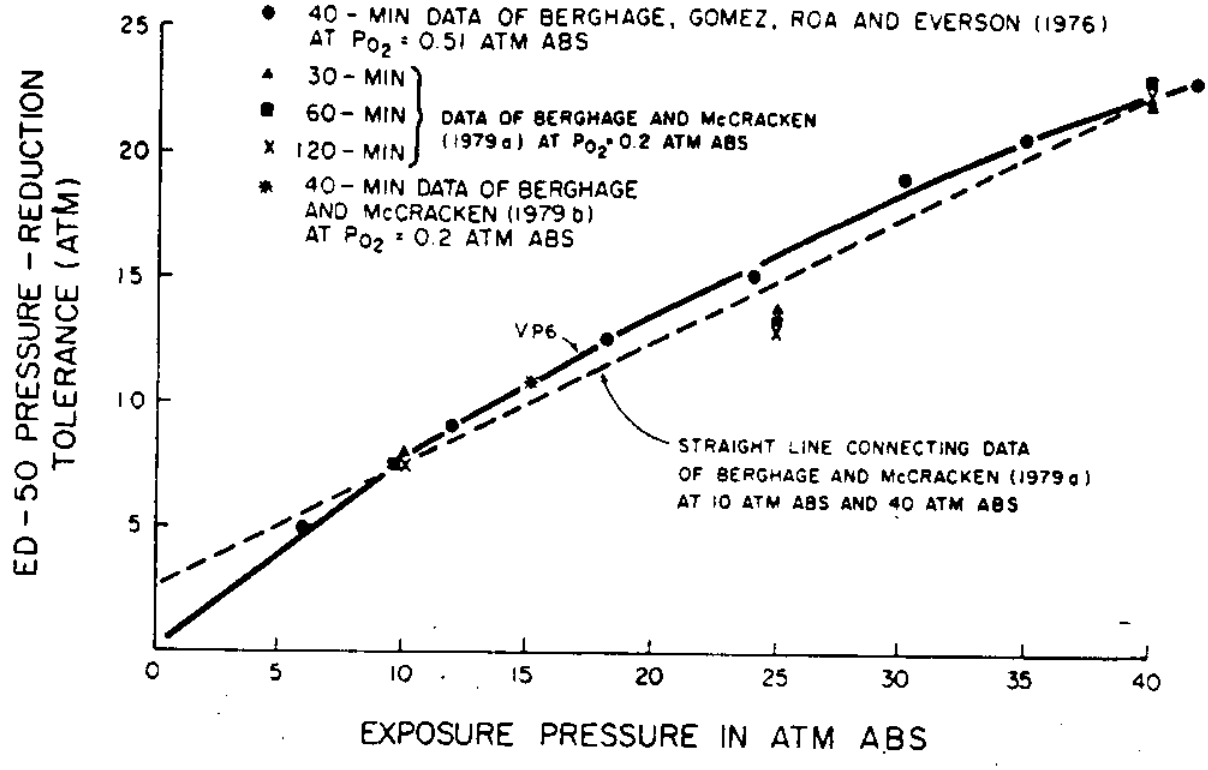

Fig. 6 - Compilation of pressure-reduction tolerances versus exposure pressure for albino rats. ED-50 is the pressure reduction needed to produce decompression sickness in 50% of the animals. The solid curve summarizes the VPM predictions. Note that pressure-reduction tolerance increases significantly with exposure pressure.

capable of stochastically restoring that distribution [16]. The time constant for such "nuclear regeneration" is assumed to be comparatively long, ranging from several hours to days or weeks. One implication is that divers might become "acclimated" by diving regularly and depleting the nuclear population, only to contract the bends when returning after a leave of absence, since this population has regenerated and decreased their decompression tolerance. Another situation is that of lengthy saturation dives, such as the Tektite 14-day exposure at 100 fsw. Any beneficial effect provided by crushing may have been "forgotten" prior to returning to the surface. In order to accommodate the phenomenon of nuclear regeneration, the computer program has been designed to track nuclear growth continuously following the initial compression. This is accomplished by allowing the minimum nuclear radius r_m to evolve gradually back into the original critical radius r_o. The time-dependence is approximated by the exponential relation

$$r_m(t) = r_m(0) + \{1 - \exp(-t/\tau_r)\} [\, r_o - r_m(0) \,] \quad . \qquad (2.30)$$

The time constant τ_r is the fourth and last of the free parameters used to calculate the VPM tables. It may be argued that some of the model constants, such as the impermeability threshold or the tissue compartment half-times, have been arbitrarily selected and therefore should have been included in our list. However, each of those constants was presumably fixed prior to the application of the model to the construction of diving tables, whereas the four variable parameters were optimized to "tune" the output to the body of available data on safe ascents. No variable or constant (other than the excursion profiles)

needs to be added or changed to calculate any of the literally thousands of VPM air and helium schedules represented in this work, or any new schedule within the same range. It is the physical model which facilitates our table calculations, not the inclusion of "hidden" parameters, and it is a notable feature of the nucleation approach—evident already in this naive formulation—that the usual proliferation of free pa meters (e.g., M-values) can be avoided.

Very little has bee said about the physiological processes which presumably underlie the mathematical equations in this chapter. Obviously, oxygen and carbon dioxide were taken into account, and typical ranges for the tissue half-times were assumed. However, no distinction was made between "fatty, loose tissue" and "watery, tight tissue" [29], nor was it explicitly stated where the bubbles form or how they grow, multiply, or are transported. Finally, nothing was said about such factors as solubility, diffusion versus perfusion, tissue deformation pressure, or tissue-specific differences in surface tension. Since all of the omitted items are not well understood, at least <u>in vivo</u>, the main effect of attempting to take any of them into account would be to increase the number of free parameters. For example, this number could be doubled simply by assuming a different set of nucleation parameter values for aqueous and lipid constituents.

CHAPTER III

A. ADJUSTING THE FREE PARAMETERS FOR AIR DIVES

The application of the equations in Chapters I and II to the problem of decompression sickness requires more than just a computer program. The absolute values of the four adjustable parameters are unknown, yet they determine the nature and safety of the program output. Indeed, the resultant tables can be "tuned" from overly-safe, excessively-long decompressions to short, lethal ascents. How, then, does one calibrate the free parameters?

The answer lies in the fact that, once adjusted, the parameters remain fixed throughout the whole range of table calculations. This allows a two-dimensional global decompression map of ascent times versus bottom times for constant depths to be calculated and superimposed upon similar lines of constant depth for existing tables. The total ascent times are used because the VPM decompression profiles vary systematically from their USN and RNPL counterparts, as will be discussed later in this chapter.

In principle, only four separate points (not all on one line) would be sufficient to completely specify the shape and position of the entire map. However, the ascent times for equivalent exposures may vary by as much as a factor of two between sets of tables created by different authors. Given the possibility of large errors, the use of only four points might have disastrous results. For that reason, we have chosen to try to match the entire range of decompression data. The uncertainty associated with the data points precludes the straightforward

application of a least-squares analysis, but a "reasonable" fit can be obtained by matching those points thought to be the safest and ignoring those which are known to have produced many bubbles or bends. In general, our approach has been conservative, and it emphasizes safety rather than speed.

After the final program adjustment, our first free parameter, the ratio γ/γ_c, was found to be equal to 0.697. To incorporate Hills' estimation of the surface tension for lipids in fatty and aqueous tissues in vivo [33], we have arbitrarily set γ equal to 17.9 dyn/cm, resulting in a value of 256.9 dyn/cm for γ_c. The second parameter, γ/r_o, was found to be 2.238×10^5 dyn/cm, corresponding to 0.80 μm for r_o. In preliminary calculations, the variable λ was used to quantify the supersaturation augmentation. The final derivation uses the parameter α, which is related to λ by the equation $\alpha = (\gamma/\gamma_c)\lambda$. The adjusted values of α and λ are 523 fsw-min and 7500 fsw-min, respectively. Finally, the last parameter τ_r was set at two weeks (20160 min) to allow for some regeneration during saturation dives. However, the time required for regeneration may vary widely between physically-different systems and is the subject of current research.

Once the above parameters were determined, a complete set of air decompression tables was generated using the FORTRAN computer program in Appendix 1. The only input required was the depth and bottom time for each excursion. Further modification of the four free parameters (for air dives) should not be necessary unless a particular range of diving schedules is found to be unreasonable or new physiological data becomes available.

B. A COMPARISON OF THE VPM, USN, AND RNPL NO-STOP LIMITS FOR AIR DIVES

One of the reasons for augmenting the allowed supersaturation was to accommodate those no-stop decompression limits which were thought to be safe, while keeping the same free-parameter values used for all the other air schedules. As given by Eqs. (2.16-2.20), the augmentation is larger for those dives with smaller total decompression times and therefore is the largest for the no-stop decompressions. The resultant VPM no-stop limits are listed in Table 1, along with similar data from the USN [19] and RNPL [20] air tables.

Even though some bubble formation has been permitted, the actual volume of released gas is expected to be smaller for the more restrictive VPM limits than for their USN counterparts. The VPM and RNPL predictions match almost exactly, which is quite reassuring since the VPM no-stop limits were not calculated until after the final adjustment of the four free parameters. In other words, the RNPL no-stops were duplicated in the VPM calculations simply by requiring that the staged decompressions be "reasonable." This is not surprising since the smooth VPM curves should tie together the no-stops and the staged decompressions. In none of our various free-parameter adjustments were we able to match the USN no-stops while maintaining what were considered to be safe staged decompressions. This is, in fact, the reason why our no-stop limits were not determined until after the parameters were set.

The data contained in Table 1 are plotted in Fig. 7, along with various "practical observations" compiled by Leitch and Barnard [34]. Although there are some differences in the rates of descent and ascent

TABLE 1

COMPARING THE NO-DECOMPRESSION LIMITS OF
THE VPM, RNPL, AND USN AIR TABLES

ALLOWED DEPTH (FSW)	SOURCE TABLE TYPE	ALLOWED TIME (MIN)	ALLOWED DEPTH (FSW)	SOURCE TABLE TYPE	ALLOWED TIME (MIN)
30	VPM	323	140	VPM	8
	RNPL	UNLIMITED		RNPL	7.5
	USN	UNLIMITED		USN	10
40	VPM	108	150	VPM	7
	RNPL	102		RNPL	NOT LISTED
	USN	200		USN	5
50	VPM	63	160	VPM	7
	RNPL	60		RNPL	5.5
	USN	100		USN	5
60	VPM	39	170	VPM	6
	RNPL	41		RNPL	NOT LISTED
	USN	60		USN	5
70	VPM	30	180	VPM	5
	RNPL	30		RNPL	4.5
	USN	50		USN	5
80	VPM	23	190	VPM	5
	RNPL	23		RNPL	NOT LISTED
	USN	40		USN	5
90	VPM	18	200	VPM	4
	RNPL	18		RNPL	3.5
	USN	30		USN	NOT ALLOWED
100	VPM	15	210	VPM	4
	RNPL	15		RNPL	NOT LISTED
	USN	25		USN	NOT ALLOWED
110	VPM	12	220	VPM	4
	RNPL	NOT LISTED		RNPL	3
	USN	20		USN	NOT ALLOWED
120	VPM	11	230	VPM	4
	RNPL	10		RNPL	NOT LISTED
	USN	15		USN	NOT ALLOWED
130	VPM	10	240	VPM	NOT ALLOWED
	RNPL	NOT LISTED		RNPL	NOT ALLOWED
	USN	10		USN	NOT ALLOWED

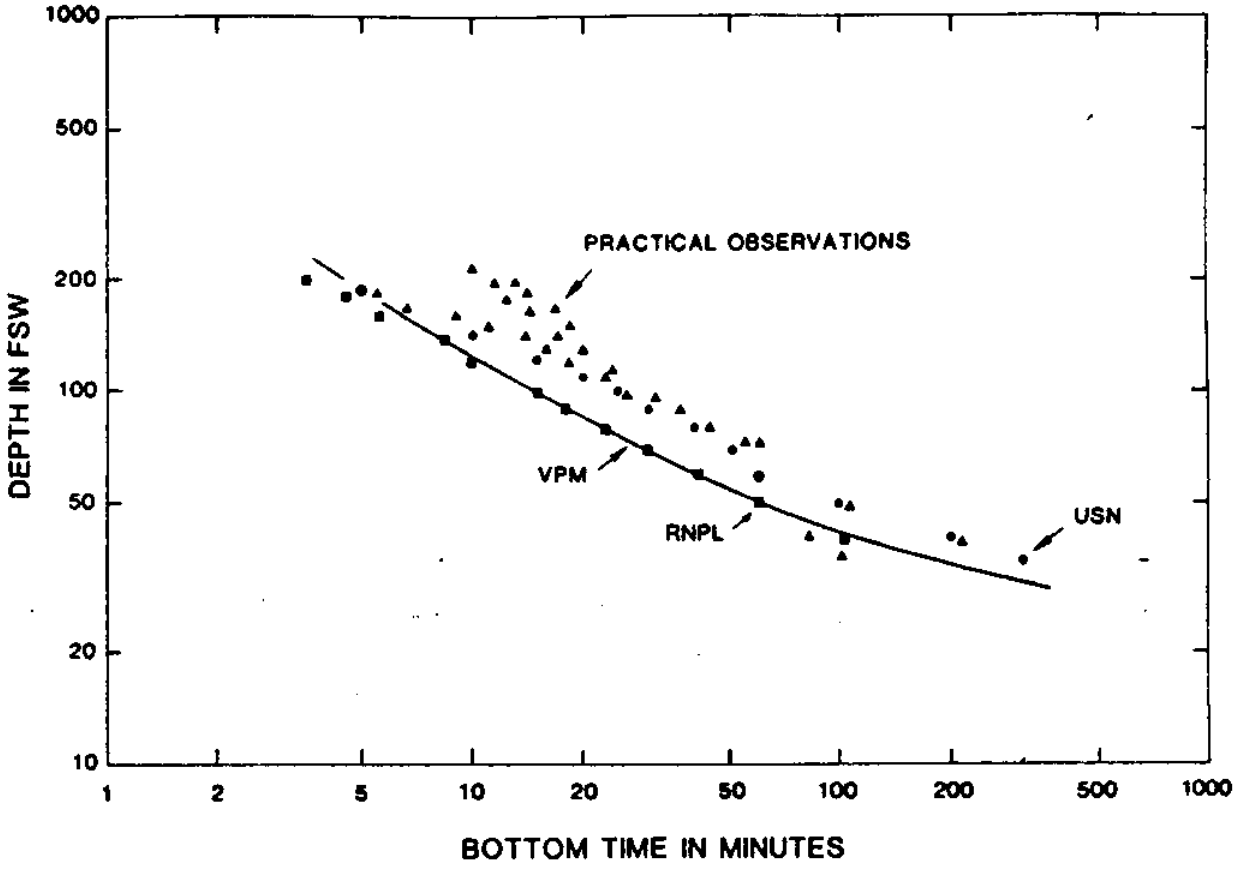

Fig. 7 - Plot of VPM, RNPL, and USN air table no-decompression limits including various practical observations, i.e., ascents which yielded no symptoms or very mild symptoms. The VPM curve lies near or just below the USN and RNPL recommendations over the entire range, and it therefore serves as a conservative and useful lower bound.

and in the exposure conditions [34], the absence of prolonged decompression stages makes this type of data nearly independent of the overall surfacing strategy. As mentioned above, the VPM curve follows the RNPL points very closely, and both come into agreement with the USN points at about 180 fsw. Over its entire range, the VPM line serves as a conservative, tight, and therefore useful lower bound. The fact that it is systematically lower than most of the practical observations reflects the general conservatism of the tables as a whole. A bolder and faster set of tables could, of course, be computed by using different values for the free parameters.

C. A COMPARISON OF THE VPM, USN, AND RNPL AIR DECOMPRESSIONS FROM 200 FSW

The salient features of the VPM, USN, and RNPL staged decompressions can be compared by studying a single, typical decompression schedule. A representative sample is given in Table 2, which repeats the stop depths and durations listed in the three sets of tables for a 60-min, 200-fsw excursion. This dive is considered to be an "exceptional exposure," imposing a greater-than-normal risk. The method of surfacing differs qualitatively among the table types. In the case of the VPM and USN schedules, all descent and ascent rates are taken to be 60 fsw/min. For the RNPL, the descent rate is not to exceed 100 fsw/min, the ascent to the first stop is made at 50 fsw/min, and the ascents between stops are at 10 fsw/min. Also, in the VPM and USN schedules, the stop durations do not include the times between stages, but for the RNPL schedule they are included (except for the final ascent

TABLE 2

COMPARING THE VPM, USN, AND RNPL AIR DECOMPRESSION SCHEDULES FOR A 60-MIN, 200-FSW EXCURSION

STOP DEPTH (FSW)	VPM WAIT (MIN)	USN WAIT (MIN)	RNPL WAIT (MIN)
130	1		
120	3		
110	3		
100	4		5
90	7		0
80	6		0
70	7		5
60	11	2	5
50	16	13	10
40	17	17	35
30	22	24	45
20	39	51	180
10	52	89	2*
TOTAL ASCENT TIME:	191:20	199:20	289:00

* NO WAIT AT 10 FSW, RATE OF ASCENT FROM 20 FSW IS 10 FSW/MIN.

from 20 fsw, which is listed explicitly). In all cases, the descent time is counted as part of the "bottom time."

The VPM and USN schedules for the 60-min, 200-fsw exposure are compared graphically in Fig. 8. The total times required to reach the surface are quite similar. However, the obvious and most important difference is the deeper first stop required by the VPM schedule, being 130 fsw instead of 60 fsw for the USN case. This is a persistent feature of the literally hundreds of comparisons we have made between the VPM tables and the conventional tables now in use. Our calculations indicate that the longer "first pull" of the existing tables results in a larger supersaturation, a larger bubble number, and, ultimately, in a larger volume of released gas. For equivalent-exposures and total decompression times, we therefore assume that the VPM tables will produce a smaller maximum volume of free gas and lead to safer ascents.

Another, related feature is the difference in the durations of the shallow stops. The longer first pulls of the USN profiles initiate bubble formation which must later be controlled. The longer stops near the surface prevent the bubbles from growing too large, although they are probably detectable by Doppler monitoring. The RNPL tables, created in an effort to decrease the incidence of bends and of osteonecrosis [20], generally have deeper first stops and longer shallow stops than the USN tables. However, the price for extra safety is paid in extra decompression time, and the resultant RNPL totals are, for the most part, much larger than their USN counterparts. The VPM schedules, based upon a physical model, begin

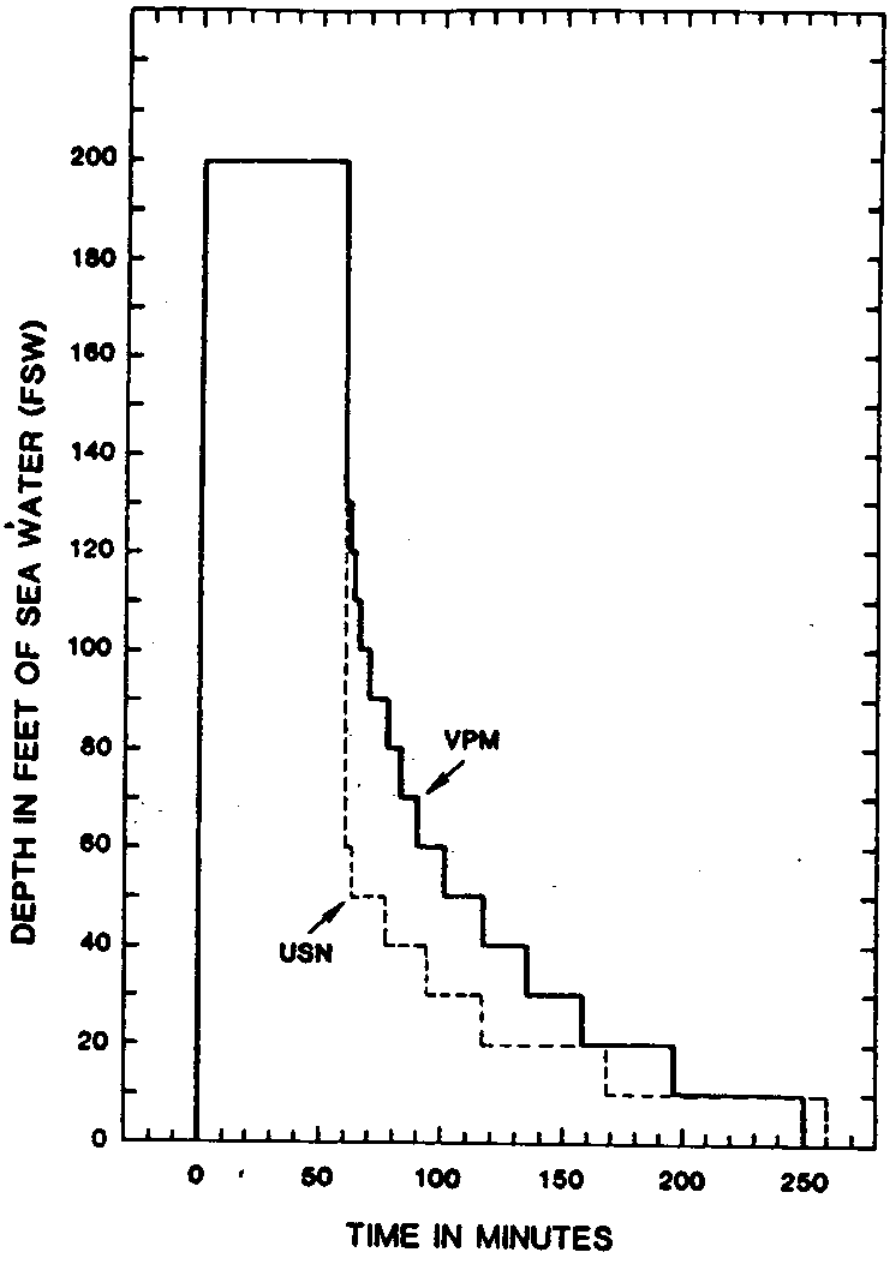

Fig. 8 - Plot of VPM and USN decompression profiles for a 60-Min, 200-fsw air excursion. The longer "first pull" of conventional air tables results in a larger supersaturation, a larger bubble number, and a larger maximum volume of released gas.

limiting bubble formation prior to the first stop and do not require excessively long shallow stops. In addition, they are remarkably self-consistent and are therefore well-suited to interpolation and extrapolation. It should be reiterated here that the VPM tables are conservative in nature and not designed for maximum speed.

The total ascent times for the VPM, USN, and RNPL tables are plotted as functions of the bottom time at 200 fsw in Fig. 9. The VPM curve is close to the USN points for bottom times that extend all the way from 5 to 360 min. The large difference in the USN and RNPL total ascent times (which, in this figure, are often larger than a factor of two) illustrates the wide divergence in opinion that still exists, even among highly-respected investigators in the diving field.

Looking at excursions shallower than 200 fsw, we find that the VPM total decompression times usually lie between the USN and RNPL values for similar exposures. This is illustrated in Fig. 10 for 100 fsw. For excursions deeper than 200 fsw, however, the VPM times tend to be shorter than their correspondents, particularly for longer bottom times. We believe that there are two reasons for this qualitative difference. The first and primary reason is that the "crushing effect" imposed upon bubble nuclei is greater at deeper depths, and, since the smaller nuclei form macroscopic bubbles less readily, the allowed supersaturation is larger.

The second reason is found in the inherent "inefficiency" of conventional tables. Deeper excursions obviously require more decompression time, but how that time is distributed between the stops is of paramount importance. Current tables that are (or were at one

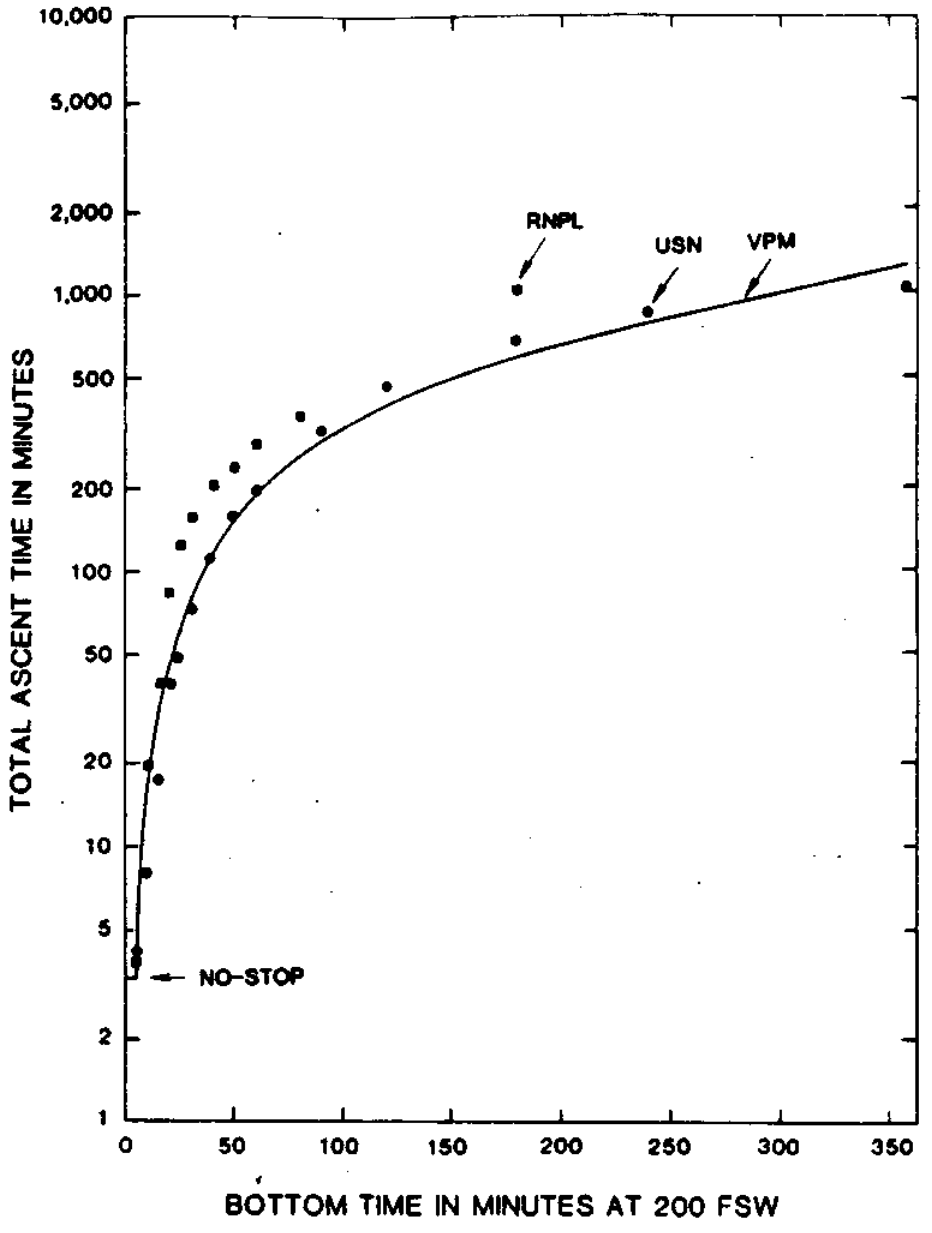

Fig. 9 - Plot of total ascent times versus bottom times at 200 fsw for the VPM, RNPL, and USN air tables. The total ascent times for the USN and RNPL air tables often differ by more than a factor of two.

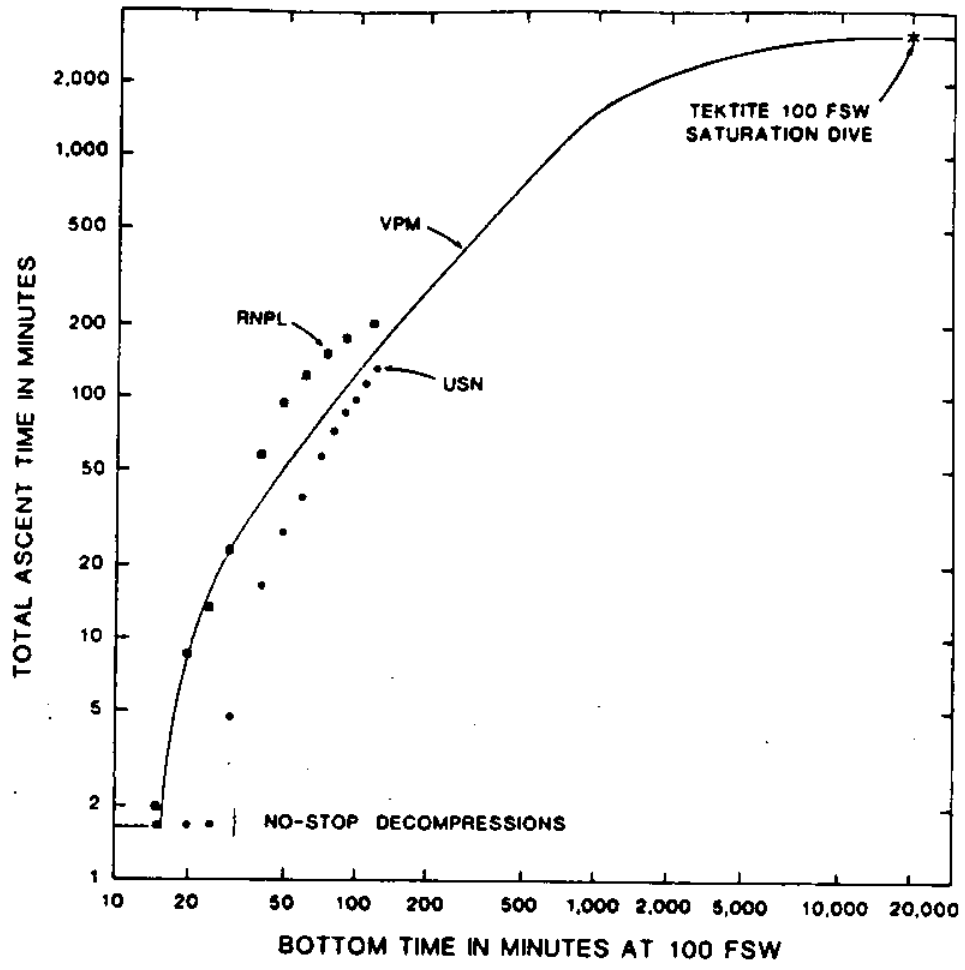

Fig. 10 - Plot of total ascent times versus bottom times for VPM, USN, and RNPL at 100 fsw on air. The VPM line lies comfortably between the USN and RNPL points for similar exposures, yet it spans the entire range from no-stops to saturation dives with the same four parameters.

time) based on the Haldanian ratio method typically have long first pulls and long shallow stops. In addition, their empirical nature suggests that extra decompression time is often added to "marginal" schedules to improve their safety. Through lack of an adequate physical model, the extra time is added to the shallow stops, a practice which may be effective but is quite inefficient. Existing U. S. Navy tables have sometimes been referred to as "treatment tables" because they provide long waits at shallow depths to "treat" the bubbles that form during the initial ascents.

Should it later be found that the VPM tables are unsafe for excursions in excess of 200 fsw, they can be further adjusted by assuming an earlier onset of impermeability and reducing the value of P^*. The result of such an adjustment would be to increase the resistance of bubble nuclei to the effect of crushing and to lengthen the total decompression times required for these deeper dives.

D. AN OVERVIEW OF THE VPM AIR TABLES

One very practical reason for attempting to optimize decompression procedures from first principles is the hope that, if a correct global theory can be formulated, it will someday be possible to describe the whole range of decompression experience with only a few equations and parameter values. Instead of "titrating" a handful of "volunteers" to develop a new table or determine a new "M-value" [19], a method which necessarily has limited statistical accuracy, one will be able to use a pre-calibrated theory to interpolate or extrapolate, thereby bringing to bear the full statistical weight of a much larger data base. This idea

is illustrated in Fig. 11, which summarizes total ascent times versus bottom times for VPM decompressions from excursions to 60, 100, 200, and 300 fsw.

In an earlier illustration of the global approach, Fig. 10 smoothly connected the no-stop decompressions of Fig. 7 with the 14-day, 100-fsw Tektite saturation dive [35]. The latter has been used by humans without incident. However, the close agreement is partly fortuitous because the VPM calculation was done using 10-fsw increments, while the Tektite stops were 5 rather than 10 fsw apart. Also, the VPM schedule used air as the breathing gas, while pure oxygen was breathed at various times during the Tektite decompression. A more precise comparison is given in Table 3, where the VPM schedule was calculated for a 14-day exposure at the 126-fsw equivalent air depth [30] of the Tektite dive, with more numerous stops being made at the closer 5-fsw intervals.

By replacing our earlier assumption of constant bubble number with a dynamic critical-volume hypothesis, we were able to prepare a comprehensive set of air diving tables. Although untested, these tables seem in all respects to be quite reasonable. It should not be forgotten, however, that the constant-bubble-number criterion worked well in the rudimentary cases in which it was first applied [11,12]. One might ask whether our new criterion gives similar results for those special situations, that is, does it obey a form of the correspondence principle? The answer, of course, is yes.

An example of the correspondence between the two methods is given by Fig. 12, in which the allowed pressure reduction $P_1 - P_2$ is plotted

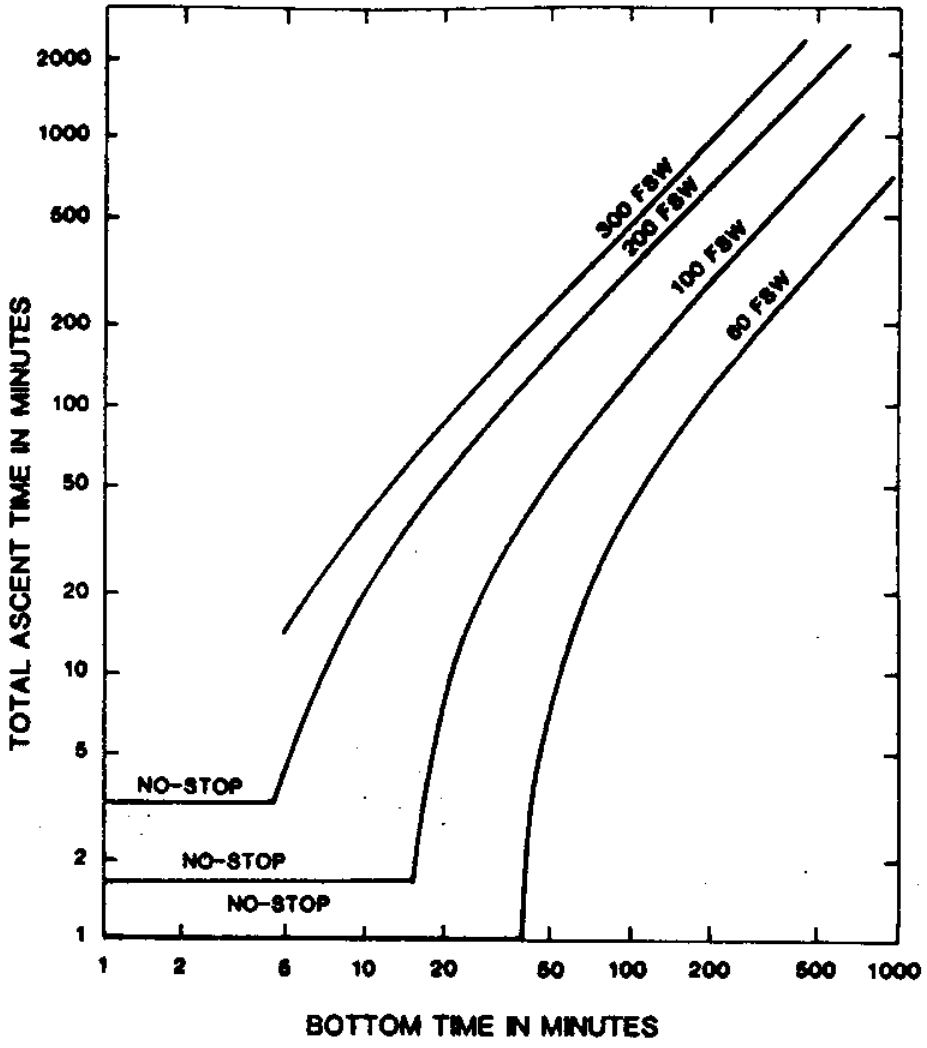

Fig. 11 - Plot of VPM total ascent times versus bottom times for 60, 100, 200, and 300-fsw air excursions. This figure illustrates how a two-dimensional map of decompression experience can be described by a global theory using a small number of equations and parameter values.

TABLE 3

COMPARING THE 14-DAY, 100-FSW TEKTITE AIR DECOMPRESSION SCHEDULE WITH THE 126-FSW VPM EQUIVALENT

Depth (fsw)	Time at stop (min) TEKTITE	Time at stop (min) VPM
100-90	10 air	
90	60 air	
85	90 air	36 air
80	100 air	159 air
75	110 air	165 air
70	120 air	170 air
65	360 air	176 air
60	140 air	182 air
55	160 air	190 air
50	160 air	197 air
45	10 oxygen 150 air	205 air
40	130 air	214 air
35	20 oxygen 150 air	224 air
30	360 air	235 air
25	30 oxygen 150 air	246 air
20	150 air	260 air
15	50 oxygen 150 air	273 air
10	160 air	290 air
5	60 oxygen	308 air
Total:	2960 air + 170 oxygen	3530 air

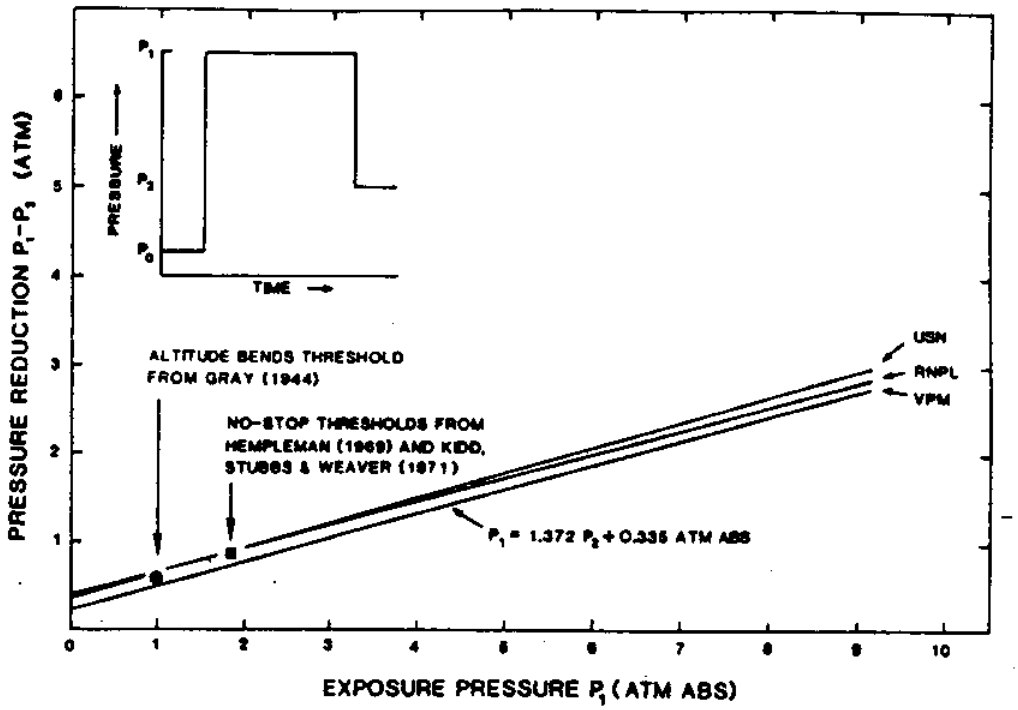

Fig. 12 - Plot of allowed pressure reduction versus exposure pressure for VPM, USN, and RNPL air tables. The VPM line lies below the no-stop and altitude bends thresholds and is therefore assumed to be "safer."

versus the exposure pressure P_1 for the VPM, USN, and RNPL tables. The subjects are first saturated at some elevated pressure P_1 and then supersaturated by reducing the pressure from P_1 to the final setting P_2. In experiments with human subjects, $P_1 - P_2$ is usually defined as the greatest pressure reduction which can be sustained without the onset of decompression sickness. This condition can be simulated by selecting dives with bottom times of 720 min and taking P_2 to be the depth of the first decompression stop. The simulation provides a reasonable approximation to a single-step decompression because, in this limit, the rate at which gas is permitted to come out of solution is only slightly larger than that which the body can dissipate and therefore tolerate indefinitely.

In the permeable region of the model ($P_1 < 9.2$ atm abs), this procedure yields the linear relationship for the VPM tables of

$$P_1 = 1.372\ P_2 + 0.335 \text{ atm abs}, \tag{3.1}$$

which has a correlation coefficient higher than 0.999 for the eight combinations of $P_1 - P_2$ that were tried. Similar expressions,

$$P_1 = 1.375\ P_2 + 0.52 \text{ atm abs} \tag{3.2}$$

and

$$P_1 = 1.366\ P_2 + 0.56 \text{ atm abs}, \tag{3.3}$$

have been extracted by Hennessy and Hempleman [29] from the USN and RNPL tables, respectively.

As can be seen in Fig. 12, the three straight lines are nearly parallel, and the VPM line is 0.1 to 0.2 atm lower than those of the USN and RNPL. The fact that these lines are similar to the isopleths of constant bubble number presented for the permeable region of the model in Figs. 2, 5, and 6 verifies the aforementioned correspondence for this simple case. The "no-stop threshold," P_1 = 1.87 atm abs and $P_1 - P_2$ = 0.87 atm, was obtained by averaging the values of P_1 = 1.90 atm abs, $P_1 - P_2$ = 0.90 atm measured by Hempleman [36] with those of P_1 = 1.83 atm abs, $P_1 - P_2$ = 0.83 atm found by Kidd, Stubbs, and Weaver [37]. The VPM result, P_1 = 1.71 atm abs, $P_1 - P_2$ = 0.71 atm, is 0.16 atm lower than the "experimental average" and is therefore "safer." The "altitude bends threshold," namely P_1 = 1.00 atm abs, $P_1 - P_2$ = 1.00 - 0.40 = 0.60 atm, was calculated using the value of P_2 = 7550 m = 307 mm Hg = 0.40 atm abs measured by Gray [38]. The VPM limit of P_1 = 1.00 atm abs, $P_1 - P_2$ = 0.52 atm is again slightly lower, this time by 0.08 atm.

In contrast, the lines for USN and RNPL are both slightly higher than the experimental no-stop and altitude-bends thresholds plotted in Fig. 12. This illustrates the type of problem one encounters in attempting to extrapolate conventional tables that are based on trial-and-error rather than on a global theory. Given such problems, altitude bends and decompression sickness are usually investigated separately, as if they were different subjects. Our approach has been to treat them simultaneously and on an equal footing.

The immediate goal of this undertaking was not to produce a completely operational set of air diving tables. Instead, we wanted to

determine whether a reasonable and comprehensive set of such tables could be computed using a bubble-nucleation model and a modest number of assumptions, equations, and parameter values. The answer to this question, quite obviously, is yes.

CHAPTER IV

A. ADJUSTING THE FREE PARAMETERS FOR HELIUM DIVES

The equations of the varying-permeability model delineated in Chapter I do not depend explicitly on the type of inert gas used. Rather, they predict that each inert gas behaves in fundamentally the same way during bubble nucleation. It should be possible, then, to duplicate for helium the comprehensive table calculations previously performed for air dives. Obviously, there are significant differences between nitrogen and helium which must be taken into account during bubble growth, presumably through adjustment of the model constants and/or free parameters. Unfortunately, the data available for helium are not as extensive as those available for nitrogen, and the empirical determination of the magnitude and scope of the required parameter changes is likely to be difficult and inaccurate. In this chapter, an attempt is made to calculate a priori what adjustments should be required on the basis of the differing physical properties of the two gases. The subsequent success of the model in tracking conventional helium tables and data over the full range from no-decompression to saturation dives is demonstrated in Chapter V.

For a given pressure exposure, the model predicts that the number of bubble nuclei present in the body at the onset of decompression should be the same whether nitrogen or helium is used as the breathing gas. Indeed, bubble nuclei are assumed to have been mechanically compressed but not extinguished [10]. Although helium is expected to form bubbles more quickly upon decompression [39,40], it seems likely

that the smaller volume of dissolved gas [41] will ultimately result in somewhat smaller bubbles. This is consistent with a plot of the data obtained in Knox gelatin for several inert gases (Fig. 13) [42], in which a curve through the number of visible helium bubbles for various supersaturation pressures lies just slightly below the corresponding nitrogen curve. Similar results have been obtained for agarose gelatin samples [8].

The varying-permeability model is theoretically and empirically based upon bubble growth in aqueous media, particularly in distilled water, gelatin, and blood. While it is possible that new variables, such as the tissue deformation pressure and the inert-gas diffusion rate, may be required to adequately describe bubble formation in various tissues, it can be argued that most injurious cases of decompression sickness result from bubbles in the blood [43,44]. The respective volumes of nitrogen and helium in physical solution in whole blood at $37^{o}C$ and 1 bar are 12.831 and 8.686 ml/liter [41], and their ratio is 1.48. For a constant number of bubble nuclei, it is assumed that equivalent supersaturations will result in slightly smaller bubbles for helium as compared to nitrogen. Also, it is expected that the same volume of released gas will produce the same decompression insult for both inert gases. The number of bubbles comprising the critical volume is thus assumed to be slightly larger for helium, and the size of the critical nuclear radius r_o required to form a macroscopic bubble has been decreased accordingly (to 0.7 μm for helium vice 0.8 μm for nitrogen). This change will increase the allowed supersaturation for tissues containing helium as the sole inert gas.

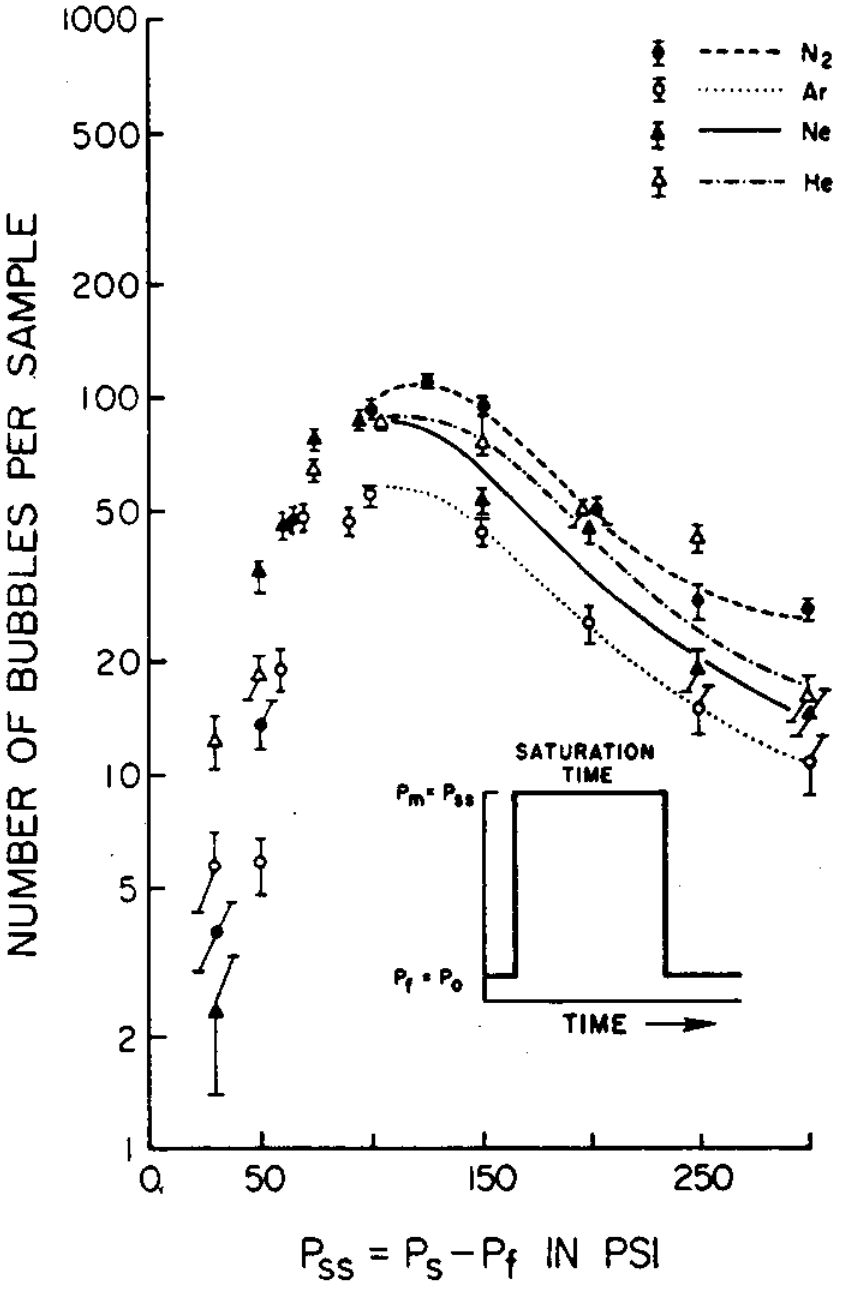

Fig. 13 - Plot of bubble number versus supersaturation pressure for various inert gases. The bubble number curves for helium and nitrogen are quite similar over the entire range of supersaturation pressures.

The decompression criterion summarized in Chapter II by Eqs. (2.16-2.20) is based upon the critical-volume hypothesis [29] and is dependent upon the the ratios γ/r_o and γ/γ_c via Eqs. (2.10) and (2.17). The surface tension and skin compression, γ and γ_c, are not affected by the change of inert gas and are therefore assigned their previous values of 17.9 and 256.9 dynes/cm, respectively.

The decompression criterion may also be adjusted directly via the parameter α (Eq. 2.19), which depends upon the critical volume of released gas V_c, the temperature T, the bubble number normalization coefficient N_o, and the physical properties of the surfactant skin molecules S, γ, and γ_c. However, none of these are expected to undergo physical or chemical changes when nitrogen is replaced by helium. Thus, the free parameter α has been carried over unchanged from the air-table calculations and has been assigned the usual value of 523 fsw-min. Similarly, the regeneration time constant τ_r characterizes a stochastic process which depends upon the ambient temperature and certain properties of the skin [16]. It does not depend upon the choice of inert gas, and hence it retains the usual air-table value of two weeks, or 20160 min.

B. DETERMINING THE IMPERMEABILITY THRESHOLD FOR HELIUM

In applying the varying-permeability model to decompression sickness, a number of physical constants are introduced that might depend upon the choice of inert gas. As mentioned before several of these have already been absorbed (unchanged) into the free parameter α, and certain others, such as the value of atmospheric pressure at sea

level, are invariant. In fact, aside from the tissue half-time series, only one constant remains to be determined for helium, and that is the threshold of impermeability P^*.

The term "varying permeability" has been used extensively in this work and requires some further qualification. Nuclear skins are assumed herein to be permeable during all compressions below the threshold crushing pressure P^* and during all decompressions. The onset of nuclear impermeability is then an immediate result of exceeding the threshold crushing pressure. However, the actual change may take place during a finite time interval and over a range of pressures, resulting in a continuous gradation of permeability which can be described by various diffusion models [45,46].

The mechanism by which impermeability manifests itself during a large radial compression from r_o to r_m is unclear. While the area occupied by each surfactant molecule might be expected to decrease and thus restrict the passage of gas molecules through the skin, another possibility exists. The surface energy required to significantly reduce the intermolecular spacing may exceed the energy required to remove surfactant molecules from the skin, thereby driving them into solution [47,48]. This idea is illustrated in Fig. 14a [48], which shows that a large change in surface pressure Π is required to produce a small change in the area per molecule of several common surfactants spread in flat monolayers. The surface pressure for a spherical skin is assumed to be generally larger, corresponding to an even smaller change in area. Since the radius of the critical nucleus decreases by as much as a factor of four during a rapid compression from P_o to P^*, the vast

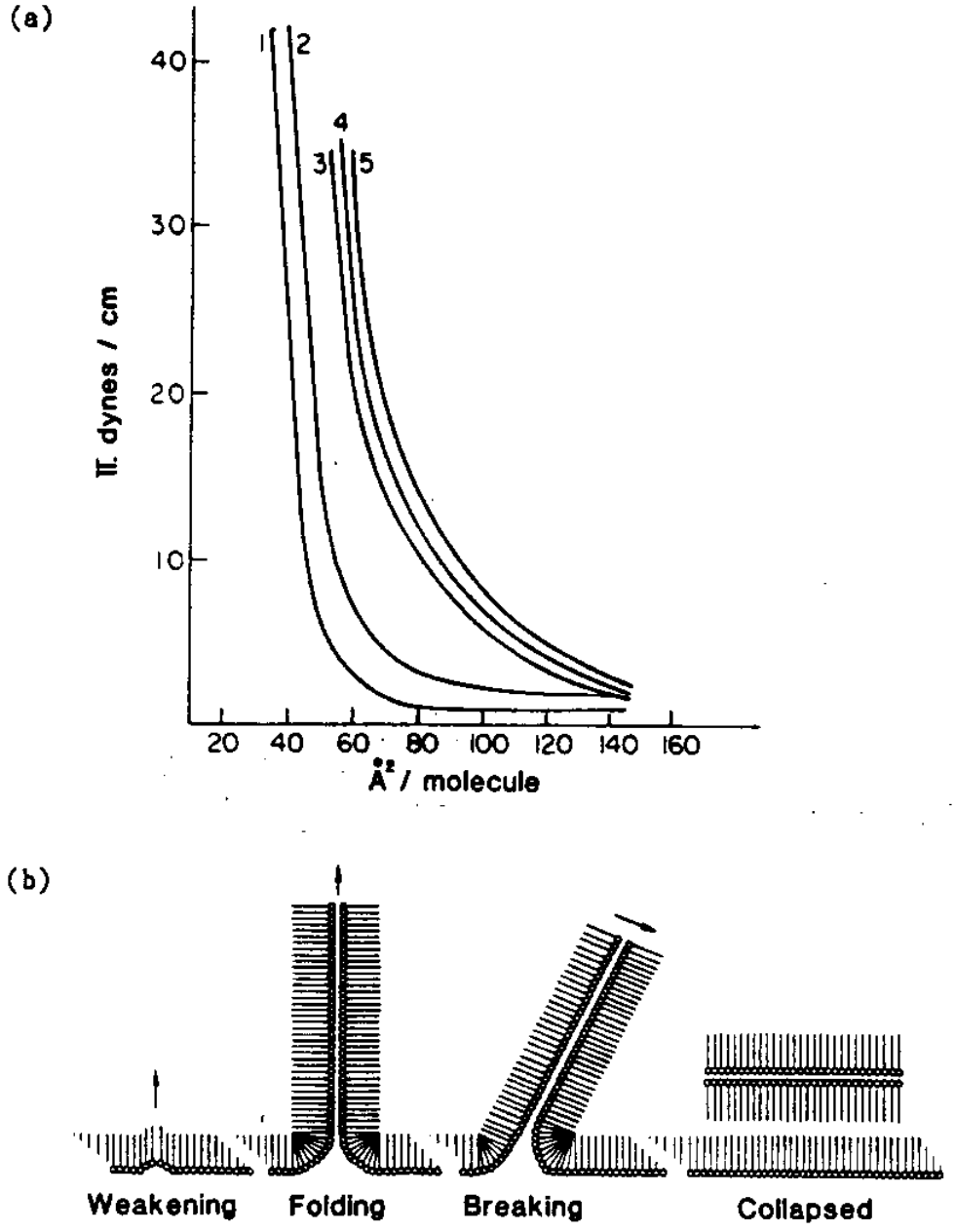

Fig. 14 - Behavior of compressed monolayers: (a) Π-A curves for typical synthetic phospholipids on a phosphate buffer (pH 7.4) at 21-24°C. Curves 1, 3, and 5 are lecithins, while curves 2 and 4 are phosphatidylethanolamines. (b) A proposed mechanism for monolayer collapse. In the varying-permeability model, Π is replaced by the constant γ_c.

majority of the component molecules must be squeezed out of the skin (Fig. 14b) [49]. These ejected molecules would then become part of a surfactant "reservoir" just outside (Fig. 15) [16], in which laminar aggregations would be likely to form whenever the local surfactant concentration exceeded a given threshold [48–50]. The onset of impermeability may thus be caused by the creation of multiple layers around the nuclear skin rather than by a reduction in the area per molecule. We favor the former possibility and assume that an excessive crushing of the nuclear skin is accompanied by a qualitative change in its structure that greatly increases its resistance to penetration by gas molecules.

Regardless of the mechanism involved, the data obtained from Knox gelatin [10] indicate that the passage of nitrogen is hindered when the crushing pressure exceeds $P^* = 9.2$ atm abs. The lack of a clear physical description, however, precludes the quantitative estimation of P^* *in vivo*, hence the use of the gelatin value in the air-table calculations. For large crushing pressures, the mechanism proposed above should rapidly increase the time required for gas molecules to penetrate the nuclear skin, rendering it effectively impermeable for either nitrogen or helium. We therefore assume that P^* is the same for both inert gases. Since P^* is not well-known, it could be used as an additional free parameter in applying the model to deeper dives.

C. DEFINING THE TISSUE HALF-TIMES FOR HELIUM

The various bodily tissue types are currently represented in the air-table calculations by a series of tissue half-times. Although no

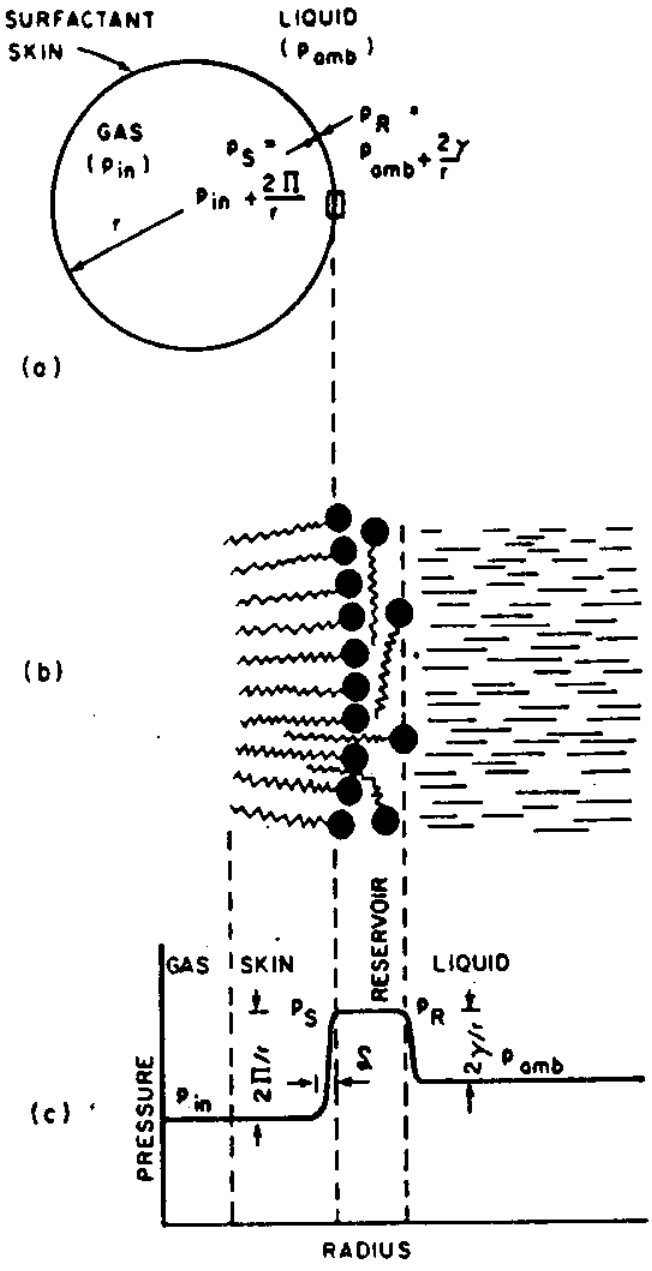

Fig. 15 - Schematic diagram of a bubble nucleus including: (a) the condition for mechanical equilibrium against small fluctuations, (b) a magnified view of the skin and the reservoir, and (c) a plot of pressure versus radius indicating where P_{in}, P_S, P_R, and P_{amb} apply.

direct correlations between these half-times and specific bodily tissues are assumed, some apparently exist [41]. In adapting the nitrogen half-times to helium, only the longest tissue must be accurately specified, as suggested by the following arguments.

First, the half-times form the basis for a set of exponential curves (Fig. 1) which generate a single "controlling-tissue" curve during staged decompressions. There are many different basis sets which would produce similar decompression profiles. During saturation dives, however, the longest tissue will always control the decompression, and basis sets with different saturation half-times will generate different schedules. The choice of the longest tissue is therefore determined empirically.

Second, there is a practical limit to the response of the system for the shortest half-times. The original nitrogen basis set, consisting of half-times ranging from 1 to 720 min, was chosen to provide complete coverage for all decompressions, including those from no-stop and saturation dives. However, an examination of the resultant air tables shows that no half-time shorter than two minutes is ever selected to control an ascent. The basis set is thus bounded on both ends.

The helium half-times must allow the same flexibility as their nitrogen counterparts. This can be assured if the nitrogen basis set is scaled down to accomodate the faster uptake and elimination of helium. The above arguments suggest that a single scale factor should suffice, although multiple empirical factors have been used [51]. The time required for complete saturation of all the tissues with helium has been

found to be 24 hours [52], and the corresponding half-time of 4 hours is widely used [31,41,51,53,54]. Comparing this with our 12-hour (720-min) maximum half-time for nitrogen, we find that the scale factor is three, which is identical to the empirical factor selected by Lambertsen for the longest tissues [51]. The basis set for helium is therefore obtained by dividing each of the nitrogen half-times by three.

CHAPTER V

A. COMPARING THE VPM AND USN HELIUM TABLES

Following the determination of the new critical radius and the insertion of the new tissue half-times into the computer program, several different sets of VPM tables were generated and compared to the current USN helium tables [31,55]. The method of calculation of the USN tables is disguised by the somewhat arbitrary assignment of M-values (maximum tissue tensions), but the discharge of residual nitrogen during helium uptake appears to be done at the faster helium rate. It is common practice to approximate a small percentage of residual nitrogen with an equivalent helium partial pressure. Empirical data suggest that the procedure is neither accurate nor safe. Because all the VPM schedules appearing in this section (including the no-stop dives) follow this practice and treat any residual nitrogen as helium, they do not represent the VPM predictions for actual dives unless the diver is acclimated to helium before any depth excursion is made. The USN schedules are suspected of providing inadequate decompression for the same reason, and for other intrinsic and extrinsic inconsistencies. All of the VPM helium SCUBA tables described in the following paragraphs use the same inert-gas fraction (0.75) as the corresponding USN tables [31], which are based on Workman's calculations [56,57]. Another source [55] requires a more modest inert-gas fraction (0.68) for the same tables.

In our first comparison, the VPM and USN no-stop decompressions are listed (Table 4) and plotted (Fig. 16) side-by-side. The VPM curve lies below all but one USN point, forming a useful lower bound. For the

TABLE 4

COMPARING THE NO-DECOMPRESSION LIMITS OF
THE VPM AND USN HELIUM TABLES

ALLOWED DEPTH (FSW)	SOURCE TABLE TYPE	ALLOWED TIME (MIN)	ALLOWED DEPTH (FSW)	SOURCE TABLE TYPE	ALLOWED TIME (MIN)
30	VPM	UNLIMITED	140	VPM	10
	USN	UNLIMITED		USN	15
40	VPM	216	150	VPM	9
	USN	260		USN	15
50	VPM	98	160	VPM	8
	USN	180		USN	10
60	VPM	58	170	VPM	7
	USN	130		USN	10
70	VPM	43	180	VPM	7
	USN	85		USN	5
80	VPM	30	190	VPM	6
	USN	60		USN	NOT LISTED
90	VPM	23	200	VPM	5
	USN	45		USN	NOT LISTED
100	VPM	19	210	VPM	5
	USN	35		USN	NOT LISTED
110	VPM	17	220	VPM	5
	USN	30		USN	NOT LISTED
120	VPM	14	230	VPM	4
	USN	25		USN	NOT LISTED
130	VPM	12	240	VPM	4
	USN	20		USN	NOT LISTED

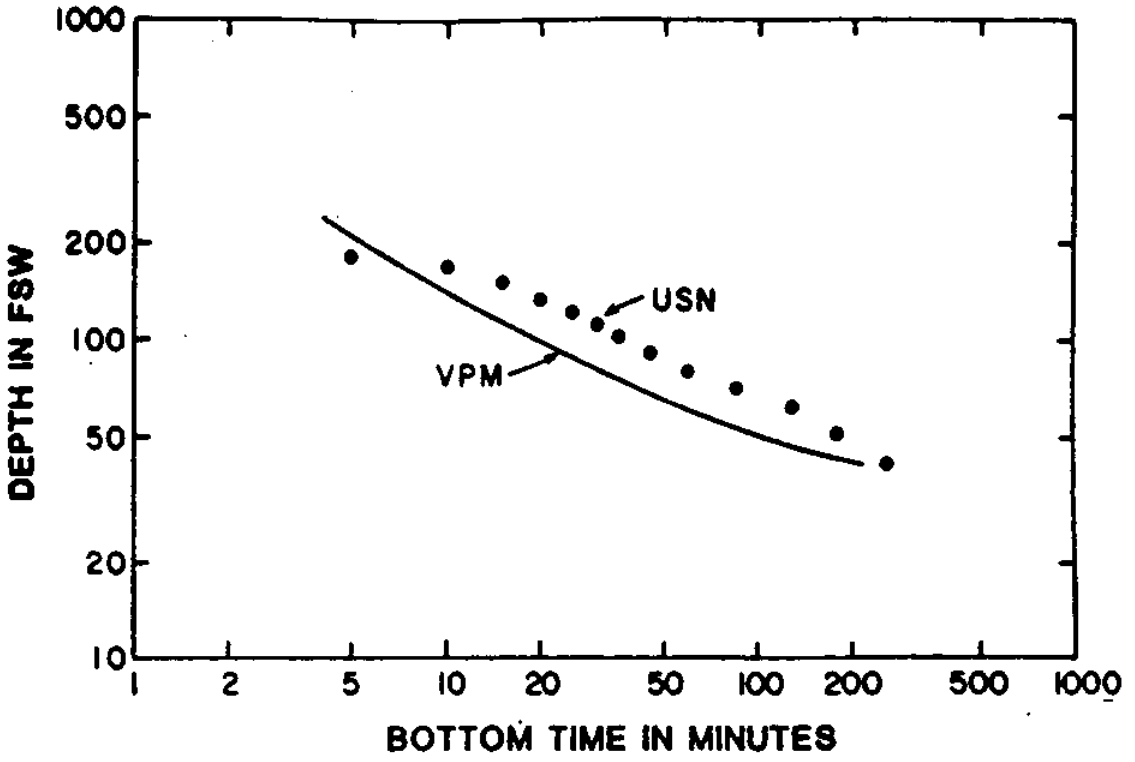

Fig. 16 - Plot of VPM and USN no-decompression limits for helium dives. Again the VPM curve lies below all but one USN point and serves as a useful lower bound.

deeper dives, the VPM crushing effect leads to larger allowed supersaturations. This should be familiar from the air-table no-stop comparison (Table 1 and Fig. 7), which shows the same trend. Some similarity between the VPM air and helium no-stop curves is to be expected since they have comparable half-time distributions and critical radii. The augmented-supersaturation parameter α varies inversely with the controlling tissue half-time and controls the shorter, deeper dives, while the critical radius limits the longer, shallower dives. This is why the VPM air and helium no-stop curves overlap at the deep end and diverge at the shallow end. The USN helium no-stops, like their air equivalents, are not expected to produce overt bends symptoms but may result in chronic and deleterious bubble formation. The VPM no-stops given in Table 4 should produce fewer bubbles, although a calculation which properly accounts for any residual nitrogen would result in even more restrictive limits.

In our second comparison, small sets of VPM and USN helium SCUBA tables are used. An integrated listing of both is supplied in Table 5. The ascent criteria for the last dive given, a 200-fsw, 30-min exposure, are specified in Table 6 and illustrated in Fig. 17. The trend is similar to that observed for the air dives, where the VPM schedules invariably require deeper first stops. A global map of the VPM helium SCUBA total decompression times versus bottom times appears in Fig. 18. The data are plotted for 60, 100, and 200-fsw excursions. While the bottom times have been extended to sixteen hours, oxygen toxicity precludes deeper dives. Such maps are convenient when comparing new decompression data with model calculations. Again, this

TABLE 5

COMPARING THE VPM AND USN HELIOX SCUBA DECOMPRESSION SCHEDULES
(ALL DEPTHS ARE IN FSW, AND ALL TIMES ARE IN MINUTES)

BOTTOM DEPTH	BOTTOM TIME	TABLE TYPE	DECOMPRESSION STOP: HELIOX 110	100	90	80	70	60	50	40	30	20	10	TOTAL TIME
40	260	VPM											5	5:40
		USN											0	0:40
50	180	VPM											22	22:50
		USN											0	0:50
	200	VPM											27	27:50
		USN											20	20:50
60	130	VPM										5	25	31:00
		USN											0	1:00
	150	VPM										8	28	37:00
		USN											20	21:00
	170	VPM										11	35	47:00
70	85	VPM										8	18	27:10
		USN											0	1:10
	100	VPM										11	23	35:10
		USN											15	16:10
	115	VPM									1	14	27	43:10
		USN											25	26:10
	130	VPM									2	17	29	49:10
		USN											40	41:00
80	60	VPM									1	6	13	21:20
		USN											0	1:20
	70	VPM									3	9	17	30:20
		USN										5	10	16:20
	80	VPM									4	12	19	36:20
		USN										10	15	26:20
	90	VPM									6	13	24	44:20
		USN										10	25	36:20
	100	VPM									8	15	27	51:20
		USN										10	35	46:20
90	45	VPM									4	5	11	20:30
		USN											0	1:30
	60	VPM									6	10	16	33:30
		USN										5	10	16:30
	70	VPM								2	6	12	20	41:30
		USN										5	20	26:30
	85	VPM								3	10	15	26	55:30
		USN										10	30	41:30

TABLE 5 (CONTINUED)

COMPARING THE VPM AND USN HELIOX SCUBA DECOMPRESSION SCHEDULES
(ALL DEPTHS ARE IN FSW, AND ALL TIMES ARE IN MINUTES)

BOTTOM DEPTH	BOTTOM TIME	TABLE TYPE	DECOMPRESSION STOP: HELIOX 110	100	90	80	70	60	50	40	30	20	10	TOTAL TIME
100	35	VPM									3	5	8	17:40
		USN											0	1:40
	50	VPM								3	5	9	14	32:40
		USN										5	15	21:40
	60	VPM								5	6	12	19	43:40
		USN										10	20	31:40
	70	VPM							1	5	9	14	23	53:40
		USN									5	15	25	46:40
110	30	VPM								1	3	5	7	17:50
		USN											0	1:50
	40	VPM							1	3	5	6	13	29:50
		USN										5	10	16:50
	50	VPM							2	5	5	11	17	41.83
		USN										10	20	31:50
	65	VPM							4	5	11	14	24	59:50
		USN									5	15	25	46:50
120	25	VPM								2	2	4	5	15:00
		USN											0	2:00
	35	VPM							2	3	5	5	13	30:00
		USN										5	10	17:00
	45	VPM						1	3	5	5	12	16	44:00
		USN									5	10	15	32:00
	55	VPM						2	4	5	10	12	21	56:00
		USN									10	15	20	47:00
130	20	VPM								2	2	3	5	14:10
		USN											0	2:10
	30	VPM						1	2	2	5	6	11	29:10
		USN										5	10	17:10
	40	VPM						2	3	5	5	11	15	43:10
		USN									5	10	15	32:10
	50	VPM					1	2	5	5	10	12	20	57:10
		USN								5	5	15	20	47:00
140	15	VPM									2	2	3	9:20
		USN											0	2:20
	25	VPM						1	2	2	4	5	9	25:20
		USN										5	10	17:20
	35	VPM					1	2	3	5	5	10	13	41:20
		USN									5	10	20	37:20
	45	VPM					2	3	5	5	9	12	19	57:20
		USN								5	5	15	25	52:20

TABLE 5 (CONTINUED)

COMPARING THE VPM AND USN HELIOX SCUBA DECOMPRESSION SCHEDULES
(ALL DEPTHS ARE IN FSW, AND ALL TIMES ARE IN MINUTES)

BOTTOM DEPTH	BOTTOM TIME	TABLE TYPE	DECOMPRESSION STOP: HELIOX 110	100	90	80	70	60	50	40	30	20	10	TOTAL TIME
150	15	VPM							1	1	2	2	4	12:30
		USN											0	2:30
	20	VPM						1	2	2	2	5	5	19:30
		USN										5	10	17:30
	30	VPM					2	2	2	5	5	8	12	38:30
		USN									5	10	15	32:30
	40	VPM				1	2	3	5	5	8	12	18	56:30
		USN								5	10	15	20	52:30
160	10	VPM										1	2	5:40
		USN											0	2:40
	20	VPM					1	1	2	2	3	5	6	22:40
		USN									5	5	10	22:40
	35	VPM				2	2	3	4	5	7	11	16	52:40
		USN								5	10	10	20	47:40
170	10	VPM									1	1	2	6:50
		USN											0	2:50
	20	VPM					1	1	2	2	4	5	8	27:50
		USN									5	5	10	22:50
	35	VPM			1	2	2	4	4	5	9	11	17	57:50
		USN								5	10	15	20	52:50
180	10	VPM							1	0	1	2	2	9:00
		USN										5	10	18:00
	20	VPM			1	1	1	2	2	3	4	5	9	31:00
		USN								5	5	10	10	33:00
	30	VPM		1	1	2	2	3	4	5	6	11	15	53:00
		USN								5	10	15	20	53:00
190	10	VPM							1	1	1	2	2	10:10
		USN										5	10	18:10
	20	VPM		1	0	1	2	2	2	3	5	5	10	34:10
		USN								5	5	10	20	43:10
	30	VPM		1	2	2	2	4	4	5	8	10	16	57:10
		USN							5	5	10	15	25	63:10
200	10	VPM						1	1	0	2	2	3	12:20
		USN										5	15	23:20
	20	VPM		1	1	1	2	2	2	4	5	5	11	37:20
		USN								5	5	10	20	43:20
	30	VPM	1	1	2	2	3	4	4	5	9	10	17	61:20
		USN							5	5	10	15	35	73:20

TABLE 6

COMPARING THE VPM AND USN HELIUM DECOMPRESSION SCHEDULES
FOR A 30-MIN, 200-FSW EXPOSURE

STOP DEPTH (MIN)	VPM WAIT (MIN)	USN WAIT (MIN)
110	1	
100	1	
90	2	
80	2	
70	3	
60	4	
50	4	5
40	5	5
30	9	10
20	10	15
10	17	35
TOTAL ASCENT TIME:	61:20	73:20

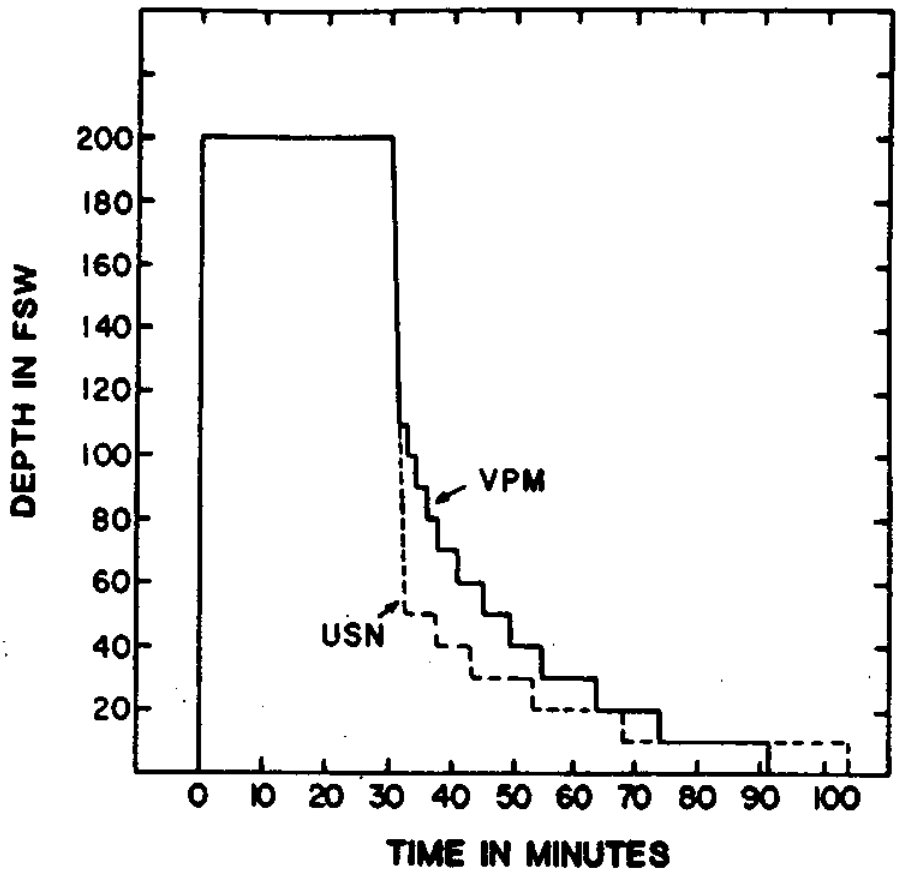

Fig. 17 - Plot of VPM and USN decompression profiles for a 30-Min, 200-fsw helium exposure. The VPM first stops are typically much deeper than their USN counterparts.

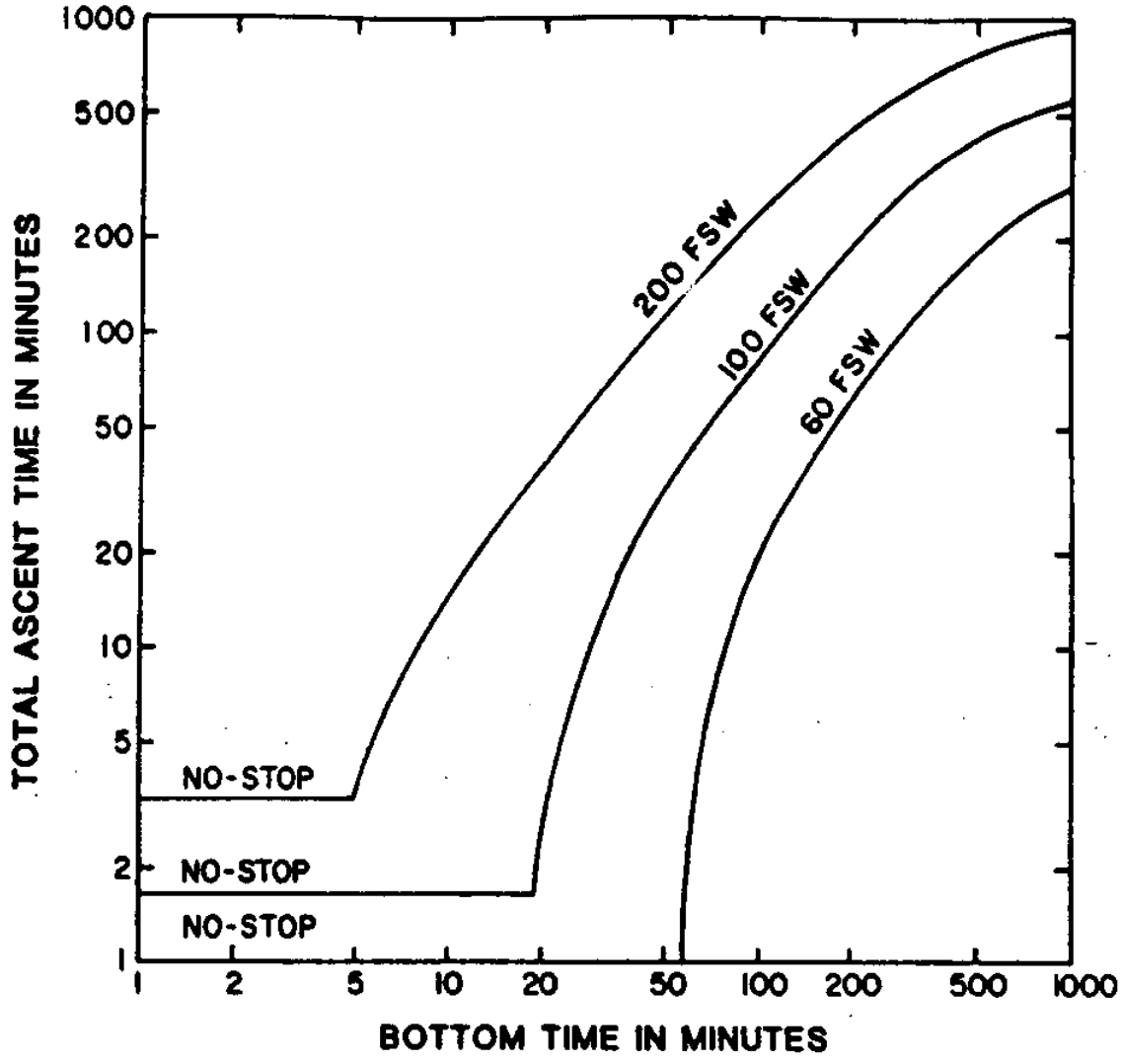

Fig. 18 - Plot of VPM total ascent times versus bottom times for 60, 100, and 200-fsw helium SCUBA excursions. The global map allows an instant comparison to be made with new helium data.

particular set of VPM tables is not expected to be adequate for divers who are initially saturated with nitrogen, and the USN tables are also questionable for the same reason. In fact, all the USN schedules appearing in Table 5 were formally tested in only 84 man-dives, eleven of which produced mild bends symptoms [31].

The VPM equivalents of the USN SCUBA tables using oxygen were also calculated. These tables shift to 100 percent oxygen at 30 fsw and surface from 20 fsw. Following Workman's method [57], we assume that the oxygen breathing apparatus is 80 percent efficient and use 0.2 for the inert-gas fraction from 30 fsw to the surface. The resultant schedules are presented in Table 7. It is apparent that these total decompression times are much shorter than those in Table 5, attesting to the efficacy of the pure-oxygen stages. The incidence of bends symptoms during the testing of the USN tables was zero for 66 man-dives [31], so safety as well as speed is included among the oxygen benefits. The agreement between the VPM and USN total times is exceptional, although the profiles are quite different, with the VPM first stops being characteristically deeper.

In our final comparison, we attempt to match several VPM schedules to the USN deep-sea helium tables [31,55], which were created by Momsen in 1939 and modified by Molumphy in 1950 [58,59]. The excursion depths must be converted to helium partial pressures using the relationship for an open-circuit breathing apparatus [31]

$$P_{He} = (D + 33)F_{He} , \qquad (4.4)$$

where D is the depth in fsw and F_{He} is the fraction of helium in the

TABLE 7

COMPARING THE VPM AND USN HELIOX SCUBA DECOMPRESSION SCHEDULES
USING PURE OXYGEN FROM 30 FSW AND SURFACING FROM 20 FSW

BOTTOM DEPTH	BOTTOM TIME	TABLE TYPE	DECOMPRESSION STOP: HELIOX 110	100	90	80	70	60	50	40	OXYGEN 30	20	TOTAL TIME
60	170	VPM										21	24:00
		USN										20	23:00
70	115	VPM										19	22:10
		USN										15	18:10
	130	VPM										23	26:10
		USN										25	28:10
80	80	VPM										15	18:20
		USN										15	18:20
	90	VPM									2	17	22:20
		USN										20	23:20
	100	VPM									3	20	26:20
		USN										25	28:20
90	70	VPM									3	15	21:30
		USN										15	18:30
	85	VPM								1	4	19	27:30
		USN										25	28:30
100	50	VPM									3	11	17:40
		USN										15	18:40
	60	VPM								3	3	15	24:40
		USN										20	23:40
	70	VPM								4	4	18	29:40
		USN									5	20	28:40
110	50	VPM								4	3	13	23:50
		USN										15	18:50
	65	VPM							2	5	5	18	33:50
		USN									5	20	28:50
120	45	VPM							2	5	3	13	27:00
		USN									5	15	24:00
	55	VPM							4	5	5	16	36:00
		USN									10	20	34:00
130	40	VPM						1	3	4	3	12	27:10
		USN									5	15	24:10
	50	VPM						2	5	4	5	16	36:10
		USN								5	5	20	34:10

TABLE 7 (CONTINUED)

COMPARISON OF VPM AND USN HELIOX SCUBA DECOMPRESSION SCHEDULES
USING PURE OXYGEN FROM 30 FSW AND SURFACING FROM 20 FSW

BOTTOM DEPTH	BOTTOM TIME	TABLE TYPE	DECOMPRESSION STOP: HELIOX 110	100	90	80	70	60	50	40	OXYGEN 30	20	TOTAL TIME
140	35	VPM						2	3	4	3	11	27:20
		USN									5	15	24:20
	45	VPM					1	3	4	5	5	15	37:20
		USN								5	5	20	34:20
150	30	VPM					1	2	2	4	3	10	26:30
		USN									5	15	24:30
	40	VPM					2	3	4	5	4	15	37:30
		USN								5	10	20	39:30
160	20	VPM						1	2	2	2	5	16:40
		USN									5	10	19:40
	35	VPM				1	2	3	4	5	3	14	36:40
		USN								5	10	20	39:40
170	20	VPM					1	1	2	2	2	6	18:50
		USN									5	10	19:50
	35	VPM			1	2	2	3	5	4	4	15	40:50
		USN								5	10	20	39:50
180	20	VPM				1	1	2	2	2	3	7	26:00
		USN								5	5	10	25:00
	30	VPM			2	1	2	3	4	5	3	13	41:00
		USN								5	10	20	40:00
190	20	VPM			1	1	1	2	2	3	3	7	25:10
		USN								5	5	15	30:10
	30	VPM		1	2	1	2	4	4	5	4	14	42:10
		USN							5	5	10	20	45:10
200	20	VPM		1	1	1	2	1	2	4	3	8	28:20
		USN								5	5	20	35:20
	30	VPM	1	1	2	2	2	4	4	5	5	14	45:20
		USN							5	5	10	25	50:20

breathing-gas mixture. In addition, a shift to pure oxygen must be made at the 50 fsw stop (if included), and surfacing is done from 40 fsw. Momsen's calculations specify that the residual nitrogen is to be treated as helium, and the modification by Molumphy merely changes the first pure-oxygen stop from 60 to 50 fsw to avoid oxygen toxicity [31]. For an inert-gas fraction of 0.75, the depth and partial pressure are equal at 100 fsw. We begin by comparing the USN deep-sea, USN SCUBA, and VPM tables for 30, 60, 120, and 240-min bottom times at that depth. The results are summarized in Table 8.

For a 30-min bottom time and a 100-fsw partial pressure, the deep-sea helium tables require a total stop time of 24 min, all of which is spent breathing pure oxygen at 40 fsw. If we follow the table - instructions [55] and double the bottom time to account for working at depth, the total stop time is 47 min, again on oxygen. However, the USN helium SCUBA tables list 35 min as the maximum no-decompression exposure at 100 fsw. Our 30-min dive falls within this limit, and we would thus be permitted to come directly to the surface. Herein lies an apparent inconsistency between two USN tables that are normally listed together. Similar observations can be made about many of the other no-stop limits. It is clearly impossible for the VPM schedule to match both sets of USN decompression criteria. In fact, the VPM requirements for this dive are 6 min on oxygen at 40 fsw, or, from the helium SCUBA table, 10 min while breathing the normal gas mixture .

Looking at the 60-min bottom time, the deep-sea table lists 47 min decompression on oxygen at 40 fsw, or 67 min if work is performed. The corresponding USN SCUBA table requires only 30 min on the normal

TABLE 8

COMPARING THE VPM, USN DEEP-SEA, AND USN SCUBA HELIUM DECOMPRESSIONS FROM 100 FSW

(ALL DEPTHS ARE IN FSW, ALL TIMES ARE IN MINUTES, AND ALL BREATHING MIXTURES ARE 75/25 HELIUM-OXYGEN OR 80/20 OXYGEN-HELIUM, WITH THE FIRST GAS BEING LISTED)

BOTTOM TIME	TABLE TYPE	WAIT AT STOP DEPTH: 50	40	30	20	10	TOTAL TIME	BREATHING GAS
30	VPM		6				7:40	OXYGEN
	VPM (SCUBA)			1	3	6	11:40	HELIUM
	USN (DEEP SEA)		24				27:00	OXYGEN
	USN (SCUBA)			(NO-STOP)			1:40	HELIUM
60	VPM		20				21:40	OXYGEN
	VPM (SCUBA)		5	6	12	19	43:40	HELIUM
	USN (DEEP SEA)		47				50:00	OXYGEN
	USN (SCUBA)				10	20	31:40	HELIUM
120	VPM	1	47				48:40	OXYGEN
	VPM (SCUBA)	3	11	18	26	43	102:40	HELIUM
	USN (DEEP SEA)		67				70:00	OXYGEN
	USN (SCUBA)			(NOT LISTED)				HELIUM
240	VPM	5	98				104:40	OXYGEN
	VPM (SCUBA)	11	23	38	58	93	224:40	HELIUM
	USN (DEEP SEA)		75				78:00	OXYGEN
	USN (SCUBA)			(NOT LISTED)				HELIUM

(NOTE: USN DEEP-SEA SCHEDULES REQUIRE 3 MIN FOR ASCENT TO FIRST STOP)

breathing mixture. The VPM results give 20 min on oxygen at 40 fsw, or 42 min from the helium SCUBA table. A pattern is beginning to emerge, in which the USN deep-sea tables appear to be more restrictive than either the USN SCUBA tables or the VPM predictions.

For the 120-min dive, the deep-sea tables use oxygen for 67 min at 40 fsw, or 75 min (working). The USN SCUBA tables do not extend that far, and the VPM prediction is 48 min on oxygen beginning at 50 fsw, which again seems quite short.

In the last dive, which has a 240-min bottom time, a change in the previous trend is seen. The deep-sea tables list 75 min on oxygen at 40 fsw, while the VPM result is 103 min beginning at 50 fsw. This inversion is to be expected as the bottom times increase since the USN calculations employ half-times terminating with 100 min [31], while the VPM basis set extends to 240 min.

Our original objective in this chapter was to create new VPM helium tables by extending the knowledge gained during the previous setting of the model parameters for air dives. We have achieved this goal, in part, by generating what appear to be viable helium no-stop, regular mixed-gas, and oxygen-assisted SCUBA decompression schedules. However, the internal inconsistencies in the USN tables preclude their use as a benchmark. The new VPM tables, by incorporating the common over-simplification of treating nitrogen as helium, may contain decompression profiles that are inadequate for a diver who is typically saturated with nitrogen at the onset of a dive. Further comparisons with empirical data are required to determine the extent of this inadequacy and to evaluate our method for its alleviation.

B. RESIDUAL NITROGEN

In order to gauge the effect that residual nitrogen has on the VPM helium tables, the computer program was modified to include an initial nitrogen partial pressure in each tissue. The only difference, then, is that the initial pressure is allowed to decay at the slower nitrogen rate. The uptake of helium is the same, with the exception that it starts from zero. At any time, the instantaneous nitrogen and helium partial pressures are combined to find the total tension in the controlling tissue. Since helium enters each tissue faster than the nitrogen escapes, the net tension is, for a period of limited duration, higher than it would be if either nitrogen or helium were used alone, and the resultant tables are more restrictive. For lengthy saturation dives, of course, the residual-nitrogen helium tables are identical to the pure helium tables. The programming additions are described in more detail in Chapter VI.

As before, we begin with the no-stop decompressions. Several empirical points [60,61] are listed in Table 9 with the new residual-nitrogen VPM limits. The data from Table 4 are replotted with these new points in Fig. 19. The residual-nitrogen curve is consistently lower (more conservative) than the original VPM helium curve, which is to be expected. It seems unlikely that overt bends symptoms would occur for any of the tables at the shallower depths, where the VPM lines diverge. However, the VPM curves are lines of constant released-gas volume, and the lack of bends symptoms does not preclude copious bubble formation. Looking at the center portion of the graph, the bends point at 116 fsw, 18 min [60] lies below the USN points and uncomfortably

TABLE 9

VPM RESIDUAL-NITROGEN NO-DECOMPRESSION LIMITS FOR HELIUM DIVES

DEPTH IN FSW	ALLOWED TIME IN MIN	(BENDS/NO BENDS POINTS ESTIMATED FROM HILLS' FIG. 67B [60]) DEPTH IN FSW	TIME IN MIN	BENDS
30	112	56	120	NO
40	59	61	240	NO
50	40	79	240	YES
60	29	91	120	YES
70	22	115	17	NO
80	18	127	18	YES
90	15			
100	13			
110	10			
120	9			
130	8			
140	7			
150	6			
160	5			
170	5			
180	4			
190	4			
200	4			

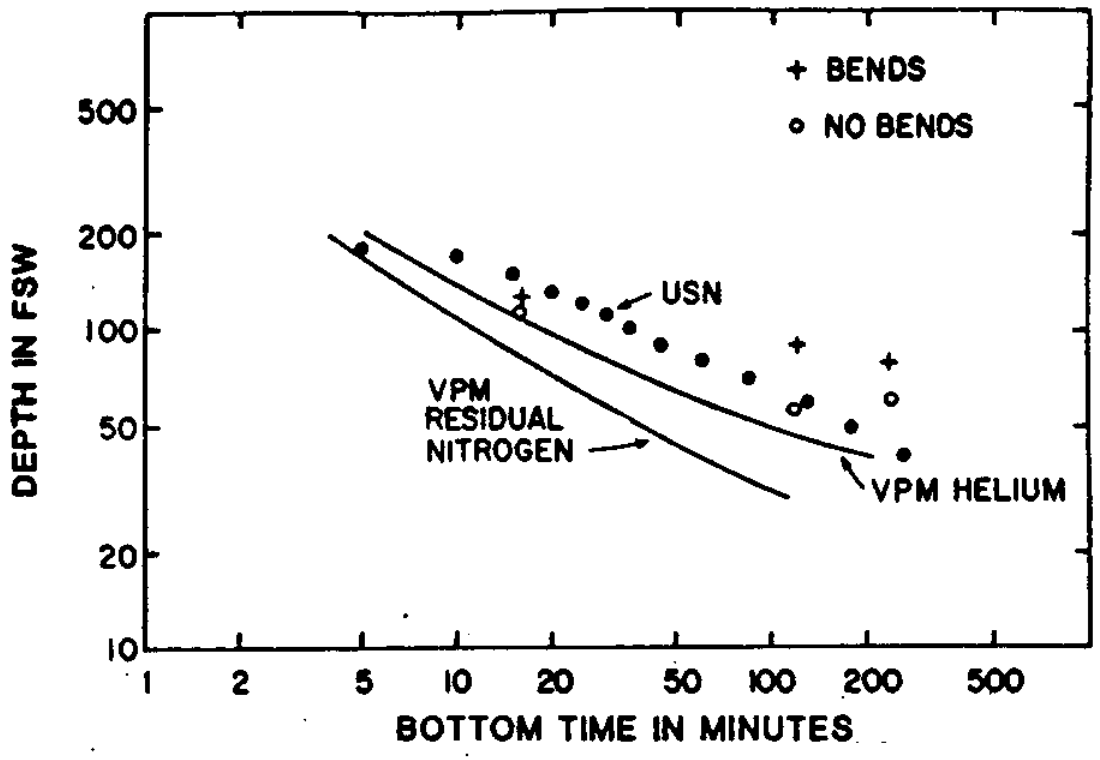

Fig. 19 - Plot of VPM residual nitrogen, VPM helium, and USN no-stop decompression limits. Several data points are included for reference. The VPM residual nitrogen curve lies in the safer region below the USN points and regions of bends incidence.

close to the VPM helium curve, indicating that the newer VPM prediction is not only safer, but necessary. All of the tables have similar limits for the deepest dives.

Our next comparison with empirical data utilizes the titration points developed by Buhlmann [41] in a series of 100-fsw dives. His method involved shortening the last stop of a comparatively-safe decompression to produce bends in nitrogen, helium, and mixed-gas dives. In each case, the divers were saturated with nitrogen at the onset of the dive.

First, we consider a bottom time of 120 min breathing 79% helium throughout the dive. Buhlmann's data indicate that a total decompression time of 316 min resulted in no bends in 20 subjects, but 232 min gave bends in 3 of 8 subjects. The USN SCUBA tables do not extend to this bottom time. However, the VPM helium SCUBA tables, which have generally-longer decompression times at 100 fsw than do their USN equivalents, predict a total decompression time of 140 min, far below the bends threshold. This unsafe condition is resolved in the VPM residual-nitrogen tables, which list the much safer time of 409 min. Of course, the shape of the profile influences the outcome, but Buhlmann's schedule is quite similar to the new VPM result, as shown in Fig. 20.

Next, the bottom times of 23 and 35 min for divers using 79% helium (exclusively) are compared. For the former, Buhlmann gives no bends in 12 subjects for a 27-min total decompression time, and bends in 6 of 12 subjects for an 18-min ascent. This 23-min bottom time is far below the 35-min no-stop limit given in the USN 75% helium SCUBA tables, once again suggesting that they are unsafe. The VPM helium prediction is

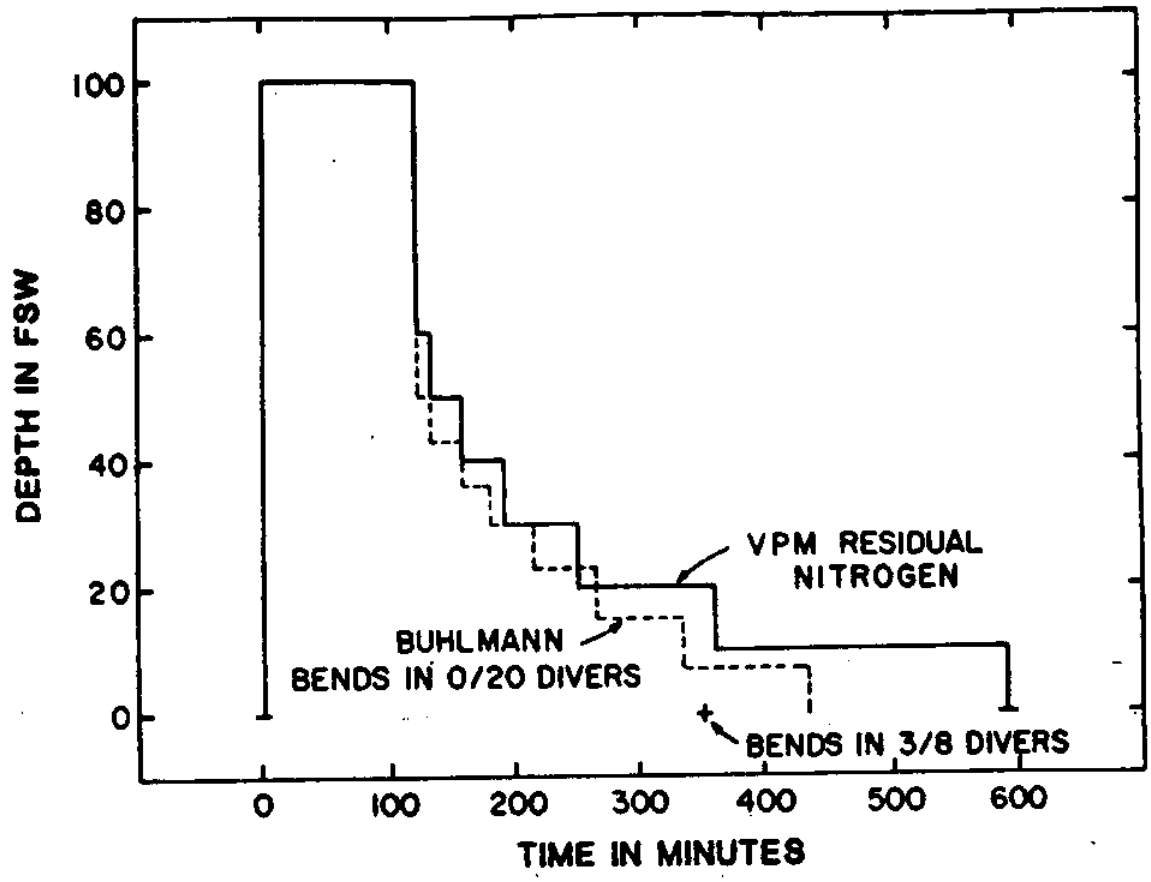

Fig. 20 - Plot of VPM residual nitrogen and Buhlmann's schedules for a 120-min, 100-fsw excursion. The profiles are quite similar, but the VPM total time is farther from the bends threshold.

also suspect, allowing only 9 min total decompression time. In contrast, the VPM residual-nitrogen helium tables are quite safe, requiring 53 min total decompression. For the 35-min bottom time, Buhlmann lists only one point, in which no bends in 19 divers were reported for an 80-min ascent. Although some decompression would be required by the USN SCUBA tables if the additional 4% inert gas were taken into account, it is unlikely that it would be more than a few minutes. The VPM helium tables give 17 min, still far too short, while the VPM residual-nitrogen result is a respectable 104 min.

In our final comparison with Buhlmann's titrations, we look again at the 120-min bottom time, but replace helium with oxygen as the breathing gas during the entire decompression period. No bends in 12 subjects were found for 83 min total decompression time, and 3 of 8 were bent in a 65-min ascent. The USN deep-sea table, for the equivalent 105-fsw helium partial pressure, requires a comparable 81 min, while the VPM residual-nitrogen prediction is 93 min. Although the USN deep-sea tables seem reasonably safe thus far, they are not expected to be valid for dives with bottom times greatly in excess of 120 min because they use the short (100-min) maximum tissue half-time [31].

In this section we have extended the VPM helium tables to include the nitrogen that is present in the diver at the onset of most SCUBA and surface-supplied dives. The new residual-nitrogen tables have been shown to correspond very well with the empirical data from two different sources. In contrast, the unaltered VPM and USN helium SCUBA tables are seen to provide inadequate decompressions. The new total decompression times versus bottom times are plotted in Fig. 21 for 60, 100, and

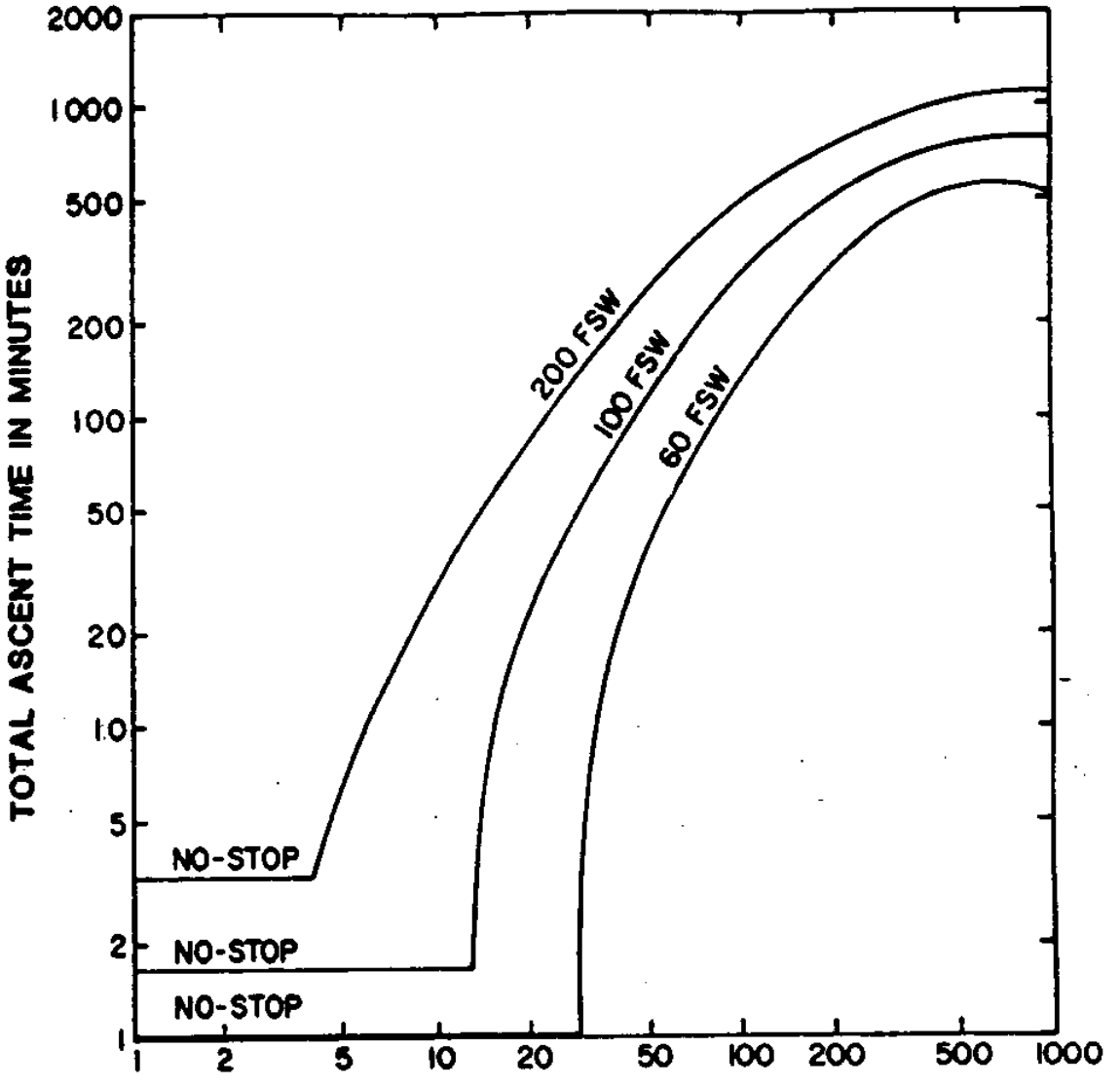

Fig. 21 - Plot of VPM residual-nitrogen helium total ascent times versus bottom times for 60, 100, and 200-fsw dives. The more-restrictive limits shift the curves to the left of those in Fig. 18.

200-fsw excursions and for bottom times to 960 min, using a 75% helium, 25% oxygen mixture. The curves are displaced to the left and above those in Fig. 18, corresponding to the more-restrictive limits, and they begin to slope downward near the 1000-min bottom time as the helium uptake falls below the nitrogen elimination.

C. CONSIDERING DEEP AND SATURATION DIVES

We have neglected dives deeper than 200 fsw on 75% helium because the high partial pressure of oxygen might result in oxygen toxicity. However, this depth limit may be increased by increasing the percentage of inert gas and by decreasing the bottom time. In the following series, we compare the USN deep-sea and VPM residual-nitrogen tables to the empirical points determined by Elliott [62] for four 270-fsw, 20-min dives conducted in a wet chamber (Fig. 22).

The first of these four dives (Fig. 22a), in which the subjects breathed 80% helium throughout and spent 156 min decompressing, resulted in bends in 8 of 25 working divers and 5 of 21 "attendants." The VPM residual-nitrogen tables require only 136 min total decompression time for this exposure, indicating that the margin of safety given by the shallower VPM tables has dwindled. We therefore invoke the prerogative which was established in Chapters III and IV, and decrease the threshold crushing pressure P^*. The air schedules in Chapter III will also be affected by any change in P^* introduced here. Fortunately, both sets of tables suffer from the same malaise and can be adjusted simultaneously. Following several air and helium trials, the lower value of 5 atm for P^* is found to cause a modest increase in the decompression times for dives

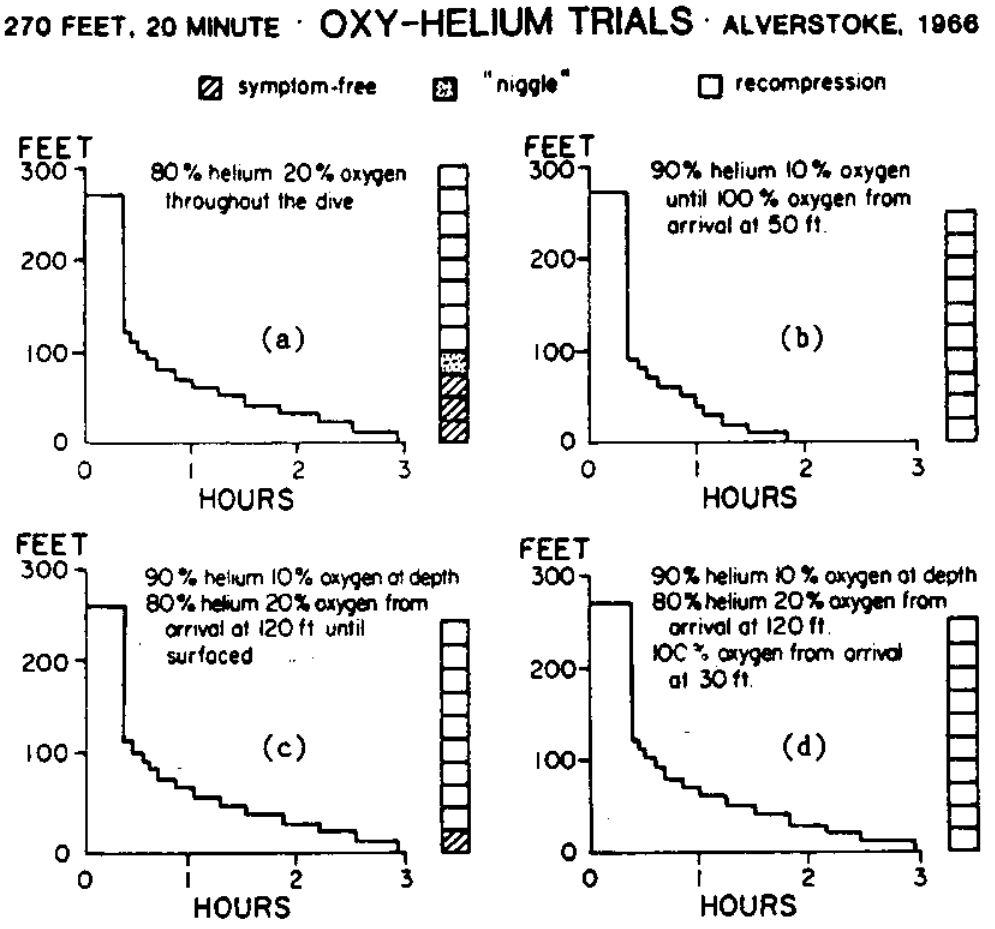

Fig. 22 - Four 20-min, 270-fsw excursions on various gas mixtures. Note the benefit of the oxygen stages in schedules (b) and (d). (Adapted from Elliott [62]).

deeper than 200 fsw. The resultant VPM output for the dive in Fig. 22a is given in Table 10. Although the total times for the two dives are still similar, the VPM schedule is expected to be safer because the first stop is at 180 fsw, nearly two atmospheres deeper than the 120-fsw first stop of Elliott. As noted in earlier chapters, the shorter "first pull" of the VPM schedule is expected to slow bubble formation and reduce the volume of released gas.

Over a two-week interval prior to each of the succeeding three dives, the subjects were given a series of short "acquainting" exposures to 180, 250, and 300 fsw. Also, the inert-gas fraction was raised to 90% for the duration of the bottom time and for the beginning of the ascent. The extra inert gas makes the corresponding VPM schedules more restrictive, increasing the depth of the first stop to 220 fsw and extending the total decompression times.

Following the profile of the second dive (Fig. 22b), the subjects breathed oxygen from 50 fsw to the surface. No bends were reported for a total decompression time of 90 min. The USN deep-sea table requires 121 min for the equivalent 272 fsw helium partial pressure (also breathing oxygen from 50 fsw, but surfacing from 40 fsw). The VPM total time is 201 min.

In the third 270-fsw dive (Fig. 22c), the 90% helium mixture is reduced to 80% upon arrival at 120 fsw. Only 1 of 10 men had bends symptoms while following the same decompression profile that was used in the first dive. The lower bends incidence in this harsher exposure provides direct evidence for the beneficial effect of acclimitization. From the VPM viewpoint, the removal of bubble nuclei during each ascent

TABLE 10

VPM RESIDUAL-NITROGEN PROGRAM OUTPUT FOR A 20-MIN, 270-FSW HELIUM DIVE

```
**************************
* TINY BUBBLES 05/05/85 *
**************************

** VALUES OF THE INPUT PARAMETERS **
GAMMA  =  17.90 DYN/CM
GAMMAC = 256.90 DYN/CM
PSTAR  =   5.00 ATM
RZERO  =   .700 MICROMETER
REGEN  = 20160. MINUTES
LAMBDA =  7500. FSW-MIN
INERT  = .80    HELIUM
INCLUDING RESIDUAL NITROGEN

** DIVE PROFILE **
MANEUVER 1  DEPTH =    .00 FSW  TIME =     .00 MIN
MANEUVER 2  DEPTH = 270.00 FSW  TIME =    4.50 MIN
MANEUVER 3  DEPTH = 270.00 FSW  TIME =   20.00 MIN

** DECOMPRESSION SCHEDULE ** ITERATION NUMBER  3   **
*****************************************************
*  FOR THE EXCURSION TO DEPTH = 270.00 FSW          *
*****************************************************
* TIME SPENT AT INITIAL DEPTH =    20.00 MIN        *
*****************************************************
* STOP *  DEPTH *  WAIT  * TISSUE *   TAU  *   PSS  *
*    1 * 180.00 *   1.00 *   3.33 * 193.98 *  29.44 *
*    2 * 170.00 *   1.00 *   3.33 * 181.89 *  29.44 *
*    3 * 160.00 *   1.00 *   6.67 * 174.65 *  30.80 *
*    4 * 150.00 *   1.00 *   6.67 * 169.04 *  30.80 *
*    5 * 140.00 *   2.00 *   6.67 * 158.52 *  30.80 *
*    6 * 130.00 *   2.00 *   6.67 * 148.41 *  30.80 *
*    7 * 120.00 *   2.00 *   6.67 * 138.64 *  30.80 *
*    8 * 110.00 *   2.00 *   6.67 * 129.14 *  30.80 *
*    9 * 100.00 *   4.00 *  13.33 * 120.56 *  31.95 *
*   10 *  90.00 *   5.00 *  13.33 * 110.63 *  31.95 *
*   11 *  80.00 *   5.00 *  13.33 * 100.98 *  31.95 *
*   12 *  70.00 *   5.00 *  13.33 *  91.57 *  31.95 *
*   13 *  60.00 *   8.00 *  26.67 *  82.62 *  32.70 *
*   14 *  50.00 *  13.00 *  26.67 *  72.41 *  32.70 *
*   15 *  40.00 *  14.00 *  40.00 *  62.59 *  32.95 *
*   16 *  30.00 *  22.00 *  40.00 *  52.68 *  32.95 *
*   17 *  20.00 *  30.00 *  53.33 *  43.03 *  33.06 *
*   18 *  10.00 *  49.00 *  80.00 *  33.08 *  33.13 *
*****************************************************
* TOTAL TIME TO REACH SURFACE =   171.50 MIN        *
*****************************************************
```

and the long time required for their regeneration result in a depleted nuclear population and a larger allowed supersaturation. However, the current model contains no provision for acclimitization. The VPM total time for this dive is 288 min, far longer than the inadequate 156-min ascent time.

The helium mixture in the final dive (Fig. 22d) is also reduced to 80% at 120 fsw, but a switch to pure oxygen is made at 30 fsw. In this case, no bends result from the 156-min decompression. The VPM total time is slightly longer at 187 min. This dive again illustrates the efficacy of pure-oxygen stages.

It is well-known that decompressions from saturation dives are controlled by the longest tissue half-time. The result is always a linear ascent, provided the partial pressure rather than the percentage of oxygen is maintained at a constant value [31,54]. The VPM residual-nitrogen program was thus modified (as described in Chapter VI) to assume a constant oxygen partial pressure of 0.5 ata, which forces the inert-gas fraction to vary continuously. In this last test, we compare the VPM residual-nitrogen predictions for saturation dives to to several long exposures described by Bornmann [63].

First, we consider the Sealab II experiment [63], in which divers were subjected to a pressure of 204 fsw for two-week periods. Using an ascent rate of 10 min/fsw, some 28 successful decompressions were conducted with only one instance of mild bends pain. Considering the length of the exposure, which is comparable to the value assumed for the regeneration time constant, some nuclear regeneration would be expected to occur. The VPM output reflects this in a slower rate, 13.6 min/fsw.

Note that all the nitrogen has escaped at depth, so the rate is constant and depends upon the longest helium half-time.

Next, in one of a set of USN EDU exposures, two subjects spent 24 hours at 300 fsw and were decompressed linearly at 8.25 min/fsw. A helium mixture containing 0.5 ata oxygen was supplied during the entire time under pressure. One man experienced slight knee pain at 55 fsw and was recompressed, while the other was unaffected. The modified VPM residual-nitrogen program requires a decompression rate that varies slightly, from 10.0 min/fsw at the start to 9.1 min/fsw at the end. The rate reduction occurs because the 24-hour bottom time is sufficient for helium saturation but not for nitrogen elimination. Lastly, subsequent exposures were made to 300 and 400 fsw by different pairs of divers. All were decompressed at 11 min/fsw without incident.

In this chapter, we have progressed through three variations of the VPM tables for helium. We successfully matched the USN helium SCUBA tables by assuming a simple, single-gas model and using the constants and free parameters derived from the air-table calculations. When it was found that these tables were unsafe, we modified the program to include the partial pressure of the residual nitrogen held by those divers who switch from air to helium just prior to diving. Finally, the problem of inadequate decompression from excursions beyond 200 fsw, which was suspected to exist in the air tables as well, was brought to light and corrected by decreasing the threshold crushing pressure. The VPM air and helium computer programs listed in Appendices 1 and 2, which contain these additions and settings, are expected to supply reasonable decompression solutions for a wide range of diving situations.

CHAPTER VI

A. NOTES ON THE APPENDICES

A documented FORTRAN program listing for air dives is given in Appendix 1. Appendix 2 contains its BASIC counterpart, modified for helium dives with residual nitrogen. An alphabetical list of all the program variables, with short descriptions, is provided in Appendix 3. Prior to any depth excursion, all tissue compartments are assumed to be saturated at some initial pressure P_o with either nitrogen or helium. Repetitive exposures are not considered. The results presented in Chapters III and V are based on a total initial pressure of 1 atm abs, although the FORTRAN input routine will accommodate an arbitrary starting depth. For simplicity, the BASIC version automatically sets the initial depth at the surface and the excursion speed at 60 fsw/min. The programs require 3 to 8 iterations to run to completion, each being of similar duration. Generally speaking, the longest decompressions will need the fewest iterations because they have the smallest supersaturation augmentation. Aside from these minor differences, the program algorithms are identical, and all further descriptions refer to both the FORTRAN and the BASIC versions unless specifically stated otherwise.

Because the documentation supplied in the appendices is extensive, we present only the fundamental principles of the program operation in this chapter. The reader may wish to consult the appropriate appendi in order to relate our discussion to specific program steps or variables.

B. THE MAIN BODY

The method of converting the equations of Chapters I and II into decompression schedules is actually quite straightforward. The tissue tension is updated by subroutine TAU, while the maximum allowed tissue supersaturation and the corresponding allowed depth are calculated by subroutine DEP. The input and output profiles are handled by subroutines INPUT and OUTPUT, respectively, leaving only bookkeeping functions for the MAIN BODY. These functions come under the headings of initiation, timing, storage, and iteration. Each will be covered in this section.

Program initiation takes place in several stages. First, some of the variables and all of the model constants are defined. The FORTRAN variables are identified in common block statements to minimize memory overhead, and the subroutines have been written using the same variable names as the main body, where applicable, to reduce confusion. All arrays are defined in the BASIC version through dimension statements. Next, the free parameters of the model are defined as constants, and the INPUT subroutine is called. The input formats are described in detail later in this chapter and in the program documentation.

After the input routine, the tissue compartments (matrix HALFTI) are filled with the constant half-times selected to span the range between very short and very long tissues. The descent speed is set equal to the initial depth divided by the duration of the descent (always 60 fsw/min for the BASIC version), and the ascent speed is set equal to the descent speed. A different ascent speed (variable ASPEED) can be inserted here if required.

The inert-gas tension in each tissue compartment (matrix CPTO) is set equal to the product of the starting depth and the inert-gas fraction (variable FR), and the descent to the bottom is made by calling subroutine TAU to find the subsequent tissue tensions. Finally, the minimum critical radius r_m for each tissue compartment (matrix RM) is calculated from Eq. (1.6) using the method detailed by Eqs. (1.8-1.14). This matrix is used by subroutine DEP in the calculation of the allowed supersaturation. Having completed the initiation sequence, the program begins the calculation of decompression stops.

The timing sequence is started by setting the internal clock (variable TIM) equal to the total elapsed time prior to surfacing. Subroutines TAU and DEP are called to determine the shallowest allowed depth (variable DEPNEW), which is then rounded off to the next deeper depth increment. That increment (variable AJUMP) is presently defined to be 10 fsw, but it can be changed if desired. The current time and depth are recorded (as variables TIMEO and DEPTH), and an ascent to the first stop is accomplished by adding the calculated ascent time (variable AT) to the clock and setting the current depth (interim variable DEPOLD) equal to the allowed depth. During long "first pulls," the controlling tissue half-time may change, so the allowed depth is recalculated after making the ascent. If it is found to be deeper than the previously-calculated first stop, the ascent is retracted by restoring the recorded time and depth, and a safer ascent is made to the deeper first stop.

All further decompression stops are made in fixed depth increments (the size of which is determined by AJUMP). The internal clock is

shifted to count one-minute intervals, and a comparison is made after each interval to determine whether the new allowed depth returned by DEP permits an incremental ascent. If so, an ascent to the next stop (variable DNEXT) is made. This process is repeated until the surface is reached.

Every time a decompression stop is completed, the stop number (loop index M), stop depth (matrix ADEP), stop duration (matrix ADUR), controlling tissue half-time (matrix AHT), controlling tissue tension (matrix ADPT), and allowed supersaturation (matrix APSS) are stored in the common block. Also, the total time required to reach the surface, measured from the start of the first ascent, is calculated and recorded (in variable DTIME) for use in subsequent program iterations. These values comprise the bulk of the desired decompression schedule and will be printed by subroutine OUTPUT if the program is on the last iteration.

It was mentioned in Chapter II that the allowed supersaturation, given by Eq. (2.20), is dependent upon the total decompression time (DTIME) and must be iterated to convergence. For the first iteration, the decompression time is zero, and the resultant schedule corresponds to the no-bubble safe-ascent criterion. The second iteration of the augmented supersaturation equation uses the decompression time found in the first, and so on for each subsequent iteration until two successive passes produce the essentially same value for DTIME. The entire program, with the exception of the initialization steps, must be repeated until DTIME converges. The number of iterations (variable IT) and the decompression schedule are then printed when subroutine OUTPUT is called.

C. THE INPUT SUBROUTINE

This edition of the program is specifically designed to calculate decompression schedules for "square-wave" dives, that is, for profiles which begin at the surface, transit downward, remain at constant depth throughout the remainder of the bottom time, and return to the surface. As mentioned earlier, the BASIC input routine has been modified to accept only an excursion depth and bottom time, while the FORTRAN routine requires three specific points in the profile. The input format for each is detailed in Table 11.

The INPUT subroutine first prints the program header, containing the title and the date of the last revision. In the FORTRAN version, the COMMON/SIX statement passes the values of the model parameters from the MAIN BODY to INPUT, which prints them to logical unit 2. Then the dive profile is read from logical unit 1 and printed on unit 2. The profile is made available to the other program sections via COMMON/ THREE. The BASIC program inputs from and outputs to the terminal device (keyboard/CRT). A sample of the complete program output is presented presented in Table 12, which contains all the information printed by subroutine INPUT and by subroutine OUTPUT.

The FORTRAN input allows the descent speed to be varied since a different time of arrival at the bottom corresponds to a different descent rate. The ascent rate is always the same as the descent rate unless the variable ASPEED is redefined. Again, the BASIC version automatically assumes 60 fsw/min rates for descent and ascent.

TABLE 11

FORTRAN INPUT FORMAT

The FORTRAN input routine reads three lines, each having format 2f8.2. As an example, the input for a 200-fsw, 60-min dive starting from the surface and descending at 60 fsw/min is:

(Depth)	(Time)	
0.00	0.00	(Start the descent here.)
200.00	3.33	(Arrive at the bottom.)
200.00	60.00	(Start the ascent here.)

The descent speed is determined by the time of arrival at the bottom (shown on line two). The ascent speed will automatically be set equal to the descent speed. To be consistent with various existing tables, the "bottom time" (shown on line three) includes the time required for descent.

BASIC INPUT FORMAT

The BASIC user will be prompted by

" PLEASE INSERT EXCURSION DEPTH, TIME?"

To input the example dive profile given above, only the information in line three is required, and the user's response would be

200.00, 60.00

All descent and ascent rates in the BASIC version are preset in the INPUT subroutine to 60 fsw/min.

TABLE 12

FORTRAN SAMPLE OUTPUT

```
**************************
* TINY BUBBLES 05/05/85 *
**************************

** VALUES OF THE INPUT PARAMETERS **
GAMMA  =  17.90 DYN/CM
GAMMAC = 256.90 DYN/CM
PSTAR  =   5.00 ATM
RZERO  =   .800 MICROMETER
REGEN  = 20160. MINUTES
LAMBDA =  7500. FSW-MIN
INERT  = .79    NITROGEN

** DIVE PROFILE **
MANEUVER 1  DEPTH =    .00 FSW  TIME =      .00 MIN
MANEUVER 2  DEPTH = 200.00 FSW  TIME =     3.33 MIN
MANEUVER 3  DEPTH = 200.00 FSW  TIME =    60.00 MIN

** DECOMPRESSION SCHEDULE ** ITERATION NUMBER  3   **
*****************************************************
*  FOR THE EXCURSION TO DEPTH = 200.00 FSW          *
*****************************************************
* TIME SPENT AT INITIAL DEPTH =    60.00 MIN        *
*****************************************************
* STOP *  DEPTH *  WAIT  * TISSUE *   TAU  *   PSS  *
*    1 * 140.00 *    .00 *   5.00 * 152.32 *  26.66 *
*    2 * 130.00 *   2.00 *  10.00 * 144.22 *  27.28 *
*    3 * 120.00 *   2.00 *  10.00 * 137.02 *  27.28 *
*    4 * 110.00 *   3.00 *  10.00 * 126.68 *  27.28 *
*    5 * 100.00 *   5.00 *  20.00 * 116.67 *  27.64 *
*    6 *  90.00 *   6.00 *  20.00 * 107.44 *  27.64 *
*    7 *  80.00 *   7.00 *  20.00 *  97.18 *  27.64 *
*    8 *  70.00 *   7.00 *  20.00 *  87.43 *  27.64 *
*    9 *  60.00 *  12.00 *  40.00 *  77.46 *  27.75 *
*   10 *  50.00 *  16.00 *  40.00 *  67.58 *  27.75 *
*   11 *  40.00 *  17.00 *  40.00 *  57.69 *  27.75 *
*   12 *  30.00 *  25.00 *  80.00 *  47.51 *  27.70 *
*   13 *  20.00 *  39.00 *  80.00 *  37.67 *  27.70 *
*   14 *  10.00 *  56.00 * 120.00 *  27.52 *  27.62 *
*****************************************************
* TOTAL TIME TO REACH SURFACE =   200.33 MIN        *
*****************************************************
```

D. THE TISSUE TENSION SUBROUTINE

Subroutine TAU calculates any changes in the tensions of the various tissues. The MAIN BODY initializes the inert gas tension in all the compartments (matrix CPTO). Then TAU is called to find the total gas tensions after every subsequent excursion, including those which merely mark time and result in no depth change. Each excursion is represented by an initial depth (variable DEPTHO), an ascent or descent speed (variable SPEED), and a duration (variable DUR). When SPEED is set to zero, the program marks time (hovers). The FORTRAN version passes these variables to TAU via COMMON/ONE, and the inert gas tensions are returned through COMMON/TWO (in matrix CPT) to the MAIN BODY, where they will be stored (again in matrix CPTO) as the "initial" tensions for the next excursion.

The calculation of the total gas tension is performed separately for each tissue compartment, using the method outlined in section B of Chapter II. First, the contribution of the active gases is found (variable ACT). Next, all of the half-times stored in matrix HALFTI are successively inserted into Eqs. (2.28) and (2.29), resulting in a new inert gas tension for each tissue (matrix CPT). Finally, the two contributions are added to obtain the total tissue tensions. If residual nitrogen is included, there will be another term (variable DNITRO) added to each total. The residual nitrogen modification will be discussed in section G. Subroutine DEP receives the tissue tensions (in matrix DPT) and utilizes them in the determination of the allowed depth. In the FORTRAN version these variables are passed via COMMON/THREE and COMMON/FOUR.

E. THE ALLOWED-SUPERSATURATION SUBROUTINE

Subroutine DEP calculates the allowed supersaturation, finds the tissue compartment that is "controlling" the ascent, and predicts the allowed depth. Since square-wave dives always result in the selection of progressively longer controlling tissue half-times during decompressions, a compartment index (variable J) is used to represent the minimum compartment number to be used whenever a loop over all the compartments is made. This feature significantly shortens the program execution time and is essential for microcomputer operation. Each time DEP is called, the compartment index is updated to correspond to the current controlling tissue. All further loops over the tissue compartments will begin with the compartment index (variable J) and end with the highest compartment number (constant NTC).

For the FORTRAN program, DEP is interfaced through the use of common blocks. The tissue tension and half-time (matrices DPT and HALFTI), maximum crushing pressure (matrix PCRUSH), and minimum critical radius (matrix RM) are made available for each selected compartment through COMMON/THREE and COMMON/FOUR. The model parameters and some other pre-defined constants are passed via COMMON/SIX and COMMON/SEVEN, and the total decompression time from the previous program iteration (variable DTIME) enters via COMMON/NINE. The allowed supersaturation (variable PSSJ), the controlling tissue compartment tension (variable DPTJ), and the allowed depth (variable DEPNEW) are returned to the MAIN BODY through COMMON/EIGHT, while the controlling tissue compartment index (variable J) enters and exits through COMMON/ONE. All of these variables are the same in the BASIC version.

The first step in determining the allowed supersaturation is to apply Eq. (2.30), which adjusts the minimum critical radius for regenerative growth. The no-bubble supersaturation (variable PSAFE) is then calculated from Eq. (1.4), and the augmented supersaturation (variable PNEW) is found using Eqs. (2.16-2.20). Following Eq. (2.22), the new allowed supersaturation is subtracted from the current tissue tension to find the allowed depth. Each time a new tissue compartment is used, the resultant allowed depth (variable DEPA) is compared to the maximum depth predicted by previously-used compartments (variable DOLD), and the larger of the two is retained (in variable DNEW), along with its corresponding compartment index (variable J) and its current tension (variable DPTJ). After all the compartments have been tried, the one which remains will be the controlling compartment and will result in the deepest (most restrictive) allowed depth. This new allowed depth (variable DEPNEW) is then passed to the MAIN BODY, as are the corresponding allowed supersaturation, the controlling tissue compartment tension, and the compartment index. Whenever a decompression stop is completed, these variables and others are used by the MAIN BODY to prepare information for subroutine OUTPUT.

F. THE OUTPUT SUBROUTINE

Subroutine OUTPUT writes the decompression schedule to logical unit 2 (or to the CRT in BASIC). A representative sample of the FORTRAN program output is given in Table 12, and the BASIC output is nearly identical. Of course, subroutine INPUT is responsible for printing the header, the model parameters, and the dive profile, leaving only the

printing of the decompression schedule to OUTPUT. Again, the variables are identical in the BASIC and FORTRAN versions. In the FORTRAN program, the number of program iterations required for convergence (variable IT), the number of decompression stops (variable M), and the total decompression time (variable DTIME) are transferred from the MAIN BODY through COMMON/NINE. In addition, the excursion depth (included in matrix DDEPTH) and the bottom time (in matrix TTIME) are passed via COMMON/THREE. Lastly, the stop depth (matrix ADEP), stop duration (matrix ADUR), controlling tissue compartment half-time (matrix AHT), controlling tissue tension (matrix ADPT), and allowed supersaturation (matrix APSS) are all received via COMMON/FIVE.

OUTPUT begins by writing the number of iterations required for DTIME to converge. The excursion depth and bottom time are then printed, followed by the header for the decompression schedule. For each decompression stop, the stop depth, stop duration, controlling tissue compartment half-time, controlling tissue tension, and allowed supersaturation are written under separate column headings. Finally, the total time required for ascent is printed. Control is then passed back to the MAIN BODY, which ends program execution.

G. PROGRAM MODIFICATIONS

Each of the program modifications used in previous chapters will be discussed in this section. First, to convert the program from air to helium, we begin with the MAIN BODY by changing the constant RO from 0.800 to 0.700 (micrometers) and by defining the helium inert-gas fraction FRO for the dive. Next, all the half-times in matrix HALFTI

are divided by three, and the initial helium tension is set to zero by changing the line

```
CPTO(I) = FR*(DEPTHO + 33.)
```

to read

```
CPTO(I) = 0.0    .
```

For cosmetic purposes, the word "NITROGEN" may be changed to "HELIUM" in subroutine INPUT, where the inert gas fraction (variable FR) is printed, and another print line may be added to say "RESIDUAL NITROGEN INCLUDED." Residual nitrogen is added by inserting the programming line

```
DNITRO = 0.79*33.*EXP(-TIM*TWOLN/(3*HALFTI(I)))
```

into subroutine TAU immediately following the calculation of CPT(I) and by changing the definition of DPT(I) to read

```
DPT(I) = CPT(I) + ACT + DNITRO    .
```

To change the BASIC program to accommodate air dives, the reverse procedure should be followed.

To convert either program to a constant oxygen partial pressure, we set FRO in the constant definition section of the MAIN BODY equal to the initial (surface) fraction of inert gas. Then we add two lines at the beginning of subroutine TAU,

PO2 = 0.5 (defines constant O_2 pressure)

and

FR = 1 - PO2/(DEPTH + 33.).

Note that the inert-gas fraction appearing on the printout will be the surface value only.

Lastly, to include simple changes in the inert-gas fraction, we turn to the loop over the number of stops (M) in the main body. A few lines above the CONTINUE (NEXT M) statement, conditional statements may be inserted, just after the DEPTH = DNEXT assignment. For instance, to shift to 80% oxygen at 50 fsw, we add either

IF(DEPTH .LE. 50.) FR = 0.2 (FORTRAN)

or

IF(DEPTH <= 50) THEN FR = 0.2 (BASIC).

Any number of conditional statements may be added in this fashion to accommodate various shifts in the percentage of a single inert gas.

APPENDIX 1

FORTRAN PROGRAM LISTING FOR AIR DIVES

```
C            TINY BUBBLES—VERSION 05/05/85—FOR AIR DIVES
C
C                          THE TINY BUBBLE GROUP
C                          DEPARTMENT OF PHYSICS
C                            AND ASTRONOMY
C                          UNIVERSITY OF HAWAII
C                          2505 CORREA ROAD
C                          HONOLULU, HAWAII 96822
C
C
C  THIS PROGRAM ACCEPTS A SQUARE-WAVE DIVE PROFILE AND CALCULATES A
C  THEORETICAL DECOMPRESSION SCHEDULE USING THE EQUATIONS AND PARAMETERS
C  OF THE VARYING-PERMEABILITY MODEL.  THE SCHEDULES SO PRODUCED ARE NOT
C  INTENDED FOR GENERAL USE BY THE DIVING COMMUNITY, AND NO CLAIM IS
C  MADE FOR THEIR VALIDITY.  PROGRAM FEATURES INCLUDE CONTINUOUS
C  TRACKING OF THE MINIMUM NUCLEAR RADIUS REQUIRED TO FORM A MACROSCOPIC
C  BUBBLE UPON DECOMPRESSION, CONTINUOUS TRACKING OF THE TENSIONS IN
C  EACH OF SEVERAL SPECIFIED TISSUES USING A PERFUSION-LIMITED EQUATION,
C  CALCULATION OF THE ALLOWED SUPERSATURATION IN EACH TISSUE BASED ON A
C  CRITICAL VOLUME OF RELEASED GAS, AND CONSTRUCTION OF A DECOMPRESSION
C  SCHEDULE USING THE DEPTHS ALLOWED BY THOSE TISSUES FOUND TO BE
C  CONTROLLING THE ASCENT.
C
C       THE PROGRAM CONSISTS OF A MAIN BODY AND THE FOUR SUBROUTINES
C  LISTED HERE:
C
C            INPUT -- READS IN THE DIVE PROFILE.  PRINTS THE PROGRAM
C                     HEADER, THE DIVE PROFILE, AND THE MODEL
C                     PARAMETERS.
C            TAU   — CALCULATES THE TISSUE TENSIONS IN
C                     THE SPECIFIED TISSUES.
C            DEP   — FINDS THE ALLOWED SUPERSATURATION
C                     AND THE RESULTANT ALLOWED DEPTH.
C            OUTPUT— PRINTS THE SCHEDULE OF DECOMPRESSION
C                     STOPS (DIVE SUMMARY).
C
C  THESE SUBROUTINES ARE NON-INTERACTIVE, THAT IS, THEY DO NOT CALL ONE
C  ANOTHER.  NOTE:  THIS VERSION OF THE PROGRAM IS NOT DESIGNED TO WORK
C  WITH OTHER THAN SQUARE-WAVE DIVE PROFILES.  FOR INPUT INFORMATION,
C  SEE SUBROUTINE "INPUT."
C
C
C     PROGRAM MAIN
C
C  ESTABLISH THE COMMON BLOCKS WHICH WILL ALLOW EFFICIENT TRANSFER OF
C  INFORMATION TO/FROM THE SUBROUTINES AND MINIMIZE MEMORY OVERHEAD:
```

```
      COMMON/ONE/SPEED,NTC,DEPTH,DEPTHO,DUR,J,TIM
      COMMON/TWO/CPT(16),CPTO(16)
      COMMON/THREE/DDEPTH(3),TTIME(3),HALFTI(16),FR
      COMMON/FOUR/DPT(16),DPTO(16),PCRUSH(16),RM(16)
      COMMON/FIVE/ADEP(100),ADUR(100),AHT(100),ADPT(100),APSS(100)
      COMMON/SIX/GAMMA,GAMMAC,PCSTAR,RZERO,REGEN,XLAM
      COMMON/SEVEN/RO,DYNES,TWOGAM,PSTAR,RSTAR,GAM,ALPHA
      COMMON/EIGHT/DEPNEW,PSSJ,DPTJ
      COMMON/NINE/DTIME,M,IT

C  DEFINE FILES FOR LOGICAL UNITS 1 AND 2:

      OPEN(1,FILE='INPUT.DAT',STATUS='OLD')
      OPEN(2,FILE='OUTPUT.DAT',STATUS='NEW')

C  DEFINE THE MODEL PARAMETERS AND READ THE DIVE PROFILE:

      GAMMA = 17.9
      GAMMAC = 256.9
      RZERO = 0.800
      REGEN = 20160.
      XLAM = 7500.
      PCSTAR = 5.00
      FRO = 0.79
      FR = FRO
      CALL INPUT

C  DEFINE SOME CONSTANTS AND CONVERSION FACTORS FOR SUBROUTINE DEP:

      RO = RZERO*1.E-4
      DYNES = 1.0133E6/33.
      TWOGAM = 2*(GAMMAC-GAMMA)
      PCSTAR = PCSTAR*33.
      PSTAR = PCSTAR*DYNES
      RSTAR = RO/(1.+PSTAR*RO/TWOGAM)
      GAM = GAMMA/GAMMAC
      ALPHA = GAM*XLAM

C  FILL THE HALF-TIME MATRIX (HALFTI) -- THE SHORTEST HALF-TIMES CONTROL
C  THE NO-STOP DECOMPRESSIONS, WHILE THE LONGEST CONTROL THE LINEAR
C  DECOMPRESSIONS FROM SATURATION DIVES, SUCH AS THE TEKTITE DIVE:

      HALFTI(1) = 1.
      HALFTI(2) = 2.
      HALFTI(3) = 5.
      HALFTI(4) = 10.
      HALFTI(5) = 20.
      HALFTI(6) = 40.
      HALFTI(7) = 80.
      HALFTI(8) = 120.
      HALFTI(9) = 160.
      HALFTI(10)= 240.
```

```
      HALFTI(11)= 320.
      HALFTI(12)= 400.
      HALFTI(13)= 480.
      HALFTI(14)= 560.
      HALFTI(15)= 720.

C  THE CRITICAL-VOLUME HYPOTHESIS REQUIRES AN ITERATION OVER THE TOTAL
C  DECOMPRESSION TIME -- INITIALIZE AND INCREMENT THE ITERATION COUNTER:

      IT = 0.0
      DTIME = 0.0
   10 IT = IT+1
      FR = FRO

C  SET THE INITIAL DEPTH AT THE SURFACE AND MAKE THE DIVE BY SETTING THE
C  CURRENT DEPTH AT THE BOTTOM.  LET THE DESCENT SPEED EQUAL THE DEPTH
C  EXCURSION DIVIDED BY ITS DURATION AND FOR SQUARE-WAVE DIVES LET THE
C  ASCENT SPEED EQUAL THE DESCENT SPEED:

      DEPTHO = DDEPTH(1)
      DEPTH = DDEPTH(2)
      DUR = TTIME(2) - TTIME(1)
      SPEED = (DDEPTH(2)-DDEPTH(1))/DUR
      ASPEED = - SPEED
      TIM = TTIME(2)

C  INITIALIZE THE TISSUE COUNT (NTC) AND THE COUNT INDEX (J).  SINCE
C  SQUARE-WAVE DIVES SELECT PROGRESSIVELY LONGER TISSUES, LATER UPDATING
C  OF "J" WILL ALLOW THE MAIN AND SUB-PROGRAMS TO LOOP OVER ONLY THOSE
C  TISSUES EQUAL TO OR LARGER THAN THE LATEST CONTROLLING TISSUE, WHICH
C  DRAMATICALLY SHORTENS THE EXECUTION TIME FOR MICROCOMPUTERS:

      NTC = 15
      J = 1

C  INITIALIZE THE INERT-GAS TENSION IN EACH TISSUE AND CALL SUBROUTINE
C  TAU TO FIND THE TENSIONS AFTER THE FIRST DEPTH EXCURSION.  SAVE THESE
C  FOR THE NEXT TIME TAU IS CALLED.  DETERMINE THE CRUSHING PRESSURE
C  IMPOSED ON EACH TISSUE BY TAKING THE DIFFERENCE BETWEEN THE AMBIENT
C  PRESSURE AND THE TISSUE TENSION.  IF THE CRUSHING EFFECT EXTENDS INTO
C  THE IMPERMEABLE NUCLEAR REGIME, GO TO LINE 31 AND SOLVE THE MODEL
C  CUBIC EQUATION FOR THE MINIMUM NUCLEAR RADIUS.  IF NOT, USE THE VALUE
C  APPROPRIATE TO THE PERMEABLE REGIME AND CONTINUE:

      DO 20 I = J,NTC
   20 CPTO(I) = FR*(DEPTHO+33.)
      CALL TAU
      DO 32 I = J,NTC
        CPTO(I) = CPT(I)
        DPTO(I) = DPT(I)
        PCRUSH(I) = DEPTH+33.-DPTO(I)
        PC = PCRUSH(I)*DYNES
```

```
            IF (PCRUSH(I) .GT. PCSTAR) GO TO 31
            RM(I) = 1./(PC/TWOGAM + 1./RO)
            GO TO 32
   31       PZERO = DPTO(I)*DYNES
            DENOM = PC-PSTAR+PZERO+TWOGAM/RSTAR
            P = -TWOGAM/DENOM
            Q = -PZERO*RSTAR**3/DENOM
            A = -P**2/3.
            B = 2.*P**3/27. + Q
            ROOT = SQRT(B**2/4. + A**3/27.)
            CA = (-B/2 + ROOT)**0.333333
            CB = (-B/2 - ROOT)**0.333333
            RM(I) = CA + CB - P/3.
   32     CONTINUE

C  MAINTAINING THE DEPTH AT THE BOTTOM, SET THE ELAPSED TIME EQUAL TO
C  THE TOTAL DIVE TIME PRIOR TO SURFACING.  FIND THE CURRENT TISSUE
C  TENSIONS AND STORE THEM, THEN FIND THE ALLOWED SUPERSATURATION BY
C  CALLING SUBROUTINE DEP, WHICH RETURNS THE ALLOWED DEPTH (DEPNEW):

         DEPTHO = DEPTH
         DEPTH = DDEPTH(3)
         TIM = TTIME(3)
         DUR = TTIME(3)-TTIME(2)
         SPEED = (DDEPTH(3)-DDEPTH(2))/DUR
         CALL TAU
         CALL DEP
         DEPTHO = DEPTH
         SPEED = ASPEED
         DO 40 I = J,NTC
   40    CPTO(I) = CPT(I)

C  SET THE DEPTH INCREMENT TO 10 FSW.  ROUND OFF TARGET DEPTH (DEPNEW)
C  TO THE NEXT DEEPER 10 FSW LEVEL.  SAVE THE STARTING DEPTH AND TIME,
C  THEN MAKE THE ASCENT:

         AJUMP = 10.
   50    IF(DEPNEW .LE. DDEPTH(1)) DEPNEW = DDEPTH(1)
         DEPNEW = DEPNEW/AJUMP
         DEPNEW = (INT(DEPNEW)+1)*AJUMP
         DEPOLD = DEPNEW
         AT = (DEPNEW-DEPTH)/SPEED
         TIMEO = TIM
         TIM = TIM + AT
         DUR = AT

C  A NEW CONTROLLING TISSUE MAY COME TO PREDOMINATE DURING THE ASCENT,
C  SO RECHECK THE ALLOWED DEPTH -- IF IT IS DEEPER THAN THE CURRENT
C  DEPTH, RETRACT THE ASCENT TIME AND BEGIN AGAIN USING THE DEEPER
C  TARGET DEPTH (EXECUTE LINES 60 THEN 50):

         CALL TAU
```

```
      CALL DEP
      IF (DEPNEW .GT. DEPOLD) GO TO 60
      GO TO 70
   60 TIM = TIMEO
      DEPNEW = DEPOLD + AJUMP
      GO TO 50
   70 DEPTH = DEPOLD
C  AFTER ARRIVING AT THE FIRST STOP, CONTINUE BY FINDING THE NEW TISSUE
C  TENSIONS AND THE NEXT ALLOWED DEPTH.  IF IT IS NOT PERMITTED TO GO
C  ANOTHER 10 FSW, KEEP INCREMENTING THE TIME IN ONE-MINUTE STEPS UNTIL
C  THE NEXT STOP CAN BE REACHED:

      DO 110 M = 1,100
        DEPTHO = DEPTH
        SPEED = 0.
        DO 80 I = J,NTC
   80   CPTO(I) = CPT(I)
        DNEXT = DEPTH - AJUMP
        TIM = TIM -1.
        DUR = -1.
   90   TIM = TIM + 1.
        DUR = DUR + 1.
        CALL TAU
        CALL DEP
        IF (DEPNEW .GT. DNEXT) GO TO 90

C  WHEN THE ASCENT IS ALLOWED, RECORD THE DEPTH, WAIT, CONTROLLING
C  TISSUE, CONTROLLING TISSUE TENSION, AND ALLOWED SUPERSATURATION FOR
C  STOP NUMBER (M).  THEN MAKE THE ASCENT AND EXIT LOOP M IF THE SURFACE
C  HAS BEEN REACHED.  IF NOT, UPDATE THE TISSUE TENSIONS AND REPEAT THE
C  LOOP (LINE 110) TO OBTAIN THE NEXT STOP:

        ADEP(M) = DEPTH
        ADUR(M) = DUR
        AHT(M) = HALFTI(J)
        ADPT(M) = DPTJ
        APSS(M) = PSSJ
        DO 100 I = J,NTC
  100   CPTO(I) = CPT(I)
        SPEED = ASPEED
        DEPTH = DNEXT

C  INSERT INERT-GAS FRACTION CONDITIONAL STATEMENTS HERE

        AT = (DEPTH-DEPTHO)/SPEED
        TIM = TIM + AT
        IF(DEPTH .LE. DDEPTH(1)) GO TO 120
        DUR = AT
        CALL TAU
  110 CONTINUE

C  ONCE THE SURFACE IS REACHED, FIND THE TOTAL DECOMPRESSION TIME
```

```
C  (DTIME) AND COMPARE IT TO THE CORRESPONDING TIME FOR THE PRECEEDING
C  PROGRAM ITERATION.  IF THE TIMES ARE THE SAME, THE ITERATION HAS
C  CONVERGED AND THE RUN IS COMPLETE.  IF NOT, RESTART THE PROGRAM AT
C  LINE 10, SAVING THE TOTAL TIME (TOLD):

 120  DTIME = TIM  - TTIME(3)
      IF (ABS(TOLD-DTIME) .LE. 1.) GO TO 130
      TOLD = DTIME
      GO TO 10

C  IF THE RUN IS COMPLETE, CALL SUBROUTINE OUTPUT, WHICH PRINTS THE
C  FINAL DECOMPRESSION SCHEDULE:

 130  CALL OUTPUT
      STOP
      END



      SUBROUTINE INPUT

C  THIS SUBROUTINE WRITES THE PROGRAM HEADER AND THE MODEL PARAMETERS
C  TO LOGICAL UNIT 2.  IT THEN READS THE DIVE PROFILE FROM UNIT 1 AND
C  WRITES IT TO UNIT 2:

      COMMON/THREE/DDEPTH(3),TTIME(3),HALFTI(16),FR
      COMMON/SIX/GAMMA,GAMMAC,PCSTAR,RZERO,REGEN,XLAM

C  WRITE THE PROGRAM HEADER AND THE MODEL PARAMETERS:

      WRITE(2,20)
   20 FORMAT(1H ,8X,25('*'),/,1H ,8X,'* TINY BUBBLES 05/05/85 *',
     +/,1H ,8X,25('*'))
      WRITE(2,30)
   30 FORMAT(1H ,/,1H ,8X,'** VALUES OF THE INPUT PARAMETERS **')
      WRITE(2,40) GAMMA
   40 FORMAT(1H ,8X,'GAMMA  = ',F6.2,' DYN/CM')
      WRITE(2,50) GAMMAC
   50 FORMAT(1H ,8X,'GAMMAC = ',F6.2,' DYN/CM')
      WRITE(2,60) PCSTAR
   60 FORMAT(1H ,8X,'PSTAR  = ',F6.2,' ATM')
      WRITE(2,70) RZERO
   70 FORMAT(1H ,8X,'RZERO  = ',F6.3,' MICROMETER')
      WRITE(2,80) REGEN
   80 FORMAT(1H ,8X,'REGEN  =',F7.0,' MINUTES')
      WRITE(2,90) XLAM
   90 FORMAT(1H ,8X,'LAMBDA =',F7.0,' FSW-MIN')
      WRITE(2,95) FR
   95 FORMAT(1H ,8X,'INERT  =',F4.2,'    NITROGEN')

C  THE PROFILE IS READ IN THREE LINES USING FORMAT 2F8.2, IE, FOR A
C  100-FSW, 30 MIN DIVE STARTING FROM THE SURFACE AT TIME ZERO AND
```

```
C  DESCENDING AT 60 FSW/MIN:
C
C                        (DDEPTH) (TTIME)
C                          0.00     0.00        (START DESCENT HERE)
C                        200.00     3.33        (ARRIVE AT BOTTOM)
C                        200.00    60.00        (START ASCENT HERE)
C
C
C  WRITE THE DIVE PROFILE:

      WRITE(2,100)
 100  FORMAT(1H ,/,1H ,8X,'** DIVE PROFILE **')
      DO 130 I = 1,3
        READ(1,110) DDEPTH(I),TTIME(I)
 110    FORMAT(2F8.2)
        WRITE(2,120) I,DDEPTH(I),TTIME(I)
 120    FORMAT(1H ,8X,'MANEUVER ',I1,2X,'DEPTH = ',
     +  F6.2,' FSW',2X,'TIME = ',F8.2,' MIN')
 130  CONTINUE
      WRITE(2,140)
 140  FORMAT(1H )
      RETURN
      END



      SUBROUTINE TAU

C  THIS SUBROUTINE CALCULATES THE TENSION IN EACH OF THE TISSUES FOR
C  WHICH HALF-TIMES ARE GIVEN.

      COMMON/ONE/SPEED,NTC,DEPTH,DEPTHO,DUR,J,TIM
      COMMON/TWO/CPT(16),CPTO(16)
      COMMON/THREE/DDEPTH(3),TTIME(3),HALFTI(16),FR
      COMMON/FOUR/DPT(16),DPTO(16),PCRUSH(16),RM(16)
      TWOLN = ALOG(2.)

C  LET THE INERT GAS PRESSURE EQUAL ABSOLUTE PRESSURE IN FSW:

      PO = DEPTHO + 33.

C  SUBTRACT THE OXYGEN WINDOW FROM THE INSPIRED OXYGEN TO GET THE CONT-
C  RIBUTION OF ACTIVE GASES, ABOUT 4.429 FSW (102 MMHG).  FOR OXYGEN
C  PARTIAL PRESSURES ABOVE 1500 MM HG, TREAT THE EXCESS AS AN INERT GAS:

      DEPTHA = 65.1/(1-FR) - 33.
      ACT = 4.429
      IF(DEPTH .GT. DEPTHA) ACT = 4.429 + ((1-FR)*(DEPTH+33.) - 65.1)

C  USING THE PERFUSION-LIMITED EQUATION WITH A SOLUTION OF THE FORM
C
C              TAU = A*EXP(-TIME/HALFTIME) + B*TIME + C
```

```
C
C  FIND THE INERT GAS TENSION IN EACH TISSUE AND STORE THE RESULTS IN
C  MATRIX CPT FOR THE COMMON BLOCK:

  20  DO 30 I = J,NTC
        A = CPTO(I) - FR*(PO-SPEED*HALFTI(I)/TWOLN)
        ARG = TWOLN*DUR/HALFTI(I)
        E = EXP(-ARG)
        CPT(I) = A*E + FR*(PO+SPEED*(DUR-HALFTI(I)/TWOLN))

C  INSERT RESIDUAL-NITROGEN MODIFICATION HERE

C  ADD THE ACTIVE GAS CONTRIBUTION TO THE INERT GAS TENSION TO GIVE THE
C  TOTAL TISSUE TENSION AND STORE THE RESULT IN MATRIX DPT FOR THE
C  COMMON BLOCK:

        DPT(I) = CPT(I) + ACT
  30  CONTINUE
      RETURN
      END



      SUBROUTINE DEP

C  THIS SUBROUTINE CALCULATES THE ALLOWED SUPERSATURATION FOR EACH
C  TISSUE, DESIGNATES THE CONTROLLING TISSUE, AND PREDICTS THE ALLOWED
C  DEPTH.  THE CRUSHING AND REGENERATION OF BUBBLE NUCLEI ARE INCLUDED.
C  PARAMETER SIGMA AUGMENTS THE NO-BUBBLE SUPERSATURATION TO PERMIT
C  BUBBLE FORMATION.  HOWEVER, SIGMA DEPENDS ON THE T     DECOMPRESSION
C  TIME, AND ITERATION OVER THE WHOLE DECOMPRESSION S    ULE IS
C  REQUIRED UNTIL SIGMA CONVERGES.  CONVERGENCE IS EV    NT WHEN TWO
C  SUCCESSIVE PASSES GIVE THE SAME TOTAL DECOMPRESSION TIME (DTIME),
C  INDICATING THAT THE CRITICAL VOLUME OF FREE GAS HAS BEEN REACHED.

      COMMON/ONE/SPEED,NTC,DEPTH,DEPTHO,DUR,J,TIM
      COMMON/THREE/DDEPTH(3),TTIME(3),HALFTI(16),FR
      COMMON/FOUR/DPT(16),DPTO(16),PCRUSH(16),RM(16)
      COMMON/SIX/GAMMA,GAMMAC,PCSTAR,RZERO,REGEN,XLAM
      COMMON/SEVEN/RO,DYNES,TWOGAM,PSTAR,RSTAR,GAM,ALPHA
      COMMON/EIGHT/DEPNEW,PSSJ,DPTJ
      COMMON/NINE/DTIME,M,IT

C  FIND THE TIME ALLOWED FOR REGENERATION (T), AND INITIALIZE ALPHA AND
C  THE ALLOWED DEPTH (DNEW).  NOTE: SIGMA IS ZERO FOR THE FIRST PASS.

      T =  TTIME(3) - TTIME(2)
      ALPHA1 = 0.0
      DNEW = 0.0
      IF(DTIME .GT. 0.0) ALPHA1 = ALPHA
      TWOLN = ALOG(2.)
```

```
C  FIND THE MINIMUM NUCLEAR RADIUS (RMT) AFTER REGENERATION AND
C  CALCULATE THE NO-BUBBLE SUPERSATURATION.  ADD SIGMA AND FIND THE
C  ALLOWED UPWARD DEPTH EXCURSION, UPDATING THE CURRENT CONTROLLING
C  TISSUE INDEX (J) AS WELL.  STORE THE CONTROLLING TISSUE TENSION IN
C  DPTJ, THE ALLOWED SUPERSATURATION IN PSSJ, AND THE ALLOWED DEPTH IN
C  DEPNEW FOR THE COMMON BLOCK:

      DO 40 I = J,NTC
   20   RMT = RM(I) + (1-EXP(-T/REGEN))*(RO-RM(I))
        PSAFE = GAM*TWOGAM/(RMT*DYNES)
        SIGMA = ALPHA1 / (DTIME + HALFTI(I)/TWOLN)
        PS = PSAFE + SIGMA
        PNEW = (PS + SQRT( PS**2 - 4*GAM*PCRUSH(I)*SIGMA))*0.5
        DEPA = DPT(I) - PNEW
        DOLD = DNEW
        IF(DEPA .GT. DNEW) DNEW = DEPA
        IF(DNEW .GT. DOLD) GO TO 30
        GO TO 40
   30   J = I
        DPTJ = DPT(I) - 33.
        PSSJ = PNEW
   40 CONTINUE
      DEPNEW = DNEW-33.
      RETURN
      END


      SUBROUTINE OUTPUT

C  THIS SUBROUTINE WRITES THE DECOMPRESSION SCHEDULE IN COLUMNAR FORMAT
C  TO LOGICAL UNIT 2:

      COMMON/THREE/DDEPTH(3),TTIME(3),HALFTI(16),FR
      COMMON/FIVE/ADEP(100),ADUR(100),AHT(100),ADPT(100),APSS(100)
      COMMON/NINE/DTIME,M,IT

C  WRITE THE HEADER WITH THE NUMBER OF ITERATIONS REQUIRED FOR
C  CONVERGENCE.  WRITE THE EXCURSION DEPTH AND DIVE DURATION:

      WRITE(2,10) IT
   10 FORMAT(1H ,8X,'** DECOMPRESSION SCHEDULE ** ITERATION NUMBER ',I2,
     +'   **')
      WRITE(2,15)
   15 FORMAT(1H ,8X,53('*'))
      WRITE(2,20) DDEPTH(3)
   20 FORMAT(1H ,8X,'*  FOR THE EXCURSION TO DEPTH = ',
     +F6.2,' FSW          *',/,1H ,8X,53('*'))
      WRITE(2,30) TTIME(3)
   30 FORMAT(1H ,8X,'* TIME SPENT AT INITIAL DEPTH = ',
     +F8.2,' MIN        *',/,1H ,8X,53('*'))
      WRITE(2,40)
```

```
   40  FORMAT(1H ,8X,
     +'* STOP *  DEPTH *  WAIT  * TISSUE *   TAU  *   PSS  *')

C  WRITE IN TABULAR FORM THE STOP NUMBER (M), THE STOP DEPTH (ADEP),
C  THE STOP DURATION (ADUR), THE CONTROLLING TISSUE HALF-TIME (AHT),
C  THE TENSION IN THE CONTROLLING TISSUE (ADPT), AND THE ALLOWED
C  SUPERSATURATION (APSS) FOR ALL THE REQUIRED STOPS.  WRITE THE TOTAL
C  TIME NEEDED TO REACH THE SURFACE (DTIME):

      DO 60 L = 1,M
        WRITE(2,50) L,ADEP(L),ADUR(L),AHT(L),ADPT(L),APSS(L)
   50   FORMAT(1H ,8X,'*  ',I3,5(' * ',F6.2),' *')
   60 CONTINUE
      WRITE(2,70) DTIME
   70 FORMAT(1H ,8X,53('*'),/,1H ,8X,'* TOTAL TIME TO REACH SURFACE = ',
     +F8.2,' MIN        *',/,1H ,8X,53('*'),//)
      RETURN
      END
```

APPENDIX 2

BASIC PROGRAM LISTING

TINY BUBBLES—VERSION 05/05/85—FOR HELIUM DIVES

THE TINY BUBBLE GROUP
DEPARTMENT OF PHYSICS
AND ASTRONOMY
UNIVERSITY OF HAWAII
2505 CORREA ROAD
HONOLULU, HAWAII 96822

THIS PROGRAM ACCEPTS A SQUARE-WAVE DIVE PROFILE AND CALCULATES A THEORETICAL DECOMPRESSION SCHEDULE USING THE EQUATIONS AND PARAMETERS OF THE VARYING-PERMEABILITY MODEL. THE SCHEDULES SO PRODUCED ARE NOT INTENDED FOR GENERAL USE BY THE DIVING COMMUNITY, AND NO CLAIM IS MADE FOR THEIR VALIDITY. PROGRAM FEATURES INCLUDE CONTINUOUS TRACKING OF THE MINIMUM NUCLEAR RADIUS REQUIRED TO FORM A MACROSCOPIC BUBBLE UPON DECOMPRESSION, CONTINUOUS TRACKING OF THE TENSIONS IN EACH OF SEVERAL SPECIFIED TISSUES USING A PERFUSION-LIMITED EQUATION, CALCULATION OF THE ALLOWED SUPERSATURATION IN EACH TISSUE BASED ON A CRITICAL VOLUME OF RELEASED GAS, AND CONSTRUCTION OF A DECOMPRESSION SCHEDULE USING THE DEPTHS ALLOWED BY THOSE TISSUES FOUND TO BE CONTROLLING THE ASCENT.

THE PROGRAM CONSISTS OF A MAIN BODY AND THE FOUR SUBROUTINES LISTED HERE:

INPUT — READS IN THE DIVE PROFILE. PRINTS THE PROGRAM HEADER, THE DIVE PROFILE, AND THE MODEL PARAMETERS.
TAU — CALCULATES THE TISSUE TENSIONS IN THE SPECIFIED TISSUES.
DEP — FINDS THE ALLOWED SUPERSATURATION AND THE RESULTANT ALLOWED DEPTH.
OUTPUT— PRINTS THE SCHEDULE OF DECOMPRESSION STOPS (DIVE SUMMARY).

THESE SUBROUTINES ARE NON-INTERACTIVE, THAT IS, THEY DO NOT CALL ONE ANOTHER. NOTE: THIS VERSION OF THE PROGRAM IS NOT DESIGNED TO WORK WITH OTHER THAN SQUARE-WAVE DIVE PROFILES. FOR INPUT INFORMATION, SEE SUBROUTINE "INPUT."

PROGRAM MAIN

BEGIN BY DIMENSIONING ALL ARRAYS:

```
10    DIM DDEPTH(3),TTIME(3),HALFTI(16)
20    DIM CPT(16),CPTO(16),DPT(16),DPTO(16),PCRUSH(16),RM(16)
30    DIM ADEP(100),ADUR(100),AHT(100),ADPT(100),APSS(100)
```

DEFINE THE MODEL PARAMETERS AND READ THE DIVE PROFILE:

```
40    GAMMA = 17.9
50    GAMMAC = 256.9
60    RZERO = .7
70    REGEN = 20160
80    XLAM = 7500
90    PCSTAR = 5
100   FRO = .75
110   GOSUB 1380                REM INPUT
```

DEFINE SOME CONSTANTS AND CONVERSION FACTORS FOR SUBROUTINE DEP, SO THEY DO NOT HAVE TO BE REDEFINED EACH TIME IT IS CALLED:

```
120   RO = RZERO*.0001
130   DYNES = 1013300.*33.
140   TWOGAM = 2*(GAMMAC-GAMMA)
150   PCSTAR = PCSTAR*33.
160   PSTAR = PCSTAR*DYNES
170   RSTAR = RO/(1.+PSTAR*RO/TWOGAM)
180   GAM = GAMMA/GAMMAC
190   ALPHA = GAM*XLAM
```

FILL THE HALF-TIME MATRIX (HALFTI) -- THE SHORTEST HALF-TIMES CONTROL THE NO-STOP DECOMPRESSIONS, WHILE THE LONGEST CONTROL THE LINEAR DECOMPRESSIONS FROM SATURATION DIVES:

```
200   HALFTI(1) = 1/3
210   HALFTI(2) = 2/3
220   HALFTI(3) = 5/3
230   HALFTI(4) = 10/3
240   HALFTI(5) = 20/3
250   HALFTI(6) = 40/3
260   HALFTI(7) = 80/3
270   HALFTI(8) = 120/3
280   HALFTI(9) = 160/3
290   HALFTI(10)= 240/3
300   HALFTI(11)= 320/3
310   HALFTI(12)= 400/3
320   HALFTI(13)= 480/3
330   HALFTI(14)= 560/3
340   HALFTI(15)= 720/3
```

THE CRITICAL-VOLUME HYPOTHESIS REQUIRES AN ITERATION OVER THE TOTAL DECOMPRESSION TIME -- INITIALIZE AND INCREMENT THE ITERATION COUNTER:

```
350   IT = 0
360   DTIME = 0.0
```

```
370   IT = IT+1
380   FR = FRO
```

SET THE INITIAL DEPTH AT THE SURFACE AND MAKE THE DIVE BY SETTING THE CURRENT DEPTH AT THE BOTTOM. LET THE DESCENT SPEED EQUAL THE DEPTH EXCURSION DIVIDED BY ITS DURATION AND FOR SQUARE-WAVE DIVES LET THE ASCENT SPEED EQUAL THE DESCENT SPEED:

```
390   DEPTHO = DDEPTH(1)
400   DEPTH = DDEPTH(2)
410   DUR = TTIME(2) - TTIME(1)
420   SPEED = (DDEPTH(2)-DDEPTH(1))/DUR
430   ASPEED = - SPEED
435   TIM = TTIME(2)
```

INITIALIZE THE TISSUE COUNT (NTC) AND THE COUNT INDEX (J). SINCE SQUARE-WAVE DIVES SELECT PROGRESSIVELY LONGER TISSUES, LATER UPDATING OF "J" WILL ALLOW THE MAIN AND SUB-PROGRAMS TO LOOP OVER ONLY THOSE TISSUES EQUAL TO OR LARGER THAN THE LATEST CONTROLLING TISSUE, WHICH DRAMATICALLY SHORTENS THE EXECUTION TIME FOR MICROCOMPUTERS:

```
440   NTC = 15
450   J = 1
```

INITIALIZE THE INERT-GAS TENSION IN EACH TISSUE AND CALL SUBROUTINE TAU TO FIND THE TENSIONS AFTER THE FIRST DEPTH EXCURSION. SAVE THESE FOR THE NEXT TIME TAU IS CALLED. DETERMINE THE CRUSHING PRESSURE IMPOSED ON EACH TISSUE BY TAKING THE DIFFERENCE BETWEEN THE AMBIENT PRESSURE AND THE TISSUE TENSION. IF THE CRUSHING EFFECT EXTENDS INTO THE IMPERMEABLE NUCLEAR REGIME, GO TO LINE 580 AND SOLVE THE MODEL CUBIC EQUATION FOR THE MINIMUM NUCLEAR RADIUS. IF NOT, USE THE VALUE APPROPRIATE TO THE PERMEABLE REGIME AND CONTINUE:

```
460   FOR I = J TO NTC
470       CPTO(I) = 0.0
480   NEXT I
490   GOSUB 1650   .      REM TAU
500   FOR I = J TO NTC
510       CPTO(I) = CPT(I)
520       DPTO(I) = DPT(I)
530       PCRUSH(I) = DEPTH+33.-DPTO(I)
540       PC = PCRUSH(I)*DYNES
550       IF (PCRUSH(I) > PCSTAR) GOTO 580
560       RM(I) = 1/(PC/TWOGAM + 1/RO)
570       GOTO 680
580       PZERO = DPTO(I)*DYNES
590       DENOM = PC-PSTAR+PZERO+TWOGAM/RSTAR
600       P = -TWOGAM/DENOM
610       Q = -PZERO*RSTAR^3/DENOM
620       A = -P^2/3
630       B = 2.*P^3/27 + Q
640       ROOT = SQR(B^2/4 + A^3/27)
```

```
650       CA = (-B/2 + ROOT)^.333333
660       CB = (-B/2 - ROOT)^.333333
670       RM(I) = CA + CB - P/3
680   NEXT I
```

MAINTAINING THE DEPTH AT THE BOTTOM, SET THE ELAPSED TIME EQUAL TO THE TOTAL DIVE TIME PRIOR TO SURFACING. FIND THE CURRENT TISSUE TENSIONS AND STORE THEM, THEN FIND THE ALLOWED SUPERSATURATION BY CALLING SUBROUTINE DEP, WHICH RETURNS THE ALLOWED DEPTH (DEPNEW):

```
690   DEPTHO = DEPTH
700   DEPTH = DDEPTH(3)
710   TIM = TTIME(3)
720   DUR = TTIME(3)-TTIME(2)
730   SPEED = (DDEPTH(3)-DDEPTH(2))/DUR
740   GOSUB 1650          REM TAU
750   GOSUB 1800          REM DEP
760   DEPTHO = DEPTH
770   SPEED = ASPEED
780   FOR I = J TO NTC
790       CPTO(I) = CPT(I)
800   NEXT I
```

SET THE DEPTH INCREMENT TO 10 FSW. ROUND OFF TARGET DEPTH (DEPNEW) TO THE NEXT DEEPER 10 FSW LEVEL. SAVE THE STARTING DEPTH AND TIME, THEN MAKE THE ASCENT:

```
810   AJUMP = 10
820   IF(DEPNEW <= DDEPTH(1)) THEN DEPNEW = DDEPTH(1)
830   DEPNEW = DEPNEW/AJUMP
840   DEPNEW = (INT(DEPNEW)+1)*AJUMP
850   DEPOLD = DEPNEW
860   AT = (DEPNEW-DEPTH)/SPEED
870   TIMEO = TIM
880   TIM = TIM + AT
890   DUR = AT
```

A NEW CONTROLLING TISSUE MAY COME TO PREDOMINATE DURING THE ASCENT, SO RECHECK THE ALLOWED DEPTH — IF IT IS DEEPER THAN THE CURRENT DEPTH, RETRACT THE ASCENT TIME AND BEGIN AGAIN USING THE DEEPER TARGET DEPTH (EXECUTE LINES 920 THEN 820):

```
900   GOSUB 1650          REM TAU
910   GOSUB 1800          REM DEP
920   IF (DEPNEW > DEPOLD) GOTO 940
930   GOTO 970
940   TIM = TIMEO
950   DEPNEW = DEPOLD + AJUMP
960   GOTO 820
970   DEPTH = DEPOLD
```

AFTER ARRIVING AT THE FIRST STOP, CONTINUE BY FINDING THE NEW TISSUE

TENSIONS AND THE NEXT ALLOWED DEPTH. IF IT IS NOT PERMITTED TO GO ANOTHER 10 FSW, KEEP INCREMENTING THE TIME IN ONE-MINUTE STEPS UNTIL THE NEXT STOP CAN BE REACHED:

```
980   FOR M = 1 TO 100
1000      DEPTHO = DEPTH
1010      SPEED = 0
1020      FOR I = J TO NTC
1030          CPTO(I) = CPT(I)
1040      NEXT I
1050      DNEXT = DEPTH - AJUMP
1060      IF (DNEXT < DDEPTH(1)) THEN DNEXT = DDEPTH(1)
1070      TIM = TIM -1
1080      DUR = -1
1090      TIM = TIM + 1
1100      DUR = DUR + 1
1110      GOSUB 1650                REM TAU
1120      GOSUB 1800                REM DEP
1130      IF (DEPNEW > DNEXT) GOTO 1090
```

WHEN THE ASCENT IS ALLOWED, RECORD THE DEPTH, WAIT, CONTROLLING TISSUE, CONTROLLING TISSUE TENSION, AND ALLOWED SUPERSATURATION FOR STOP NUMBER (M). THEN MAKE THE ASCENT AND EXIT LOOP M IF THE SURFACE HAS BEEN REACHED. IF NOT, UPDATE THE TISSUE TENSIONS AND REPEAT THE LOOP (NEXT M) TO OBTAIN THE NEXT STOP:

```
1140      ADEP(M) = DEPTH
1150      ADUR(M) = DUR
1160      AHT(M) = HALFTI(J)
1170      ADPT(M) = DPTJ
1180      APSS(M) = PSSJ
1190      FOR I = J TO NTC
1200          CPTO(I) = CPT(I)
1210      NEXT I
1220      SPEED = ASPEED
1230      DEPTH = DNEXT
1240      AT = (DEPTH-DEPTHO)/SPEED
1250      TIM = TIM + AT
1260      IF(DEPTH <= DDEPTH(1)) GOTO 1300
1270      DUR = AT
1280      GOSUB 1650
1290  NEXT M
```

ONCE THE SURFACE IS REACHED, FIND THE TOTAL DECOMPRESSION TIME (DTIME) AND COMPARE IT TO THE CORRESPONDING TIME FOR THE PRECEEDING PROGRAM ITERATION. IF THE TIMES ARE THE SAME, THE ITERATION HAS CONVERGED AND THE RUN IS COMPLETE. IF NOT, RESTART THE PROGRAM AT LINE 370, SAVING THE TOTAL TIME (TOLD):

```
1300 DTIME = TIM - TTIME(3)
1310 IF(ABS(DTIME-TOLD) <= 1) GOTO 1340
1320 TOLD = DTIME
```

```
1330 GOTO 370
```

IF THE RUN IS COMPLETE, CALL SUBROUTINE OUTPUT, WHICH PRINTS THE FINAL DECOMPRESSION SCHEDULE:

```
1340 GOSUB 2050          REM OUTPUT
1350 STOP
1360 END
```

THIS SUBROUTINE WRITES THE HEADER AND THE MODEL PARAMETERS

```
1380 REM ***** SUBROUTINE INPUT *****
1390 REM
1400 PRINT"        **********************"
1410 PRINT"        * BUBBLES 05/05/85 *"
1420 PRINT"        **********************"
1430 PRINT
1440 PRINT"        ** VALUES OF THE INPUT PARAMETERS **"
1450 PRINT"        GAMMA  = ";GAMMA;"  DYN/CM"
1460 PRINT"        GAMMAC = ";GAMMAC;" DYN/CM"
1470 PRINT"        PSTAR  = ";PCSTAR;"      ATM"
1480 PRINT"        RZERO  = ";RZERO;"    MICROMETER"
1490 PRINT"        REGEN  = ";REGEN;" MINUTES"
1500 PRINT"        LAMBDA = ";XLAM;"  FSW-MIN"
1510 PRINT"        INERT  = ";FRO;"   HELIUM
1520 PRINT"        INCLUDING RESIDUAL NITROGEN"
1525 PRINT
```

THE PROFILE IS READ IN ON LINE 1540 AS A BOTTOM DEPTH AND TIME SEPARATED BY A COMMA, THEN THE DIVE PROFILE IS PRINTED, E.G., FOR A 100 FSW DIVE DESCENDING AT 60 FSW/MIN:

```
                      (DDEPTH) (TTIME)
                         0.00     0.00        (START DESCENT HERE)
                       100.00     1.67        (ARRIVE AT BOTTOM)
 (INPUT THIS LINE)     100.00    30.00        (START ASCENT HERE)
```

```
1530 PRINT"        ** DIVE PROFILE **"
1540 INPUT "        PLEASE INSERT EXCURSION DEPTH,TIME ";DD,TT
1550 DDEPTH(1) = 0
1560 DDEPTH(2) = DD
1570 DDEPTH(3) = DDEPTH(2)
1580 TTIME(1)  = 0
1590 TTIME(2)  = (DDEPTH(2)-DDEPTH(1))/60
1600 TTIME(3)  = TT
1610 PRINT
1620 PRINT
1630 RETURN
1640 END
```

THIS SUBROUTINE CALCULATES THE TENSION IN EACH OF THE TISSUES FOR WHICH HALF-TIMES ARE GIVEN.

```
1650 REM ***** SUBROUTINE TAU *****
1660 TWOLN = LOG(2)
```

LET THE INERT GAS PRESSURE EQUAL ABSOLUTE PRESSURE IN FSW:

```
1670 PO = DEPTHO + 33
```

SUBTRACT THE OXYGEN WINDOW FROM THE INSPIRED OXYGEN TO GET THE CONTRIBUTION OF ACTIVE GASES, ABOUT 4.429 FSW (102 MMHG). FOR OXYGEN PARTIAL PRESSURES ABOVE 1500 MM HG, EXECUTE LINE 1700, WHICH TREATS THE EXCESS AS AN INERT GAS:

```
1680 DEPTHA = 65.1/(1-FR) - 33
1690 ACT = 4.429
1700 IF (DEPTH > DEPTHA) THEN ACT = 4.429 + ((1-FR)*(DEPTH+33) - 65.1)
```

USING THE PERFUSION-LIMITED EQUATION WITH A SOLUTION OF THE FORM

$$TAU = A*EXP(-TIME/HALFTIME) + B*TIME + C$$

FIND THE INERT GAS TENSION IN EACH TISSUE AND STORE THE RESULTS IN MATRIX CPT.

```
1710 FOR I = 1 TO NTC
1720     A = CPTO(I) - FR*(PO-SPEED*HALFTI(I)/TWOLN)
1730     ARG = TWOLN*DUR/HALFTI(I)
1740     E = EXP(-ARG)
1750     CPT(I) = A*E + FR*(PO+SPEED*(DUR-HALFTI(I)/TWOLN))
1755     DNITRO = 0.79*33*EXP(-TIM*TWOLN/(3*HALFTI(I)))
```

ADD THE ACTIVE GAS CONTRIBUTION TO THE INERT GAS TENSION TO GIVE THE TOTAL TISSUE TENSION AND STORE THE RESULT IN MATRIX DPT.

```
1760     DPT(I) = CPT(I) + ACT + DNITRO
1770 NEXT I
1780 RETURN
1790 END
```

THIS SUBROUTINE CALCULATES THE ALLOWED SUPERSATURATION FOR EACH TISSUE, DESIGNATES THE CONTROLLING TISSUE, AND PREDICTS THE ALLOWED DEPTH. THE CRUSHING AND REGENERATION OF BUBBLE NUCLEI ARE INCLUDED. PARAMETER SIGMA AUGMENTS THE NO-BUBBLE SUPERSATURATION TO PERMIT BUBBLE FORMATION. HOWEVER, SIGMA DEPENDS ON THE TOTAL DECOMPRESSION TIME, AND ITERATION OVER THE WHOLE DECOMPRESSION SCHEDULE IS REQUIRED UNTIL SIGMA CONVERGES. CONVERGENCE IS EVIDENT WHEN TWO SUCCESSIVE PASSES GIVE THE SAME TOTAL DECOMPRESSION TIME (DTIME), INDICATING THAT THE CRITICAL VOLUME OF FREE GAS HAS BEEN REACHED.

```
1800 REM ***** SUBROUTINE DEP *****
```

FIND THE TIME ALLOWED FOR REGENERATION (T), AND INITIALIZE ALPHA AND THE ALLOWED DEPTH (DNEW) (NOTE: SIGMA IS ZERO FOR THE FIRST PASS):

```
1810 T =  TTIME(3) - TTIME(2)
1820 ALPHA1 = 0
1830 DNEW = 0
1840 IF(DTIME > 0) THEN ALPHA1 = ALPHA
1850 TWOLN = LOG(2)
```

FIND THE MINIMUM NUCLEAR RADIUS (RMT) AFTER REGENERATION AND CALCULATE THE NO-BUBBLE SUPERSATURATION. ADD SIGMA AND FIND THE ALLOWED UPWARD DEPTH EXCURSION, UPDATING THE CURRENT CONTROLLING TISSUE INDEX (J) AS WELL. STORE THE CONTROLLING TISSUE TENSION IN DPTJ, THE ALLOWED SUPERSATURATION IN PSSJ, AND THE ALLOWED DEPTH IN DEPNEW.

```
1860 FOR I = J TO NTC
1870      RMT = RM(I) + (1-EXP(-T/REGEN))*(RO-RM(I))
1880      PSAFE = GAM*TWOGAM/(RMT*DYNES)
1890      SIGMA = ALPHA1 / (DTIME + HALFTI(I)/TWOLN)
1900      PS = PSAFE + SIGMA
1910      PNEW = (PS + SQR( PS^2 - 4*GAM*PCRUSH(I)*SIGMA))*.5
1920      DEPA = DPT(I) - PNEW
1930      DOLD = DNEW
1940      IF(DEPA > DNEW) THEN DNEW = DEPA
1950      IF(DNEW > DOLD) GOTO 1970
1960      GOTO 2000
1970      J = I
1980      DPTJ = DPT(I) - 33.
1990      PSSJ = PNEW
2000 NEXT I
2010 DEPNEW = DNEW-33
2020 RETURN
2030 END
2040 REM
```

THIS SUBROUTINE WRITES THE DECOMPRESSION SCHEDULE.

```
2050 REM ***** SUBROUTINE OUTPUT *****
```

WRITE THE HEADER WITH THE NUMBER OF ITERATIONS REQUIRED FOR CONVERGENCE. WRITE THE EXCURSION DEPTH AND DIVE DURATION:

```
2070 PRINT"        ******************************************************"
2080 PRINT"        ** DECOMPRESSION SCHEDULE ** ITERATION NUMBER ";IT;"    *"
2090 PRINT"        ******************************************************"
2100 PRINT"        *  FOR THE EXCURSION TO DEPTH = ";
2110 PRINT USING "###.##";DDEPTH(3);
2120 PRINT"              *"
2130 PRINT"        * TIME SPENT AT INITIAL DEPTH = ";
2140 PRINT USING "###.##";TTIME(3);
2150 PRINT"              *"
```

WRITE IN TABULAR FORM THE STOP NUMBER (M), THE STOP DEPTH (ADEP), THE STOP DURATION (ADUR), THE CONTROLLING TISSUE HALF-TIME (AHT),

```
   THE TENSION IN THE CONTROLLING TISSUE (ADPT), AND THE ALLOWED
   SUPERSATURATION (APSS) FOR ALL THE REQUIRED STOPS.   WRITE THE TOTAL
   TIME NEEDED TO REACH THE SURFACE (DTIME):

2160 PRINT"        ********************************************************"
2170 PRINT"        * STOP *  DEPTH *  WAIT  * TISSUE *   TAU  *   PSS   *"
2180 PRINT"        ********************************************************"
2190 FOR L = 1 TO M
2200     PRINT "        *";
2210     PRINT USING " ###. ";L;
2220     PRINT USING "  ###.## "; ADEP(L),ADUR(L),AHT(L),ADPT(L),APSS(L);
2230 PRINT"*"
2240 NEXT L
2250 PRINT"        ********************************************************"
2260 PRINT"        * TOTAL TIME TO REACH SURFACE = ";
2270 PRINT USING "#####.##";DTIME;
2280 PRINT"           *"
2290 PRINT"        ********************************************************"
2295 RETURN
2300 END
```

APPENDIX 3

ALPHABETICAL LISTING OF PROGRAM VARIABLES

VARIABLE	LOCATION	DESCRIPTION
A	MAIN	Impermeable equation variable
A	TAU	Tension equation variable
ACT	TAU	Active gas addition to inert gas tension
ADEP(100)	COMMON/FIVE	Stores stop depths
ADPT(100)	COMMON/FIVE	Stores controlling tensions
ADUR(100)	COMMON/FIVE	Stores stop durations
AHT(100)	COMMON/FIVE	Stores controlling compartments
AJUMP	MAIN	Ascent stop interval in fsw
ALPHA	COMMON/SEVEN	Equals: (gamma/gammac)*xlam
ALPHA1	DEP	Same as alpha but zero on first pass
APSS(100)	COMMON/FIVE	Stores for allowed supersaturations
ARG	TAU	Tension equation variable
ASPEED	MAIN	Ascent speed
AT	MAIN	Excursion ascent time
B	MAIN	Impermeable equation variable
CA	MAIN	Impermeable equation variable
CB	MAIN	Impermeable equation variable
CPT(16)	COMMON/TWO	Inert gas tissue tension (absolute)
CPTO(16)	COMMON/TWO	Previous inert gas tension (absolute)
DD	INPUT	Depth profile input (BASIC only)
DDEPTH(3)	COMMON/THREE	Depth profile input
DENOM	MAIN	Impermeable equation variable
DEPA	DEP	Allowed depth in fsw
DEPNEW	COMMON/EIGHT	New allowed depth
DEPOLD	MAIN	Stores excursion starting depth
DEPTH	COMMON/ONE	Current depth
DEPTHO	COMMON/ONE	Previous depth
DNEW	DEP	Allowed supersaturation equation variable
DNEXT	MAIN	Next higher stop during ascent
DNITRO	TAU	Residual nitrogen inert-gas contribution
DOLD	DEP	Allowed depth intermediate variable
DPT(16)	COMMON/FOUR	Total tissue tension (absolute)
DPTJ	COMMON/EIGHT	Current controlling tissue tension
DTIME	COMMON/NINE	Total decompression time
DUR	COMMON/ONE	Duration of present excursion
DYNES	COMMON/SEVEN	Conversion from fsw to dyn/cm/cm
E	TAU	Tension equation variable
FR	COMMON/THREE	Inert gas fraction
GAM	COMMON/SEVEN	Equals: gamma / gammac
GAMMA	COMMON/SIX	Skin surface tension
GAMMAC	COMMON/SIX	Skin crumbling compression strength
HALFTI(16)	COMMON/THREE	Tissue half-time column

APPENDIX 3 (CONTINUED)

VARIABLE	LOCATION	DESCRIPTION
I	MAIN	Counter dummy index
IT	COMMON/NINE	Current number of program iterations
J	COMMON/ONE	First tissue compartment to use
M	COMMON/NINE	Current number of stops
NTC	COMMON/ONE	Number of tissue compartments
P	MAIN	Impermeable equation variable
PC	MAIN	Crushing pressure in dyn/cm/cm
PCRUSH(16)	COMMON/FOUR	Initial crushing imposed on each tissue
PCSTAR	COMMON/SIX	Impermeable crossover point in fsw
PCSTAR	MAIN	Impermeable crossover point in atm
PNEW	DEP	Augmented allowed supersaturation
PO	TAU	Tension equation starting depth (absolute)
PS	DEP	Allowed supersaturation equation variable
PSAFE	DEP	No-bubble allowed supersaturation
PSSJ	COMMON/EIGHT	Current allowed supersaturation
PSTAR	COMMON/SEVEN	Impermeable crossover point in dyn/cm/cm
PZERO	MAIN	Initial tissue tension in dyn/cm/cm
Q	MAIN	Impermeable equation variable
REGEN	COMMON/SIX	Regeneration time parameter
RM(16)	COMMON/FOUR	Minimum critical radius for each tissue
RMT	DEP	Minimum radius after regeneration
RO	COMMON/SEVEN	Initial critical radius in cm
ROOT	MAIN	Impermeable equation variable
RSTAR	COMMON/SEVEN	Nuclear radius at crossover pressure
RZERO	COMMON/SIX	Initial critical radius in microns
SIGMA	DEP	Allowed supersaturation equation variable
SPEED	COMMON/ONE	Rate of descent or ascent
T	DEP	Time during which regeneration occurs
TIM	MAIN	Internal clock
TIMEO	MAIN	Stores excursion starting time
TOLD	MAIN	Previous total decompression time
TT	INPUT	Time profile input (BASIC only)
TTIME(3)	COMMON/THREE	Time profile input
TWOGAM	COMMON/SEVEN	Equals: 2.0*(gammac - gamma)
TWOLN	DEP	Natural log of 2.0
TWOLN	TAU	Natural log of 2.0
XLAM	COMMON/SIX	Supersaturation augmentation parameter

REFERENCES

1. Yount, D.E. and R.H. Strauss. 1977. Decompression sickness. American Scientist 65(5):598-604.

2. Strauss, R.H. 1974. Bubble formation in gelatin: implications for prevention of decompression sickness. Undersea Biomed. Res. 1(2):169-174.

3. Strauss, R.H. and T.D. Kunkle. 1974. Isobaric bubble growth: a consequence of altering atmospheric gas. Science 186:443-444.

4. Kunkle, T.D. and D.E. Yount. 1975. Gas nucleation in gelatin. In: Proc. Sixth Symp. Underwater Physiol., ed. M.B. Kent, pp. 459-467. Bethesda: Federation of American Societies for Experimental Biology.

5. Yount, D.E. and R.H. Strauss. 1976. Bubble formation in gelatin: a model for decompression sickness. J. Appl. Phys. 47(11): 5081-5089.

6. Yount, D.E., C.M. Yeung, and F.W. Ingle. 1977. Determination of the radii of gas cavitation nuclei by filtering gelatin. J. Acoust. Soc. Am. 65(6):1440-1450.

7. Yount, D.E. and C.M. Yeung. 1981. Bubble formation in supersaturated gelatin: a further investigation of gas cavitation nuclei. J. Acoust. Soc. Am. 69(3):702-708.

8. D'Arrigo, J.S. 1978. Improved method for studying the surface chemistry of bubble formation. Aviat. Space Environ. Med. 49(2):358-361.

9. Paganelli, C.V., R.H. Strauss, and D.E. Yount. 1977. Bubble formation within decompressed hen's eggs. Aviat. Space Environ. Med. 48(1):48-49.

10. Yount, D.E. 1979. Skins of varying permeability: a stabilization mechanism for gas cavitation nuclei. J. Acoust. Soc. Am. 65(6):1429-1439.

11. Yount, D.E. 1979. Application of a bubble formation model to decompression sickness in rats and humans. Aviat. Space Environ. Med. 50(1):44-50.

12. Yount, D.E. 1981. Application of a bubble formation model to decompression sickness in fingerling salmon. Undersea Biomed. Res. 8(4):199-208.

13. Yount, D.E., E.W. Gillary, and D.C. Hoffman. 1982. A microscopic study of gas cavitation nuclei. In: Cavitation and Polyphase Flow Forum, ed. J.W. Hoyt, pp. 6–8. New York: The American Society of Mechanical Engineers.

14. Yount, D.E., E.W. Gillary, and D.C. Hoffman. 1984. Microscopic study of bubble formation nuclei. In: Proc. Eighth Symp. Underwater Physiol., ed. A.J. Bachrach and M.M. Matzen, pp. 119-130. Bethesda, Md: Undersea Medical Society, Inc.

15. Yount, D.E., E.W. Gillary, and D.C. Hoffman. 1984. A microscopic investigation of bubble formation nuclei. J. Acoust. Soc. Am. 76(5):1511-1521.

16. Yount, D.E. 1982. On the evolution, generation, and regeneration of gas cavitation nuclei. J. Acoust. Soc. Am. 71(6):1473-1481.

17. Yount, D.E. and D.C. Hoffman. 1983. Decompression theory: a dynamic critical-volume hypothesis. In: Proc. Eighth Symp. Underwater Physiol., ed. A.J. Bachrach and M.M. Matzen, pp. 131-146. Bethesda, Md: Undersea Medical Society, Inc.

18. Yount, D.E. and D.C. Hoffman. 1983. On the use of a cavitation model to calculate diving tables. In: Cavitation and Multiphase Flow Forum, ed. J.W. Hoyt, pp. 65–68. New York: The American Society of Mechanical Engineers.

19. U.S. Department of the Navy. 1977. U.S. Navy Diving Manual (NAVSHIPS 0994-LP-001-9010). Washington: U.S. Government Printing Office.

20. Royal Naval Physiological Laboratory. 1968. Air Diving Tables. Alverstoke, Hants. London: Her Majesty's Stationary Office.

21. Landau, L.D. and E.M. Lifshitz. 1938. Statistical Physics, pp. 225-228. Oxford: Oxford University Press.

22. Frenkel, J. 1955. The kinetic theory of liquids, chap. VII New York: Dover Publications.

23. Harvey, E.N. et al. 1944. Bubble formation in animals, I. Physical factors. J. Cell. Comp. Physiol. 24:1-22.

24. Pease, D.C. and L.R. Blinks. 1947. Cavitation from solid surfaces in the absence of gas nuclei. J. Phys. Col. Chem. 51:556-567.

25. Yount, D.E. et al. 1977. Stabilization of gas cavitation nuclei by surface-active compounds. Aviat. Space Environ. Med. 48(3):185-191.

26. Spencer, M.P. and S.D. Campbell. 1968. Development of bubbles in venous and arterial blood during hyperbaric decompression. Bull Mason Clinic 22:26-32.

27. Yount, D.E. 1983. A model for microbubble fission in surfactant solutions. J. Colloid Interface Sci. 91:349-360.

28. Albano, G. 1970. Principles and observations on the physiology of the scuba diver. Published in Italian in 1966 and translated for the Office of Naval Research, ONR Report DR0150.

29. Hennessey, T.R. and H.V. Hempleman. 1977. An examination of the critical released gas volume concept of decompression sickness. Proc. R. Soc. Lond. Biol. 197:299-313.

30. Yount, D.E. and D.A. Lally. 1980. On the use of oxygen to facilitate decompression. Aviat. Space Environ. Med. 51(6): 544-550.

31. Flynn, E.T., et al. 1981. Diving Medical Officer Student Guide, Course A-6A-0010. Naval Diving and Salvage Training Center, Panama City, FL 32407.

32. Beckman, E.L. 1976. Recommendations for Improved Air Decompression Schedules for Commercial Diving. UNIHI-SEAGRANT-TR-76-02. University of Hawaii Sea Grant College Program, Honolulu.

33. Hills, B.A. 1966. A thermodynamic and kinetic approach to decompression sickness. Ph.D. dissertation, Department of Chemical Engineering, University of Adelaide, Australia.

34. Leitch, D.R. and E.E.P. Barnard. 1982. Observations on no-stop and repetitive air and oxynitrogen diving. Undersea Biomed. Res. 9:113-129.

35. Beckman, E.L. and E.M. Smith. 1972. Tektite II: Medical supervision of the scientists in the sea. Texas Reports on Biol. and Med. 30:155-169.

36. Hempleman, H.V. 1969. Decompression theory: British practice. In: The physiology and medicine of diving and compressed air work. Eds. Bennett, P.B. and D.H. Elliott, pp. 331-347. Baltimore: Williams & Wilkins.

37. Kidd, D.J., R.A. Stubbs, and R.S. Weaver. 1971. Comparative approaches to prophylactic decompression. In: Proc. Fourth Symp. Underwater Physiol., ed. C.J. Lambertsen, pp. 167-177. New York: Academic Press.

38. Gray, J.S. 1944. Aeroembolism induced by exercise in cadets at 23,000 feet. Committee on Aviation Medicine Report 260. Washington, D.C.: United States National Research Council.

39. Beard, S.E., T.H. Allen, R.G. McIver, and R.W. Bancroft. 1967. Comparison of helium and nitrogen in production of bends in simulated orbital flights. Aerospace Med. 38(4):331-337.

40. Bennett, P.B. and A.J. Hayward. 1968. Relative decompression sickness hazards in rats of neon and other inert gases. Aerospace Med. 39(3):301-302.

41. Buhlmann, A.A. 1984. Decompression—Decompression Sickness. New York: Springer-Verlag. (Available through: Best Publishing Company, P.O. Box 1978, San Pedro, CA 90732).

42. Yount, D.E. 1978. Responses to the twelve assumptions presently used for calculating decompression schedules. In: Decompression Theory, the Seventeenth Undersea Medical Society Workshop, pp. 143-160. Bethesda, Md.: Undersea Medical Society, Inc.

43. Behnke, A.R. 1971. The Harry G. Armstrong Lecture. Decompression sickness: advances and interpretations. Aerospace Med. 42(3):255-267.

44. Gersh, I. and H.R. Catchpole. 1951. Decompression sickness: physical factors and pathologic consequences. In: Decompression Sickness, J.F. Fulton, Ed. Philadelphia: W.B. Saunders.

45. Blank, M. 1979. Monolayer permeability. Progress in Surface and Membrane Science 13:87-139.

46. Kunkle, T.D. 1979. Bubble nucleation in supersaturated fluids. Sea Grant Technical Report UNIHI-SEAGRANT-TR-80-1. NOAA Office of Sea Grant, U.S. Department of Commerce.

47. Adamson, A.W. 1976. The physical chemistry of surfaces, 3rd ed., Chapters II and III. New York: John Wiley & Sons.

48. Gaines, G.L. 1966. Insoluble monolayers at liquid-gas interfaces, Chapter IV, Sec. III. New York: John Wiley & Sons, Inc.

49. Ries, H.E., Jr. and W.A. Kimball. 1957. Proceedings of the Second International Congress of Surface Activity, Vol. I, pp. 75-84.

50. Tanford, C. 1980. The hydrophobic effect: formation of micelles and biological membranes, 2nd Ed. New York: John Wiley & Sons.

51. Lambertsen, C.J. and H. Bardin. 1973. Decompression from acute and chronic exposure to high nitrogen pressure. Aerospace Med. 44(7):834-836.

52. Buhlmann, A.A., P. Frei, and H. Keller. 1966. Saturation and desaturation with N_2 and He at 4 atm. J. Appl. Physiol. 23(4):458–462.

53. Krekler, H., G. von Nieding, K. Muysers, P. Cabarrou, and D. Fust. 1973. Washout of inert gases following hyperbaric exposure. Aerospace Med. 44(5):505–507.

54. Schreiner, H.R. and P.L. Kelley. 1966. Computation methods for decompression from deep dives. Proc. Third Symp. Underwater Physiol., C.J. Lambertsen, Ed., pp. 275–299. Baltimore: Williams and Wilkins.

55. Schilling, C.W., M.F. Werts, and N.R. Schandelmeier, Eds. 1976. The underwater handbook: a guide to physiology and performance for the engineer. New York: Plenum Press.

56. Workman, R.D. and J.L. Reynolds. 1965. Adaptation of helium-oxygen to mixed-gas SCUBA. U.S. Navy Experimental Diving Unit Research Report 1-65.

57. Workman, R.D. 1965. Calculation of decompression schedules for nitrogen-oxygen and helium-oxygen dives. U.S. Navy Experimental Diving Unit Report 6-65.

58. Molumphy, G.G. 1950. Computation of helium-oxygen decompression tables. U.S. Navy Experimental Diving Unit Report 7-50.

59. Molumphy, G.G. 1950. Helium-oxygen decompression tables. U.S. Navy Experimental Diving Unit Report 8-50.

60. Hills, B.A. 1977. Decompression sickness, Volume 1, Chapter 7. New York: John Wiley & Sons.

61. Hempleman, H.V. 1967. Decompression procedures for deep, open sea operations. In: Proc. Third Symp. Underwater Physiol., C.J. Lambertsen, Ed., pp. 255–266. Baltimore: Williams & Wilkins.

62. Elliott, D.H. 1969. Some factors in the evaluation of oxy-helium decompression schedules. Aerospace Med. 40(2):129–132.

63. Bornmann, R.C. 1966. Decompression after saturation diving. In: Proc. Third Symp. Underwater Physiol., C.J. Lambertsen, Ed., pp. 255–266. Baltimore: Williams & Wilkins.